Expression of Airway Cell Specific Secretory Proteins and Transcription Factors in the Developing Respiratory Epithelium and Tumors of the Lung

PhD Thesis

András Khoór, M.D.

Semmelweis University
Clinical Medicine Doctoral School

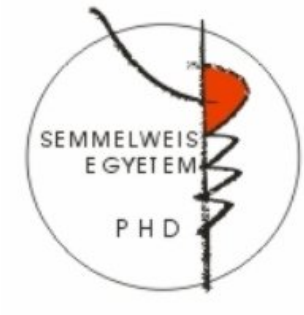

Program Director:	Prof. Péter Lakatos, M.D., Ph.D., D.Sc.
Thesis Supervisor:	Prof. Károly Cseh, M.D., Ph.D., D.Sc.
Official Reviewers:	Judit Moldvay, M.D., Ph.D. László Vass, M.D. Ph.D.
Final Examination Board:	Prof. Tamás Machay, M.D., Ph.D. (Chair) Adrien Halász, M.D., Ph.D. Prof. Tibor Kerényi, M.D., Ph.D.

Jacksonville, Florida
2011

Table of Contents

1. List of Abbreviations

ABC	avidin-biotin complex
BPD	bronchopulmonary dysplasia
CGRP	calcitonin gene-related peptide
CK	cytokeratin
CCSP	Clara cell specific protein
DAB	3,3'-diaminobenzidene
Foxa	forkhead box A
H&E	hematoxylin and eosin
h	hour
HMD	hyaline membrane disease
LSAB	labeled streptavidin-biotin
min	minute
mRNA	messenger ribonucleic acid
NE	neuroendocrine
NEB	neuroendocrine body
NSCLC	non-small cell lung carcinoma
PAP	peroxidase-antiperoxidase
pro-SP-B	surfactant protein B precursor
pro-SP-C	surfactant protein C precursor
SCLC	small cell lung carcinoma
SP-A	surfactant protein A
SP-B	surfactant protein B
SP-C	surfactant protein C
TTF-1	thyroid transcription factor 1

2. Introduction

2.1. Phases of lung development

Phases of lung development are summarized in **Table 1**. In the embryo, the developing lower respiratory tract is first seen as a groove in the floor of the primitive pharynx, caudal to the pharyngeal pouches. The groove evaginates into a distinct laryngotracheal diverticulum, which elongates caudally into the primitive mesenchyme as the primitive lung bud. Bronchial buds arise by progressive dichotomous division and the segmental, subsegmental, and more distal airways are formed. Bronchial cartilage, musculature, and connective tissues are derived from the mesenchyme surrounding the bronchial buds. The development of the major airways, termed the embryonic phase, occurs between 3 and 6 weeks of gestation.

Table 1. Phases of Lung Development*

Phase	Gestation	Major events
Embryonic	26 days to 6 weeks	Development of major airways
Pseudoglandular	6 to 16 weeks	Development of airways to terminal bronchioles
Canalicular	16 to 28 weeks	Development of the acinus and its vascularization
Saccular	28 to 36 weeks	Subdivision of saccules by secondary crests
Alveolar	36 weeks to term	Acquisition of alveoli

*From Colby et al, 1995 [1].

From approximately the 6th to 16th week of gestation, the small airways, including the terminal bronchioles, are formed; 16 weeks after conception, the formation of the conducting airways is complete. This is the pseudoglandular phase.

The next stage of development, the canalicular phase, occurs between 16 and 28 weeks; the acinus and its accompanying vascular supply develop. Terminal bronchioles give rise to respiratory bronchioles with terminal sacs representing primitive alveoli. Some respiratory function may be possible toward the end of this phase because of the presence of these vascularized terminal sacs.

The saccular phase is identifiable by the 28th week and extends to the 36th week of gestation. Saccules form and become lined by flattened Type I alveolar epithelial cells. The associated capillary network develops in the surrounding mesenchyme, and lymphatics are formed.

The alveolar phase begins at approximately 36 weeks of gestation and extends to as late as 8 years of age. Vascularized alveoli are formed and are lined by Type I and Type II pneumocytes. The visceral and parietal pleura arise within the primordial mesenchyme surrounding the developing lung.

2.2. Histology of the airway epithelium

The cells lining the airways and alveoli are endodermally derived and have a number of specialized modifications. The respiratory tract is organized to facilitate gas transfer distally (hence large numbers of attenuated Type I alveolar lining cells) and for airflow and clearance along the mucociliary escalator proximally (hence larger numbers of ciliated and mucus cells) (**Figure 1**). Submucosal glands of minor salivary type are found in the submucosa of the trachea and bronchi (but not the bronchioles).

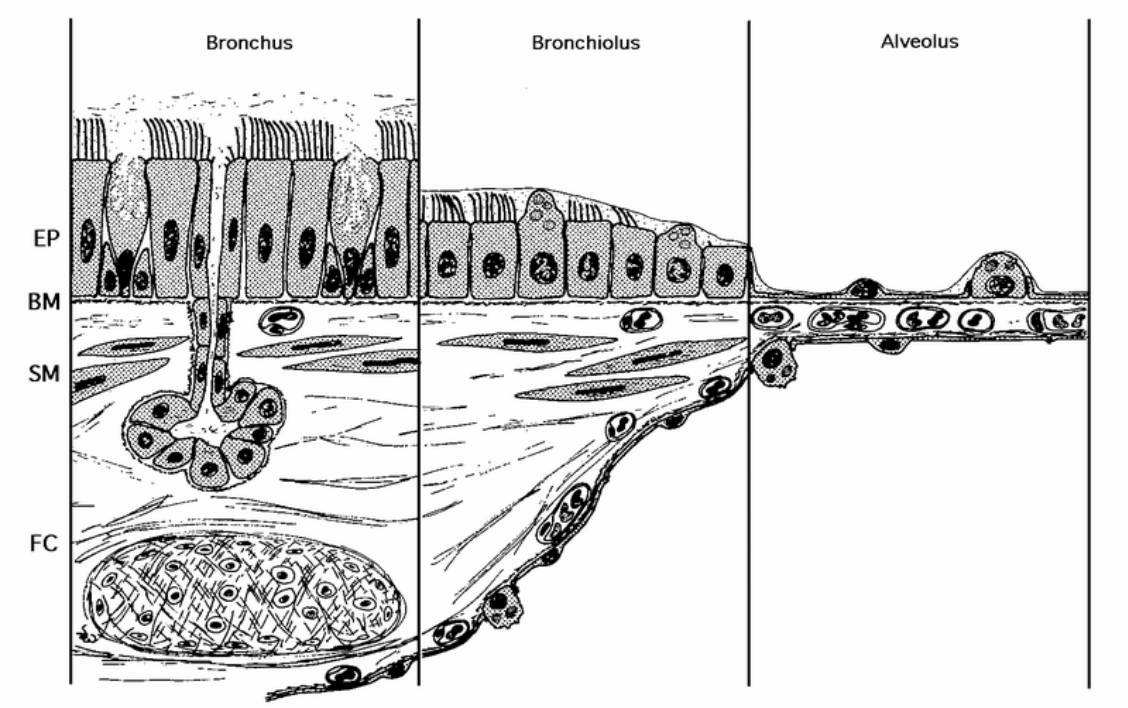

Figure 1. Schematic diagram of the respiratory epithelium. The bronchial epithelium is composed of primarily ciliated cells and goblet cells, whereas the bronchiolar epithelium is composed of ciliated cells and nonciliated bronchiolar epithelial (Clara) cells with apical protrusions containing granules. The alveolus contains attenuated Type I cells to facilitate gas transfer, interspersed with Type II cells that protrude into the alveolar lumen. From Colby et al, 1995 [1].

2.3. Classification of lung tumors

Lung cancer is the most frequently diagnosed cancer worldwide, with approximately 1.2 million new cases reported in 2000, and is the most common cause of cancer mortality in males. The highest incidence and mortality occur in North America, Europe, Australia/New Zealand, and South America. Incidence is generally a function of past trends in tobacco smoking [2]. The incidence is currently sharply increasing in developing regions such as China and Eastern Europe. Lung carcinomas account for approximately 99% of all lung cancers. In North America, the incidence of adenocarcinoma now exceeds that of squamous cell carcinoma in both men and women. This appears to be related to a true increase in incidence rather than a reflection of improved diagnostic methods. The reasons for this are not fully understood and may be related to changes in cigarette filter composition or deeper inhalation [3]. Despite better diagnostic techniques and understanding of the molecular biology of lung cancers, the overall prognosis remains poor, with an overall 5-year survival of 15% and a 60% 5-year survival for stage I tumors [4].

The current WHO Classification of malignant epithelial lung tumors is summarized in **Table 2** [5]. From a clinical standpoint, lung carcinomas are broadly divided into non-small cell lung carcinoma (NSCLC) and small cell lung carcinoma (SCLC) for treatment purposes. NSCLCs include squamous cell carcinoma, adenocarcinoma, and large cell carcinoma. To address advances in oncology, molecular biology, pathology, radiology, and surgery of lung adenocarcinoma, a new international multidisciplinary classification has been sponsored by the International Association for the Study of Lung Cancer, the American Thoracic Society, and the European Respiratory Society (**Table 3**) [6, 7]. This new classification may replace the current WHO classification in the future, but its detailed discussion is beyond the scope of this dissertation.

Table 2. 2004 WHO Classification of Malignant Epithelial Lung Tumors*

- Squamous cell carcinoma
  - Variants
    - Papillary
    - Clear cell
    - Small cell
    - Basaloid
- Small cell carcinoma
  - Variant
    - Combined small cell carcinoma
- Adenocarcinoma
  - Adenocarcinoma, mixed subtype
  - Acinar adenocarcinoma
  - Papillary adenocarcinoma
  - Bronchioloalveolar carcinoma
    - Nonmucinous
    - Mucinous
    - Mixed nonmucinous and mucinous
  - Solid adenocarcinoma with mucin production
  - Variants
    - Fetal adenocarcinoma
    - Mucinous ("colloid") carcinoma
    - Mucinous cystadenocarcinoma
    - Signet ring adenocarcinoma
    - Clear cell adenocarcinoma
- Large cell carcinoma
  - Variants
    - Large cell NE carcinoma
    - Combined large cell NE carcinoma
    - Basaloid carcinoma
    - Lymphoepithelioma-like carcinoma
    - Clear cell carcinoma
    - Large cell carcinoma with rhabdoid phenotype
- Adenosquamous carcinoma
- Sarcomatoid carcinoma
  - Pleomorphic carcinoma
  - Spindle cell carcinoma
  - Giant cell carcinoma
  - Carcinosarcoma
  - Pulmonary blastoma
- Carcinoid Tumor
  - Typical carcinoid
  - Atypical carcinoid
- Salivary Gland Tumors
  - Mucoepidermoid carcinoma
  - Adenoid cystic carcinoma
  - Epithelial-myoepithelial carcinoma

*From Travis et al, 2004 [5].

Table 3. IASLC/ATS/ERS Classification of Lung Adenocarcinoma in Resection Specimens*

- Preinvasive lesions
  - Atypical adenomatous hyperplasia
  - Adenocarcinoma in situ (≤3 cm formerly BAC)
    - Nonmucinous
    - Mucinous
    - Mixed mucinous/nonmucinous
- Minimally invasive adenocarcinoma (≤3 cm lepidic predominant tumor with ≤5 mm invasion)
  - Nonmucinous
  - Mucinous
  - Mixed mucinous/nonmucinous
- Invasive adenocarcinoma
- Lepidic predominant (formerly nonmucinous BAC pattern, with >5 mm
- invasion)
  - Acinar predominant
  - Papillary predominant
  - Micropapillary predominant
  - Solid predominant with mucin production
- Variants of invasive adenocarcinoma
  - Invasive mucinous adenocarcinoma (formerly mucinous BAC)
  - Colloid
  - Fetal (low and high grade)
  - Enteric

Abbreviations: BAC, bronchioloalveolar carcinoma; IASLC, International Association for the Study of Lung Cancer; ATS, American Thoracic Society; ERS, European Respiratory Society. *From Travis et al, 2011 [7].

2.4. Adenocarcinoma of the lung

Adenocarcinoma has now surpassed squamous cell carcinoma as the most common type of lung cancer in many countries. Clinically, adenocarcinoma most commonly presents as a peripheral nodule. Rare cases of adenocarcinoma may produce diffuse thickening of the visceral pleura, mimicking malignant mesothelioma [8]. Radiographically, peripheral adenocarcinomas produce a spectrum of ground-glass to solid opacities. The likelihood of an invasive component increases with the size of the solid component [9, 10]. Kodama and coworkers have demonstrated that the radiographic ground-glass component correlates with the BAC component in pathology specimens [11].

Histologically, adenocarcinoma of the lung is subclassified into acinar, papillary, bronchioloalveolar, and solid types [5]. Rare variants of adenocarcinoma include fetal adenocarcinoma, mucinous (colloid) carcinoma, mucinous cystadenocarcinoma, signet ring adenocarcinoma, and clear cell adenocarcinoma [5].

2.5. Neuroendocrine (NE) lung tumors

NE tumors of the lung are a distinctive subset of lung cancers which share certain morphologic, immunohistochemical, and ultrastructural features. The main tumor types include low-grade typical carcinoid, intermediate grade atypical carcinoid, and two high-grade tumors, large cell NE carcinoma and SCLC.

Typical carcinoid is defined as a NE tumor with fewer than two mitoses per 2 mm^2 and lacking necrosis, while atypical carcinoid is defined as a NE tumor with either 2 to 10 mitoses per 2 mm^2 or necrosis [5]. Most atypical carcinoids will meet both criteria but occasional atypical carcinoids will have necrosis and fewer than 2 mitoses per 2 mm^2. Studies have shown that such tumors behave as atypical carcinoids rather than typical carcinoids [12]. Both typical carcinoids and atypical carcinoids may occur in either a central or a peripheral location and tend to be predominantly, but not exclusively, endobronchial [13]

Large cell NE carcinoma is defined as a NE tumor with greater than 10 mitoses/2mm^2 and cytologic features of large cell carcinoma [5, 14]. Tumor cells tend to be polygonal with abundant cytoplasm and prominent nucleoli are often seen. Evidence of NE differentiation must be demonstrated by ancillary methods such as immunohistochemistry. Use of a specific marker such as chromogranin or synaptophysin is recommended as neuron-specific enolase (NSE) is regarded as being too nonspecific. Only tumors which show both NE morphology and positive staining should be classified as large cell NE carcinoma. It is important to note that up to 20% of conventional adenocarcinoma, squamous cell carcinoma or large cell carcinoma will stain with NE markers. Such tumors have been designated as NSCLC with NE differentiation. It is currently undetermined if NSCLC with NE differentiation has a worse prognosis or responds differently to chemotherapy than conventional NSCLC, as reports have been conflicting to date [15, 16].

SCLC is defined as a NE tumor with greater than 10 mitoses/2 mm^2 and small cell cytologic features. Cells are typically oval to slightly spindled in shape and have scant cytoplasm. Nuclei are hyperchromatic and have absent to very small nucleoli [5]. Crush artifact may be prominent on small biopsies, but is not pathognomonic for SCLC. In larger core biopsies or resected specimens, the cells may appear slightly larger than in a transbronchial biopsy and may have discernable cytoplasm. It has been demonstrated that a range of nuclear size may be present, and occasional cells may contain larger nucleoli. Frequent prominent nucleoli and large cells should not be seen.

SCLC comprises approximately 20% of all lung cancers and the vast majority present as central tumors with extensive mediastinal adenopathy [17]. Only 10% of SCLC is localized to the lung at the time of diagnosis. Five percent of SCLC present as a peripheral coin lesion.

2.6. Surfactant proteins

The alveolar surface is lined by Type II and Type I alveolar epithelial cells that are in direct contact with respiratory gases, creating collapsing forces at the air-liquid interface. To maintain inflation, these surface forces are mitigated by the presence of pulmonary surfactant that is synthesized and secreted onto the alveolar surface by Type II epithelial cells. Because pulmonary surfactant reduces surface tension, it is critical for the maintenance of lung volumes during the respiratory cycle. Lack of pulmonary surfactant in preterm infants with respiratory distress syndrome or adults with acute respiratory distress syndrome causes atelectasis leading to respiratory failure.

Pulmonary surfactant is a complex mixture of lipids, mostly phosphatidylcholine, and associated proteins. The surfactant proteins, designated as SP-A, SP-B, SP-C, and SP-D, play critical roles in various aspects of surfactant structure, function, and metabolism [18, 19]. All four are expressed at relatively high levels in Type II cells and have distinct structures (**Figures 2-4**) [20] and functions [21]. SP-B and SP-C alter lipid packing and spreading and enhance the surface tension–lowering activity of the lipids, as well as stabilizing the lipid layers during the respiratory cycle [22]. SP-A and SP-D are larger, relatively abundant, oligomeric proteins. They are structurally related members of the collectin family of C-type mammalian lectins that share distinct collagen-like and globular, carbohydrate-binding domains. SP-A is required for the formation of tubular myelin and plays diverse roles in host-defense functions of the lung [23-26]. SP-A binds lipopolysaccharides and various microbial pathogens, enhancing their clearance from the lung. Unlike SP-B and SP-C, SP-A does not play a critical role in surface functions. SP-D, however, influences the structural forms of pulmonary surfactant and is important in the regulation of alveolar surfactant pool sizes and reuptake [27-29]. SP-D is also necessary in the suppression of pulmonary inflammation and in host defense against viral, fungal, and bacterial pathogens [23, 26].

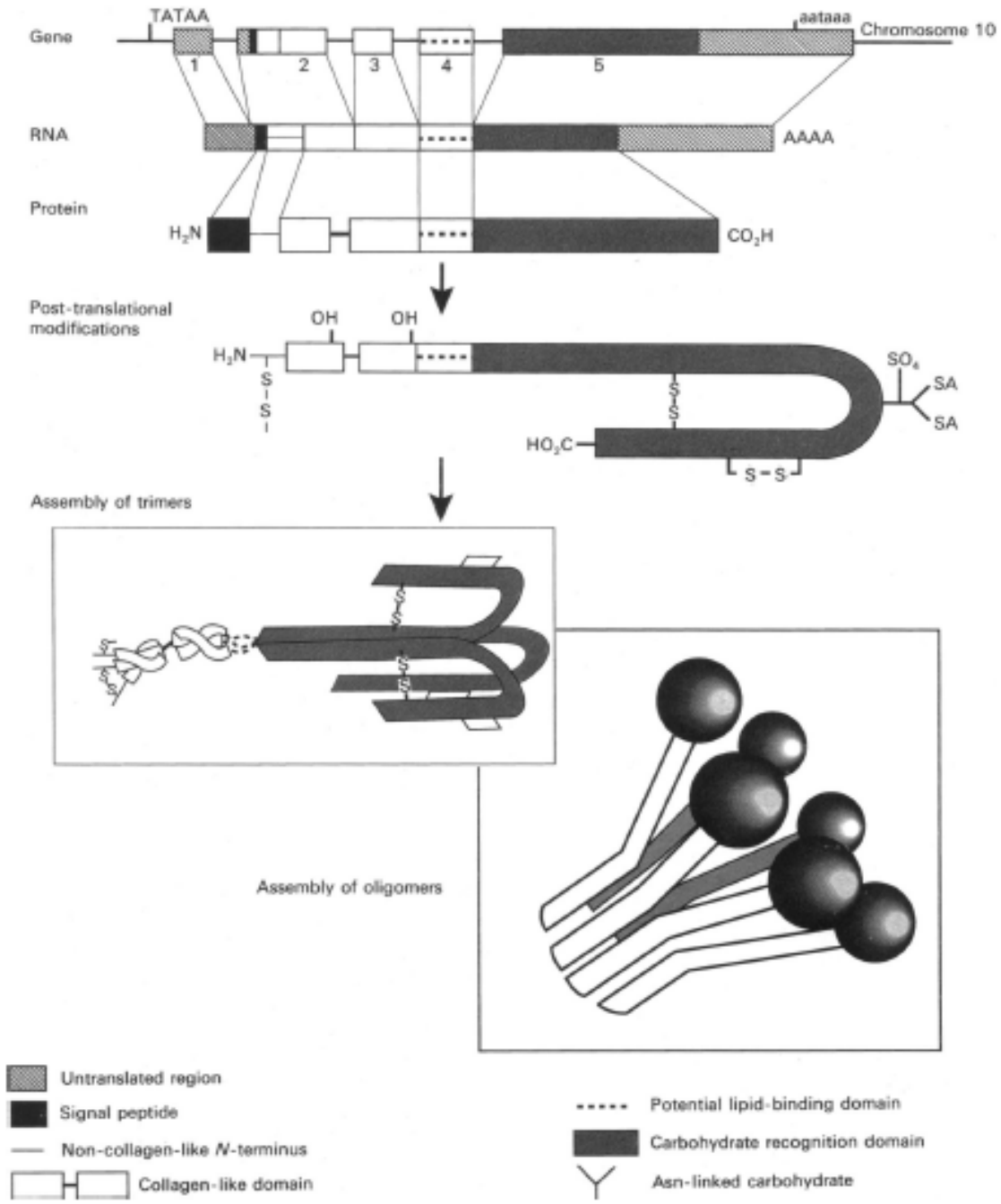

Figure 2. Gene, RNA and proposed protein structure of human SP-A. The human SP-A gene is encoded by five exons on chromosome 10. The approx. 2.2 kb SP-A mRNA encodes a protein of 248 amino acids including a 20-amino-acid signal peptide. Post-translational modifications include signal peptide cleavage, inter- and intra-chain disulphide bond formation, hydroxylation of specific proline residues and the formation of a triple helix in the collagen-like region. Mature SP-A consists of six trimers of SP-A. From Weaver and Whitsett, 1991 [20].

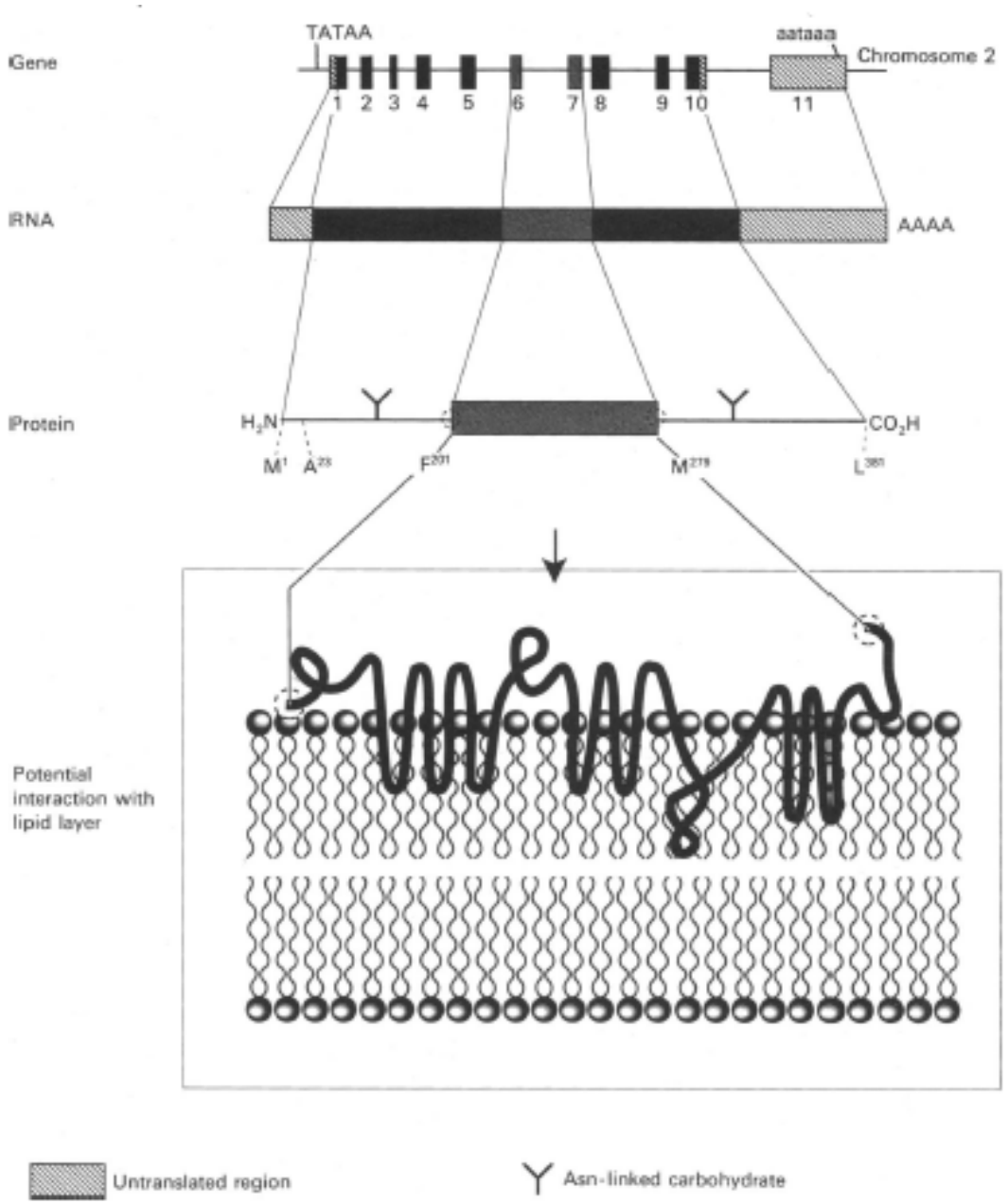

Figure 3. Gene, RNA and proposed protein structure of SP-B. The human SP-B gene is encoded by 11 exons on chromosome 2. The SP-B RNA of approx. 2 kb encodes a precursor of 381 amino acids (pro-SP-B). Processing of the precursor includes removal of a signal peptide of approximately 23 residues, and proteolytic cleavages between Gln^{200} and Phe^{201} and between Met^{279} and Asp^{280} to produce the 79 residue active airway peptide. Potential amphipathic helices may facilitate interaction of the peptide with phospholipid. From Weaver and Whitsett, 1991 [20].

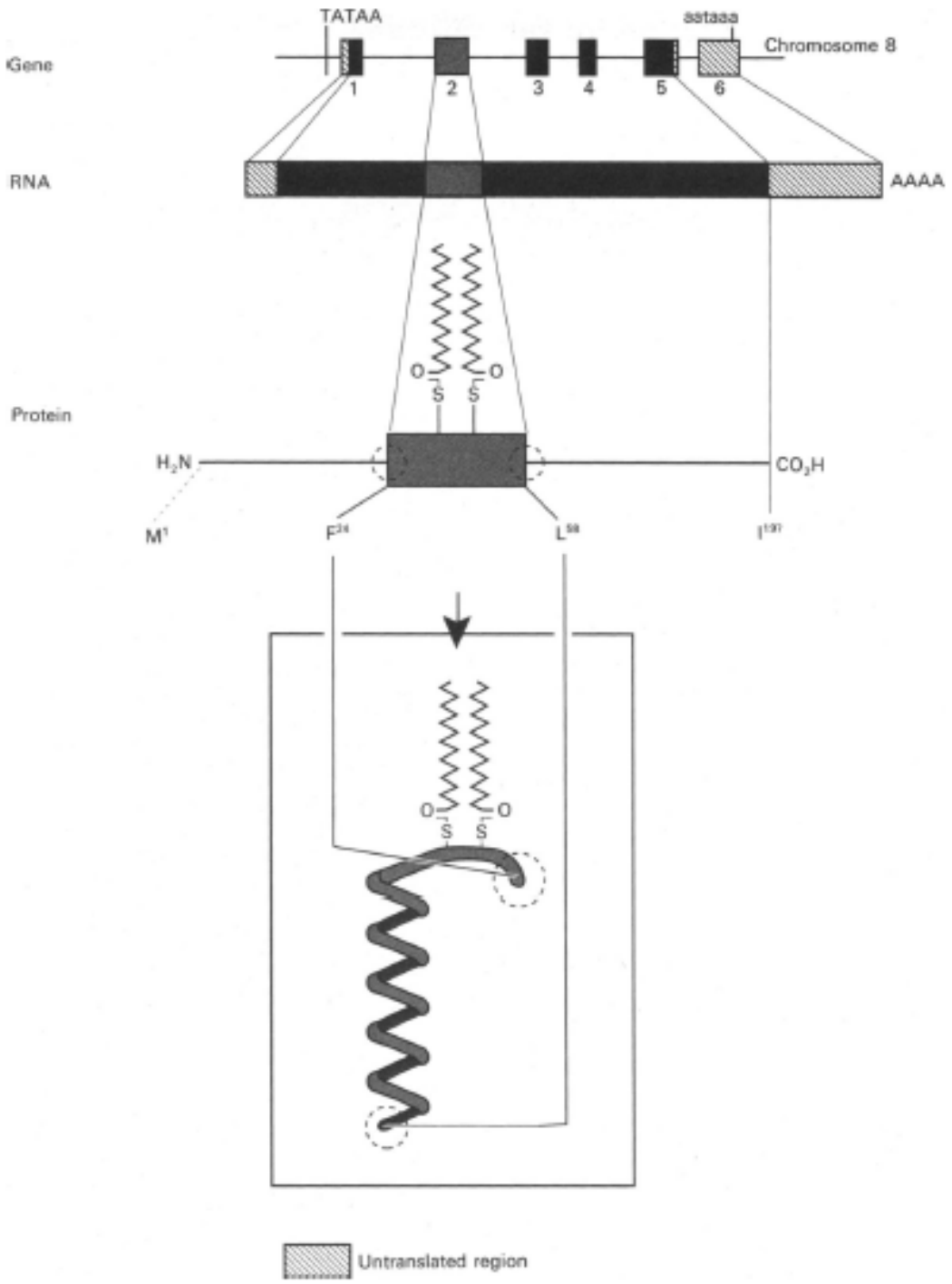

Figure 4. Gene, RNA and proposed protein structure of SP-C. The human SP-C gene is encoded by six exons on chromosome 8. SP-C RNAs of approx. 0.9 kb encode a precursor of 191-197 residues (pro-SP-C). Proteolytic cleavages between Arg^{23} and Phe^{24} and between Leu^{58} and His^{59} result in an active airway peptide of 35 residues. From Weaver and Whitsett, 1991 [20].

2.7. Clara cell specific protein (CCSP)

Human CCSP is a low-molecular-weight protein that has been isolated from bronchoalveolar lavage fluid and localized to secretory granules of Clara cells [30, 31]. The structure of this protein is similar to that of a previously described protein secreted by rabbit endometrium called uteroglobin [32]. The protein has been referred to by various names in the literature, including Clara cell 10-kDa protein (CC10). Despite elucidation of the complete amino acid sequence and the detailed X-ray diffraction crystallographic structure of the protein, the primary physiologic function of CCSP remains unknown. In vitro testing suggests that the protein suppresses inflammation [33].

2.8. Thyroid transcription factor 1 (TTF-1)

TTF-1 [also known as Nkx2.1, T/EBP (thyroid-specific-enhancer-binding protein) or TITF1], a member of the homeodomain-containing transcription factor family, activates the expression of select genes in the thyroid, lung and restricted regions of the brain [34, 35].

A homeobox is a 180 bp DNA sequence motif encoding a protein domain that can bind the DNA in a sequence-specific manner. Homeodomain-containing transcription factors play key roles in the control of embryonic development and differentiation [36]. They control the transcriptional activation of target genes by binding to specific DNA sequences via the homeodomain.

TTF-1 controls the expression of several important thyroid-specific and lung-specific genes. In the thyroid, TTF-1 controls the expression of the thyroglobulin [37], thyroperoxidase [38], thyrotropin receptor [39] and sodium iodide symporter [40] genes and, in the lung, TTF-1 is essential for the expression of SP-A [41], SP-B [42], SP-C [43], CCSP [44] and ABCA3 (ATPbinding-cassette transporter A3) [45] genes.

2.9. Forkhead box A2 (Foxa2)

The Foxa subfamily of winged helix/forkhead box (Fox) transcription factors has been the subject of genetic and biochemical study for over 20 years [46]. Three members, Foxa1, Foxa2 and Foxa3, have been found to play important roles in multiple stages of mammalian life, beginning with early development, continuing during organogenesis, and finally in metabolism and homeostasis in the adult. The genes were originally

named hepatocyte nuclear factor-3 (HNF-3) α, β, and γ until the nomenclature of all vertebrate forkhead box containing genes was standardized in 2000 [47].

Foxa2 is required for the formation of the node and notochord, and in its absence severe defects in gastrulation, neural tube patterning, and gut morphogenesis result in embryonic lethality [46]. Foxa1 and Foxa2 cooperate to establish competence in foregut endoderm and are required for normal development of endoderm-derived organs such as the liver, pancreas, lungs, and prostate. In postnatal life, members of the Foxa family control glucose metabolism through the regulation of multiple target genes in the liver, pancreas, and adipose tissue.

Foxa2 has also been implicated in the regulation of transcription of several genes expressed in respiratory epithelial cells, including SP-B (**Figure 5**), CCSP, and TTF-1 [42, 48]. Foxa2 binding sites are present in the promoter–enhancer elements of many genes, including those expressed in liver, pancreas, and lung.

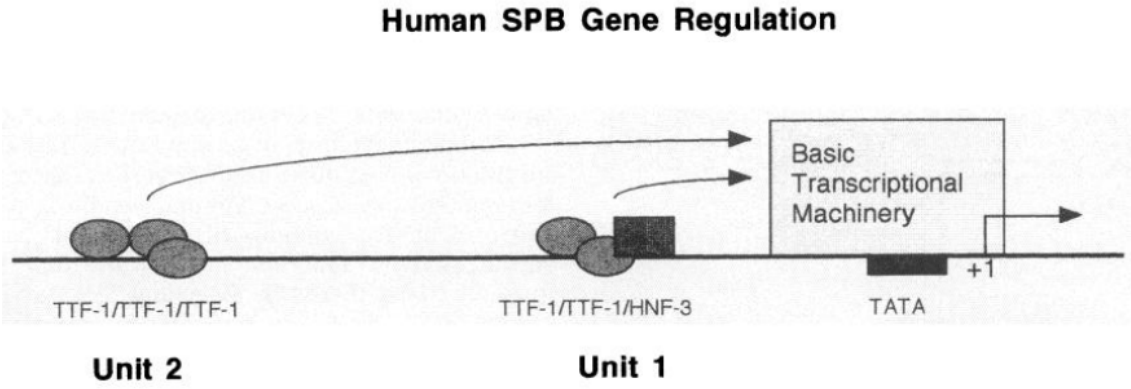

Figure 5. Transcriptional apparatus of SP-B gene. SP-B is transcribed from a pol II promoter element that interacts with tissue-specific enhancers located 5' to SP-B gene. The nuclear transcription factor TTF-1 is expressed in respiratory epithelial cells that express SP-B; TTF-1 binds to and activates transcription of SP-B gene, determining lung cell-specific gene expression. Foxa (HNF-3) transcription proteins bind to and enhance promoter activity of SP-B gene. Interactions among *cis*-acting sequences of SP-B gene and nuclear transcription proteins, in part, determine the temporal, spatial, and humoral regulation of SP-B gene. Unit 1 is proximal promoter region consisting of TTF-1 and Foxa binding sites that work in concert with SP-B promoter (transcription machinery). Unit 2 represents a cluster of TTF-1 binding sites that functions as an enhancer, activating the SP-B promoter as well as other promoters in any orientation. From Whitsett et al., 1995 [48].

3. Objectives

Our aims and objectives were as follows:

1. To analyze the expression of airway cell specific secretory proteins and their mRNAs in the developing human lung. More specifically, to analyze
    a. Expression of SP-A and SP-A mRNA;
    b. SP-B precursor (pro-SP-B) and SP-B mRNA;
    c. SP-C precursor (pro-SP-C) and SP-C mRNA; and
    d. CCSP and CCSP mRNA in the developing human lung.
2. To analyze the expression of pro-SP-B, SP-B mRNA and TTF-1 in NSCLC. More specifically, to analyze
    a. Expression of pro-SP-B and SP-B mRNA in adenocarcinoma of the lung;
    b. The utility of pro-SP-B and TTF-1 in differentiating adenocarcinoma of the lung from malignant mesothelioma;
    c. The prognostic value of pro-SP-B and TTF-1 in early stage adenocarcinoma of the lung;
    d. The utility of TTF-1 in determining the primary site for adenocarcinomas metastatic to the brain; and
    e. Expression of TTF-1 in malignant pleural effusions.
3. To analyze the expression of airway cell specific transcription factors in NE lung tumors. More specifically, to analyze
    a. Expression of TTF-1 in SCLC and Merkel cell tumor; and
    b. Expression of Foxa2 in NE lung tumors.
4. To analyze the expression of airway cell specific secretory proteins and TTF-1 in miscellaneous neoplasms, including
    a. Alveolar adenoma; and
    b. Mature teratoma of the uterine cervix with pulmonary differentiation.

4. Materials and Methods

4.1 Fetal and neonatal lung tissue

The studies on fetal and neonatal lung tissues were approved by the Committee for the Protection of Human Subjects, Vanderbilt University Medical Center, Nashville, Tennessee. Lung and tracheal tissue was available from up to 41 normal fetuses (gestational age, 10-23 weeks) and 13 newborn infants without pulmonary pathology (gestational age, 25-42 weeks; postnatal age, 15 min to 30 days) [49-51]. Immunohistochemistry and in situ hybridization for CCSP was also performed on lung tissue from 23 infants with acute hyaline membrane disease (HMD) (postnatal age, 1.5 h to 2 days), 15 infants with regenerating HMD (postnatal age, 60 h to 10 days), 15 infants with early bronchopulmonary dysplasia (BPD) (postnatal age, 12-35 days), and 9 infants with late BPD (postnatal age, 35 days to 7 months) [50].

Tissues were fixed in 10% phosphate buffered formalin, in most cases within 2 h of death, dehydrated through graded ethanols, and embedded in paraffin. Floros et al. have demonstrated that tissues harvested within this time interval are suitable for in situ hybridization [52]. Four-µm-thick sections were cut and mounted on Superfrost Plus glass slides (Fisher, Atlanta, GA).

4.2. Tumor tissues

Each study was approved by the Institutional Review Board (IRB) of the appropriate institution. To analyze the incidence and distribution of pro-SP-B and SP-B mRNA, 15 consecutive adenocarcinomas, 15 squamous cell carcinomas, and 5 large cell carcinomas (a total of 35 primary carcinomas) of the lung, and 15 nonpulmonary adenocarcinomas were selected from the surgical pathology files of the Veterans Affairs Medical Center, Nashville, Tennessee [53].

The incidence and distribution of pro-SP-B and TTF-1 immunoreactivity were analyzed in 370 NSCLCs (208 adenocarcinomas, 101 squamous cell carcinomas, and 61 large cell carcinomas) and in 95 malignant mesotheliomas (69 epithelial, 19 sarcomatous, and 7 mixed) [54].

To characterize the immunohistochemical expression of TTF-1 and Cdx2 in metastatic adenocarcinomas to the brain, 38 consecutive brain biopsies containing metastatic adenocarcinoma of known origin were retrieved from the files of the H. Lee Moffitt Cancer Center and Research Institute at the University of South Florida, Tampa

[55]. The primary sites were determined by review of the original tumor and chart review, and included lung (22); breast (10); and gastrointestinal tract (6), including esophagus (1), gastroesophageal junction (1), and colon/rectum (4).

For the TTF-1 cytology study, three consecutive years of cytopathology files were searched for cases of malignant pleural effusions at the H. Lee Moffitt Cancer Center and Research Institute at the University of South Florida [56]. A total of 56 cases (52 cases of metastatic adenocarcinoma and 4 cases of malignant mesothelioma) with known primary sites and available cell blocks were selected for the study. Twenty-one patients were male (38%) and 35 patients were female (62%). Primary sites for metastatic adenocarcinomas included breast (13), ovary (5), stomach (2), prostate (2), esophagus (1), colon (1), pancreas (1), and kidney (1). Cell blocks were prepared by the plasma/thrombin technique [57]. Briefly, pleural fluid specimens were centrifuged at 2000 rpm for 5 min. The supernatant was decanted and equal drops of plasma and thrombin were added to the sediment. The clot was placed onto a small piece of tissue paper, which was folded and placed in a cassette. The specimen was then fixed in 10% phosphate-buffered formalin and was embedded in paraffin.

Immunoreactivaty for TTF-1 and cytokeratin 20 (CK20) was analyzed in 36 SCLCs and 21 Merkel cell tumors [58]. Twelve Merkel cell tumors were identified in the files of the Dermatology Clinic, University of South Florida College of Medicine. Nine Merkel cell tumors and 10 SCLCs were retrieved from the surgical pathology files of the H. Lee Moffitt Cancer Center at the University of South Florida. The remaining 26 SCLCs were obtained from the Methodist Hospital, Baylor College of Medicine. Houston, Texas.

Immunoreactivity for Foxa2 was assessed in 17 typical carcinoids, 2 atypical carcinoids, 4 large cell NE carcinomas, 23 SCLCs, 19 adenocarcinomas, 7 squamous cell carcinomas, and 3 (non-NE) large cell carcinomas of the lung [59]. One typical carcinoid, 2 large cell NE carcinomas, and 14 SCLCs were obtained from the James A. Haley VA Medical Center, Tampa, Florida. The remaining tumors were retrieved from the surgical pathology files of the Moffitt Cancer Center at the University of South Florida.

Seventeen cases of alveolar adenoma were studied [60]. Sixteen were retrieved from the files of the Department of Pulmonary and Mediastinal Pathology at the Armed Forces Institute of Pathology; case 17 was previously published in 1996 and was submitted by Dr. E. Oliveira of the Department of Pathology, Portuguese Cancer

Institute, Lisbon [61, 62]. Clinical information and follow-up was obtained from the patient records and contributing physicians. In all 17 cases, hematoxylin and eosin (H&E) stained sections were assessed. Immunohistochemical stains were analyzed in cases for which paraffin-embedded tissue was available.

We also reported a case of a 33-year-old woman who presented with heavy vaginal bleeding and a polypoid mass of the uterine cervix [63]. The 3.5 cm mass was excised, and the specimen was sampled extensively for histopathologic evaluation and immunohistochemistry.

4.3. Antibodies

Polyclonal SP-A antibody

The antibodies most relevant to our studies are listed in **Table 4**. The polyclonal SP-A antibody was a kind gift of Dr. Jeffrey Whitsett (Children's Hospital, Cincinnati, Ohio) [49, 63]. Purification of SP-A from alveolar lavage fluid of a patient with alveolar proteinosis has previously been reported [49]. The purity of the protein was tested on a 13% acrylamide gel and the protein concentration determined by the Lowry method [64]. After endoglycosidase digestion and β-elimination, antibodies to the digested and β-eliminated SP-A were prepared in rabbits. Serum samples of antibody 63742 were subjected to absorption overnight at 4°C with red blood cells from each of the four major blood groups. The cells were separate by centrifugation and the cell-free serum tested again in an ELISA, where it proved to be active up to a dilution of 50,000. The antibody was further analyzed by immunoblot. Human SP-A and digested and β-eliminated SP-A were separated by SDS-PAGE and the proteins transferred to nitrocellulose and reacted with the antibody generated against deglycosylated SP-A. Antibody 63742 reacted strongly with both glycosylated and deglycosylated isoforms of SP-A.

Polyclonal pro-SP-B antibody

The rabbit pro-SP-B antiserum was received from Dr. Jeffrey Whitsett's laboratory [51, 53, 54, 60, 63]. The antiserum was generated against recombinant pro-SP-B expressed in E. coli as previously described [65]. This antiserum recognizes pro-SP-B and both amino- and carboxy-terminal portions of pro-SP-B but is less reactive with the active SP-B peptide [66].

Table 4. Antibodies and Staining Methods

Antibody	Type (Clone)	Source	Dilution	Staining Method (Source)	Antigen retrieval
SP-A	Rabbit polyclonal	Dr. Whitsett	1:250	PAP	
Pro-SP-B	Rabbit polyclonal	Dr. Whitsett	1:1,600	PAP; Biotin-streptavidin detection system (Super Sensitive, BioGenex, San Ramon, CA)	Microwave antigen retrieval (BioGenex)
Pro-SP-C	Rabbit polyclonal	Dr. Whitsett	1:100	PAP	
CCSP	Rabbit polyclonal	Dr. Singh	1:1,000	PAP	
TTF-1	Monoclonal (8G7G3/1)	Dr. Whitsett; Dako Corporation, Carpinteria, CA	1:250 to 1:1,000	ABC kit (Vectastain, Vector Laboratories, Burlingame, CA); Biotin-streptavidin detection system (Super Sensitive, BioGenex)	Microwave antigen retrieval (BioGenex)
Foxa2	Rabbit polyclonal	Dr. Costa	1:4,000	Biotin-streptavidin detection system (Super Sensitive, BioGenex), cobalt enhancement	Microwave antigen retrieval (BioGenex)

Polyclonal pro-SP-C antibody

The rabbit pro-SP-C antiserum was prepared in Dr. Jeffrey Whitsett's laboratory [51, 60, 63]. It was produced by repeated injection of the entire recombinant human SP-C precursor expressed in E. coli as previously described [65]. The antiserum reacts with recombinant human pro-SP-C, but does not recognize the active SP-C peptide [67]. The antiserum precipitates [^{35}S]-methionine/cystine-labeled pro-SP-C (M_r 22,000) and processing intermediates (Mr ~16,000) in fetal rat lung explant cultures and in immortalized mouse lung epithelial cells (MLE-12 cells) and does not crossreact with SP-B or its precursor protein [68].

Polyclonal CCSP antibody

The rabbit antiserum to human CCSP was received from Dr. Gurmukh Singh's laboratory (Veterans Affairs Medical Center, Pittsburgh, Pennsylvania) [50, 60, 63]. Preparation and purification of the antiserum have been described earlier [30].

Monoclonal TTF-1 antibody

Production and characterization of the monoclonal TTF-1 antibody (clone 8G7G3/1) have been reported earlier [69]. For our earlier studies, the TTF-1 antibody was received from Dr. Jeffrey Whitsett's laboratory [54, 58, 60]. When the antibody became commercially available (same clone), it was purchased from Dako Corporation (Carpinteria, California) [55].

Polyclonal Foxa2 antibody

A rabbit polyclonal Foxa2 antibody was kindly provided by Dr. Robert Costa, University of Chicago, Illinois [59]. It was generated against recombinant rat Foxa2 and purified by affinity chromatography. The specificity of this antibody has been tested previously [70].

Other antibodies

In addition to the antibodies listed above, several other commercially available antibodies were used in our studies, including Cdx2 (Novocastra Laboratories, Newcastle upon Tyne, United Kingdom) [55], CK 7 (Dako) [55], and CK 20 (Dako) [55, 58].

4.4. Immunohistochemical methods

Immunohistochemical staining was performed using standard peroxidase-antiperoxidase (PAP) complex [71], avidin-biotin complex (ABC) [72], labeled streptavidin-biotin (LSAB), and polymer-based immunohistochemistry methods [73, 74]. Schematic representation of these methods is shown in **Figures 6-9**. All avidin-biotin methods rely on the strong affinity of avidin or streptavidin for the vitamin biotin. Streptavidin (from Streptomyces avidinii) and avidin (from chicken egg) both possess four binding sites for biotin. The biotin molecule is easily conjugated to antibodies and enzymes. In the ABC method, secondary antibodies are conjugated to biotin and function as links between tissue-bound primary antibodies and an avidin-biotin-peroxidase complex (**Figure 7)** [72]. Polymer-based immunohistochemical methods utilize a technology based on a polymer backbone to which multiple secondary antibodies and enzyme molecules are conjugated (**Figure 9**) [73, 74].

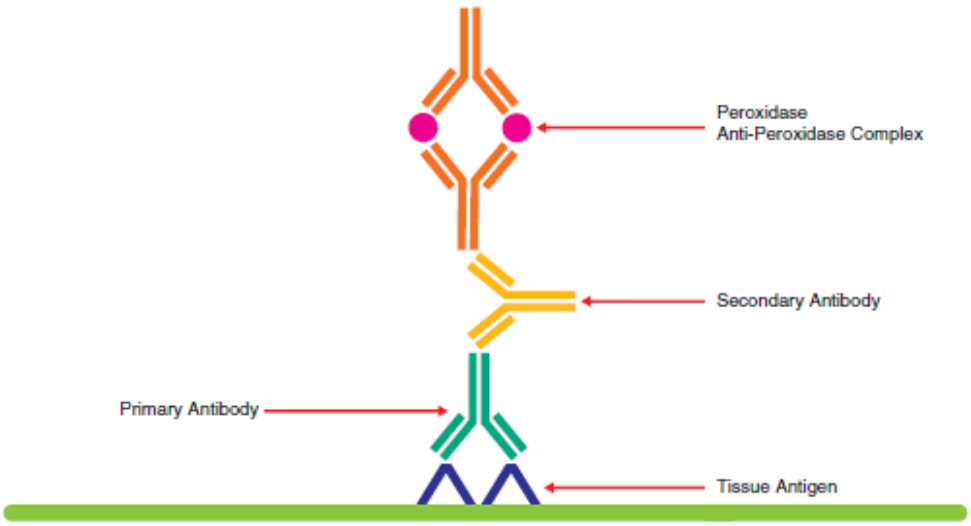

Figure 6. Peroxidase anti-peroxidase (PAP) complex method.

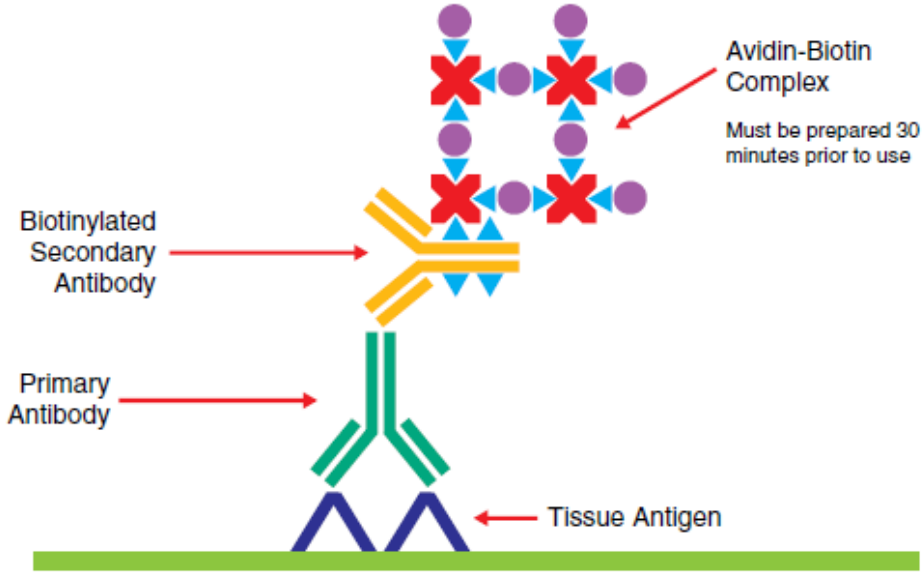

Figure 7. Avidin-biotin complex (ABC) method.

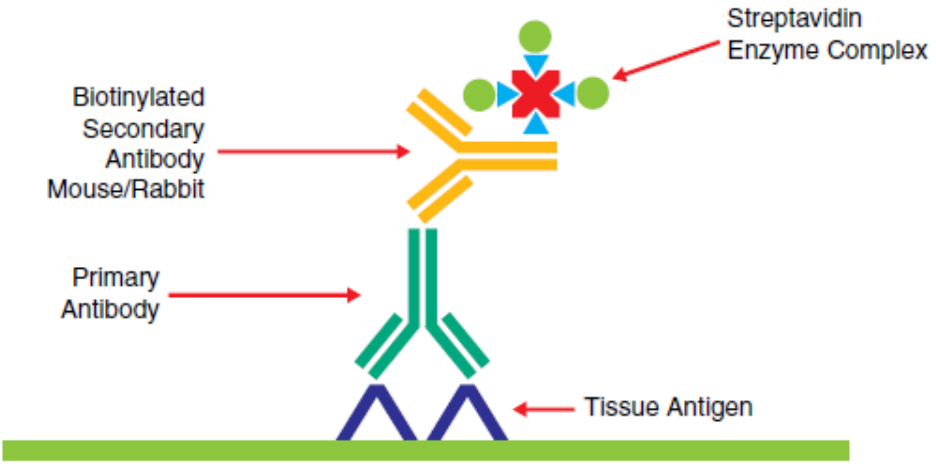

Figure 8. Labeled streptavidin-biotin (LSAB) method.

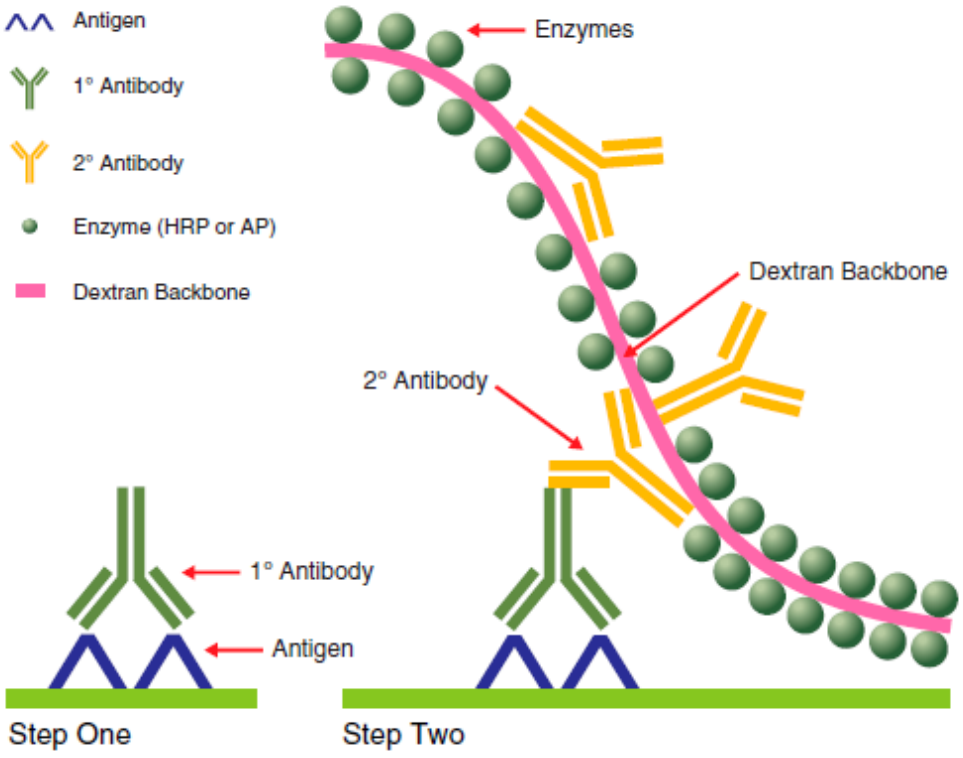

Figure 9. Two-step polymer method (EnVision™, Dako)

The staining method for each antibody is listed in **Table 4**. SP-A, pro-SP-C and CCSP were detected using the PAP complex method [49-51, 60, 63]. Sections were deparaffinized, hydrated, treated with 0.3% H_20_2 in methanol, and exposed to 10% normal swine serum to eliminate nonspecific staining. The primary antibody was applied and allowed to remain overnight at room temperature. After washing, sections were exposed to a swine antiserum to rabbit immunoglobulin, washed again, and treated with horseradish peroxidase coupled to rabbit anti-peroxidase. The peroxidase activity was then localized by reaction with a solution containing 0.05% 3,3'-diaminobenzidene (DAB) and 0.01% H_20_2 and counterstained with hematoxylin. Specificity of immunohistochemical results was tested by exposing adjacent tissue sections to nonimmune rabbit serum in place of the primary antiserum. Tissues known to contain or not to contain the antigen were used as controls.

Pro-SP-B was detected by either the PAP complex method (see above) [51, 63] or an amplified biotin-streptavidin detection system (Super Sensitive, BioGenex, San Ramon, CA), according to the manufacturer's protocol [53, 54, 60].

TTF-1 was detected using avidin/streptavidin-biotin methods. Briefly, deparaffinized sections were pretreated with a microwave antigen retrieval system (BioGenex), according to the manufacturer's protocol. After pretreatment, sections were incubated with the appropriate dilution (1:250 to 1:1,000) of the TTF-1 antibody. Antigen-antibody complexes were visualized by an ABC kit (Vectastain, Vector Laboratories, Burlingame, CA) or a biotin-streptavidin detection system (Super Sensitive, BioGenex), using DAB as the chromogen. Normal lung and thyroid tissues and a pulmonary adenocarcinoma known to express TTF-1 served as positive controls. Negative controls were prepared by substituting the TTF-1 antibody with nonspecific mouse immunoglobulin G.

Foxa2 was detected using biotin-streptavidin technology with cobalt chloride enhancement of DAB [59]. Briefly, 4-μm-thick deparaffinized sections were pretreated with a microwave antigen retrieval system (Super Sensitive, BioGenex). After pretreatment, slides were exposed to prediluted normal goat serum to block nonspecific staining. Sections were then incubated with the Foxa2 primary antibody (dilution, 1:4000) overnight. The antigen-antibody complexes were visualized with a biotin-streptavidin detection system (BioGenex), using DAB as the chromogen. Specific staining was enhanced with a 0.5% cobalt chloride solution. Slides were counterstained

with nuclear fast red. Normal rabbit serum was substituted for the primary antiserum as negative control. Normal lung tissue served as positive control.

Cytoplasmic staining was considered positive for SP-A, pro-SP-B, pro-SP-B, and CCSP and nuclear staining was judged positive for TTF-1 and Foxa2.

4.5. In situ hybridization probes

Radiolabeled SP-A probe

An 862-base fragment of a human SP-A cDNA clone was subcloned into pGEM-7Zf transcription vector (Promega, Madison, Wisconsin). This fragment contains almost the entire coding sequence of SP-A and recognizes only SP-A mRNA at 2.15 KB in Northern blot analysis of human lung RNA [75]. The orientation of the subcloned fragment with respect to T7 and SP6 promoters was determined by restriction map analysis and confirmed by Northern blotting. Sense and anti-sense RNA probes were synthesized by in vitro transcription. The reaction mixture contained a linearized DNA template, 5'[α-^{35}S]-UTP, 1000-1500 Ci/mmol (NEN, Boston, Massachusetts), and the reagents of a transcription kit (Riboprobe Gemini II Core System, Promega). Radiolabeled probes were reduced to an average length of 100 bases by limited alkaline hydrolysis [76], and separated from unincorporated nucleotides by Sephadex G-50 column chromatography. Before hybridization, probes were sized on denaturing agarose gels.

Radiolabeled SP-B and SP-C probes

A 797-BP fragment of a human SP-B cDNA clone (SP-B 7.1) and an 800-BP fragment of a human SP-C cDNA clone (SP-C 2.1) (both from American Type Culture Collection, Rockville, Maryland) were subcloned separately into Bluescript II SK transcription Vectors (Stratagene, La Jolla, California). The cDNA clones hybridize with SP-B mRNA (2.0 KB) and SP-C mRNA (1.0 KB) in Northern blot analysis of human lung RNA [77]. The orientation of the subcloned fragments with respect to T3 and T7 promoters was determined by restriction map analysis. Sense and anti-sense RNA probes were synthesized by in vitro transcription. The reaction mixture contained a linearized DNA template, 5'[α-^{35}S]-UTP, 1000-1500 Ci/mmol (NEN), reagents of a transcription kit (Riboprobe Gemini II Core System; Promega), and T3 (Stratagene) or T7 (Promega) RNA polymerase. Radiolabeled probes were reduced to an average length of 100 bases by limited alkaline hydrolysis [76] and separated from

unincorporated nucleotides by Sephadex G-50 column chromatography. Before hybridization, probes were sized on denaturing agarose gels to determine that the limited alkaline hydrolysis reduced the probe to the optimal length (100 bases).

Radiolabeled CCSP probe

The 367-BP human CCSP cDNA [78] was inserted into a pBluescript II SK+ transcription vector (Stratagene). Labeled RNA transcripts of this cDNA identify a 0.6 KB CCSP band in Northern blot analysis of human lung RNA [78]. The orientation of the subcloned cDNA with respect to the T3 and T7 promoters was determined by restriction map analysis. Sense and antisense RNA probes were synthesized by in vitro transcription. The reaction mixture contained a linearized DNA template, 5'[α-^{35}S]-UTP, 1000-1500 Ci/mmol (NEN), reagents of a transcription kit (Riboprobe Gemini II Core System), and T3 (Stratagene) or T7 (Promega) RNA polymerase. Radiolabeled probes were reduced to an average length of 100 bases by limited alkaline hydrolysis [76] and were separated from unincorporated nucleotides by Sephadex G-50 column chromatography. Before hybridization, probes were sized on denaturing agarose gels to determine that the limited alkaline hydrolysis reduced the probe to the optimal length (100 bases).

Nonradioactive digoxigenin-labeled SP-B probe

A 797-base pair fragment of a human SP-B cDNA clone (SP-B 7.1 from the American Type Culture Collection) was subcloned into a Bluescript II SK transcription vector (Stratagene). This cDNA clone hybridizes with SP-B mRNA in Northern blot analysis of human lung mRNA [77]. The orientation of the subcloned fragment with respect to the T3 and T7 promoters was assessed by restriction map analysis. Sense and antisense nonradioactive digoxigenin-labeled RNA probes were synthesized by in vitro transcription using the DIG RNA Labeling Kit (Boehringer Mannheim, Indianapolis, Indiana) according to the guidelines of the manufacturer. Each reaction mixture contained a linearized DNA template, reagents of the transcription kit, and T3 (Stratagene) or T7 (Boehringer Mannheim) RNA polymerase. The labeled probe was reduced to an average length of 100 bases by limited alkaline hydrolysis [76] and separated from unincorporated nucleotides by ethanol precipitation. After confirmation of the resultant probe length, the probes were stored at -70°C.

4.6. In situ hybridization procedures

Radioactive in situ hybridization

In situ hybridization was performed as described previously [79] with modifications. Briefly, tissue sections were deparaffinized in xylene (twice for 10 min), rehydrated through a graded ethanol series (100% to 30%), rinsed in 1 x PBS (5 min), and postfixed in a freshly prepared solution of 4% paraformaldehyde in 1 x PBS (20 min). Slides were then rinsed in 1 x PBS (twice for 5 min) and treated with a fresh solution of proteinase K (1 µg/ml) in 50 mM Tris-HCl, pH 8.0, 5 mM EDTA (30 min at 37°C). Slides were then rinsed in 1 x PBS (5 min), refixed in the same paraformaldehyde solution (5 min), quickly dipped in distilled water, and acetylated in freshly prepared 0.25% acetic anhydride in 0.1 M triethanolamine (twice for 10 min). Slides were subsequently rinsed in 1 x PBS (5 min), dehydrated through the ethanol series (30% to 100%) and dried in a slide drier (Oncor, Gaithersburg, Maryland). Tissue sections were covered with a hybridization solution that contained 2 x 10^4 cpm/µl sense or antisense probe. Tissue and probe were covered with a siliconized coverslip and hybridized in a humid chamber (overnight at 55°C). After hybridization, coverslips were removed in 5 x SSC (1 x SSC = 150 mM NaCI, 15 mM sodium citrate), 20 mM P-mercaptoethanol (BME) (1 h at 50°C). Slides were washed in 50% formamide, 2 x SSC, 200 mM BME (20 min at 65°C), rinsed in 1 x TEN (10 mM Tris, pH 7.5, 0.5 mM EDTA, 0.5 M NaCl) (twice for 10 min at 37°C), treated with a solution of RNAse A (20 µg/ml) and RNAse T1 (1 U/ml) in 1 x TEN (30 min at 37'C) and rinsed again in 1 x TEN (twice for 10 min at 37°C). Slides were then washed in 50% formamide, 2 x SSC, 200 mM BME (20 min at 65°C), in 2 x SSC (twice for 15 min at 65%), and in 0.1 x SSC (twice for 15 min at 65°C). Slides were dehydrated through graded ethanols containing 0.3 M ammonium acetate, dried, dipped in 50% Ilford K.5 emulsion in 1 % glycerol, and dried again. After 4 days (SP-B), 6 days (SP-C and CCSP) or 10 days (SP-A) of exposure, autoradiographs were developed in Kodak D-19 solution and counterstained with 0.04% toluidine blue. The length of autoradiography was determined in preliminary studies and was not changed in subsequent procedures. The specificity of hybridization was established by sense probes which did not hybridize above the background levels observed with the anti-sense probes.

Nonradioactive in situ hybridization

For nonradioactive in situ hybridization, we used a modified version of the original protocol of Springer et al. [80]. Prehybridization treatments and posthybridization washes were performed as described previously [51] The hybridization solution contained 1 ng/µl sense or antisense probe, 50% formamide, 0.3 M sodium chloride, 10 mM Tris, pH 8.0, 10 mM sodium phosphate, 0.5 mM EDTA, 1x Denhardt's solution, 10% dextran sulfate, and 0.2 mg/ml yeast RNA. The hybridization was performed overnight in a humid chamber at 55"C. Hybrids were detected by an enzyme-linked immunoassay with a nucleic acid detection kit (DIG Nucleic Acid Detection Kit, Boehringer Mannheim). The specificity of hybridization was established with a sense probe, which did not hybridize above the background level observed with the antisense probe.

4.7. Statistical analysis

Sensitivity, specificity, positive predictive value and negative predictive value were calculated using standard statistical methods [81]. Actuarial cumulative survival analyses were performed and tested by logrank (Mantel-Cox) test using StatView 4.5 (Abacus Concepts).

5. Results

5.1 Expression of SP-A and SP-A mRNA in the developing lung

We used immunohistochemistry and in situ hybridization to determine the distribution of SP-A and SP-A mRNA in lungs of human fetuses and newborn infants without pulmonary pathology [49]. The results are shown in **Table 5** (fetuses of 10-18 weeks' gestation), **Table 6** (fetuses of 19-23 weeks' gestation), **Table 7** (newborn infants of 25-42 weeks' gestation), and **Figures 10-16**. Immunoreactive SP-A was first detected in the tracheal epithelium at 13 weeks of gestation. Between 13 and 18 weeks of gestation, expression of SP-A and SP-A mRNA was limited to the tracheal and bronchial epithelium and glands. SP-A and SP-A mRNA was detected in terminal airways from 19 weeks of gestation onward. In liveborn infants, tracheal and bronchial epithelial cells and glands, non-ciliated bronchiolar epithelial (Clara) cells, cells of the bronchioloalveolar portals, and alveolar Type II cells contained SP-A and SP-A mRNA. Although some alveolar macrophages contained immunoreactive material, SP-A mRNA was never detected.

Table 5. SP-A and SP-A mRNA in Fetuses (10-18 Weeks of Gestation)

GA (wk)	BM (g)	Trachea		Bronchi			
		Ep	Gl	Ep	Gl	CB	TA
10	7	na	na	–	0	–	–
11	8	na	na	0/0	0/0	– / –	– / –
12	18	na	na	–	0	–	–
12	na	– / –	0/0	– / –	0/0	– / –	– / –
13	41	+	–	0	0	–	–
14	39	na	na	0/0	0/0	– / –	– / –
14	44	na	na	–	–	–	–
14	36	na	na	0	0	–	–
15	60	+	–	+	–	–	–
15	55	na	na	0/0	0/0	– / –	– / –
16	111	+ /na	– /na	+ / +	+ / +	– / –	– / –
16	105	+ / –	– / –	– / +	+ / –	– / –	– / –
16	99	+ / –	+ / –	0/0	0/0	– / –	– / –
17	137	+ /na	– /na	– / –	– /0	– / –	– / –
18	200	+ / –	+ / –	– / +	+ / +	– / –	– / –
18	185	+ / –	+ / –	– / +	– / –	– / –	– / –
18	175	na	na	0	0	–	–

GA, gestational age; BM, birth weight; Ep, epithelium; Gl, glands; CB, ciliated bronchioles; TA, terminal airway cells; 0, structure not present; na, not available.

Table 6. SP-A and SP-A mRNA in Fetuses (19-23 Weeks of Gestation)

GA (wk)	BM (g)	PNA	Trachea		Bronchi		CB	TA	LM
			Ep	Gl	Ep	Gl			
19	278	SB	+ /na	− /na	0/0	0/0	− / −	− / −	0
19	235	40 min	+ / +	+ / +	− /0	+ /0	− / +	+ / +	0
20	343	1 hr	+	+	−	+	−	−	+
20	296	SB	+ / +	+ / +	0/0	0/0	− / −	− / −	+
20	na	1 hr	na	na	0/0	0/0	− / −	+ / +	+
20	250	1 hr	na	na	0	0	−	+	+
20	na	SB	+ / +	+ /0	0/0	0/0	− / −	− / −	0
20	320	SB	na	na	−	+	−	−	+
21	361	4 min	na	na	−	0	−	−	0
21	412	SB	na	na	− / +	− / −	− / +	+ / +	0
21	292	SB	na	na	0	0	−	+	0
22	470	1.5 hr	+ / +	− / −	0/0	0/0	− / +	+ / +	0
22	430	30 min	na	na	− / +	+ / −	− / +	+ / +	0
22	360	SB	+	+	+	+	−	−	0
22	470	1.25	na	na	0/0	0/0	− / +	− / +	+
22	560	SB	+	+	0	0	−	−	0
23	487	SB	+ / +	+ / +	− / +	+ / +	− / −	− / +	+
23	528	SB	na	na	0/0	0/0	− / −	+ / +	0
23	410	2 hr	na	na	− / −	+ / −	− / −	− / +	+
23	460	2 hr	na	na	0/0	0/0	− / −	− / −	0
23	480	2 hr	na	na	− / −	− /0	− / −	− / −	0

GA, gestational age; BM, birth weight; PNA, postnatal age; Ep, epithelium; Gl, glands; CB, ciliated bronchioles; TA, terminal airway cells; LM, luminal material.

Table 7. SP-A and SP-A mRNA in Newborn Infants (25-42 Weeks of Gestation)

GA (wk)	BM (g)	PNA	Trachea		Bronchi		CB	BA	MII	MA	LM
			Ep	Gl	Ep	Gl					
25	725	15 min	na	na	0	0	−	−	−	0	+
26	790	SB	+	+	0	0	0	0	0	0	0
29	1106	3.5 hr	na	na	−	0	−	−	−	+	+
33	1740	SB	−	+	−	+	−	−	+	0	+
36	2960	1.5 hr	na	na	− / −	+ / −	− / −	+ / +	+ / +	0	0
36	2246	3 hr	−	+	−	+	−	−	+	0	+
37	2506	24 hr	na	na	0	0	−	+	+	0	+
38	2380	24 hr	na	na	0	0	−	+	+	0	+
38	3317	90 hr	na	na	−	+	+	−	+	+	+
40	2183	41 hr	na	na	−	+	−	−	+	0	+
40	2139	10 hr	na	na	+ / +	0/0	+ / +	+ / +	+ / +	0	+
40	3580	10 days	− / +	+ / +	− / +	+ / +	+ / +	+ / +	+ / +	+	+
42	4950	12 days	− / −	+ / +	+ / +	+ /0	+ / +	+ / +	+ / +	+	+

GA, gestational age; BM, birth weight; PNA, postnatal age; Ep, epithelium; Gl, glands; CB, ciliated bronchioles; BA, bronchioloalveolar portals; MII, Type II cells; MA, macrophages; LM, luminal material; 0, structure not present in section; na, not available.

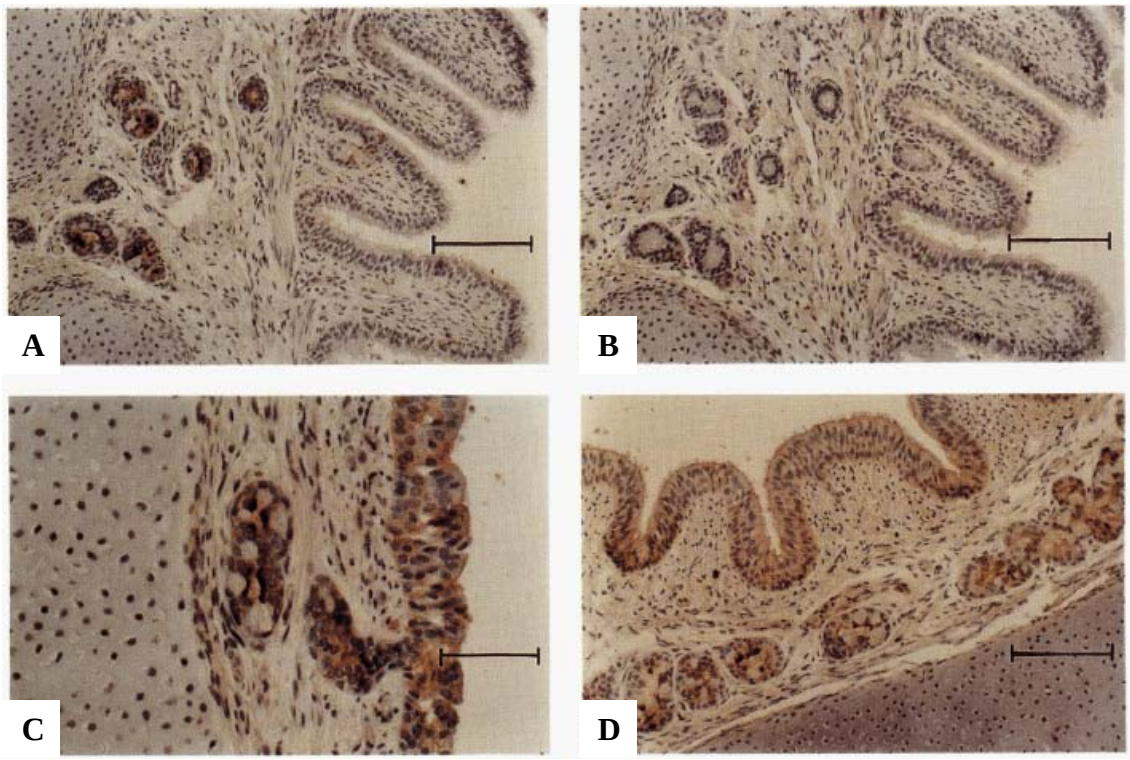

Figure 10. (A) Bronchus of a 23 week fetus. Many cells in submucosal glands are stained for SP-A. (B) Serial section of the same field shown in A. Immunostaining is ablated by incubation of the primary antibody with SP-A before use. (C) Trachea of a 19-week fetus. Scattered cells of the epithelial lining and submucosal glands are stained. (D) Trachea of a 23-week fetus. A few epithelial lining cells in the depths of folds are immunostained for SP-A. Many cells in submucosal glands are also stained.

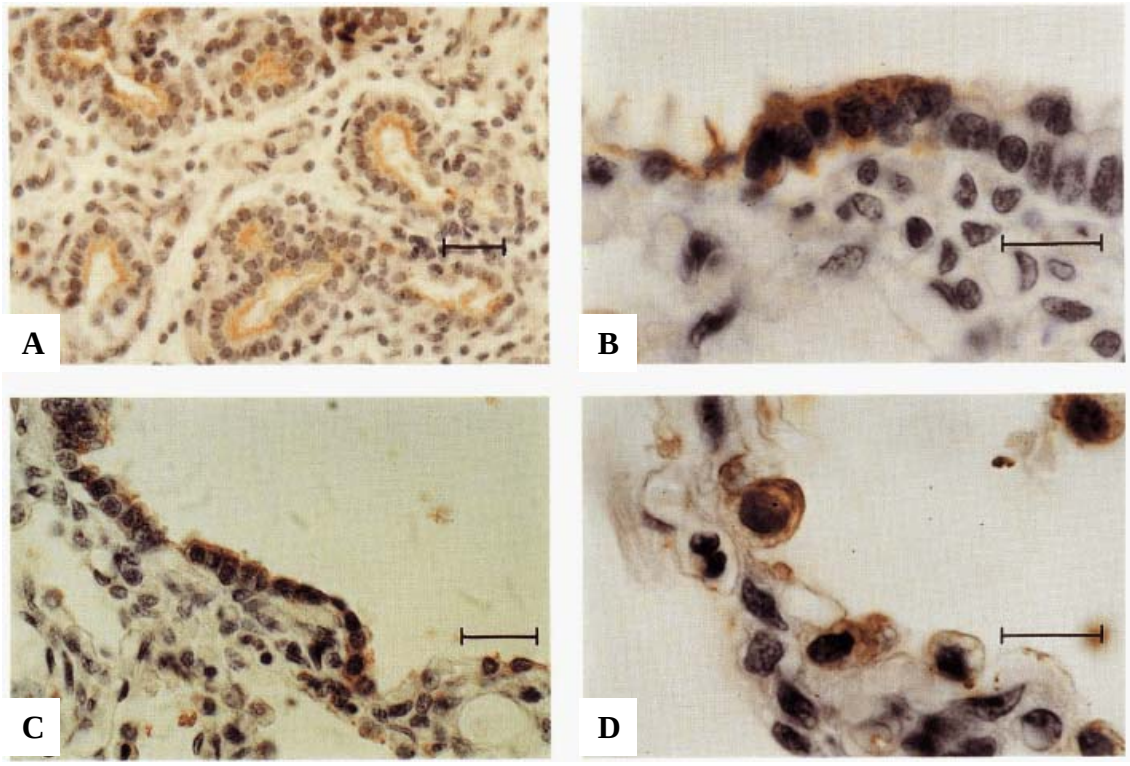

Figure 11. (A) Lung of a 20-week fetus. Cuboidal cells of the terminal airways are immunostained faintly for SP-A. (B) Lung of a term infant who survived 10 days and died of non-pulmonary causes. A bronchiole is shown, a portion of which is lined with SP-A positive cells. (C) Lung of a term infant who survived 10 days and died of non-pulmonary causes. Cells of a bronchioloalveolar portal are stained for SP-A. (D) Lung from a term infant who survived 10 days and died of non-pulmonary causes. Alveolar Type II cells show cytoplasmic staining for SP-A.

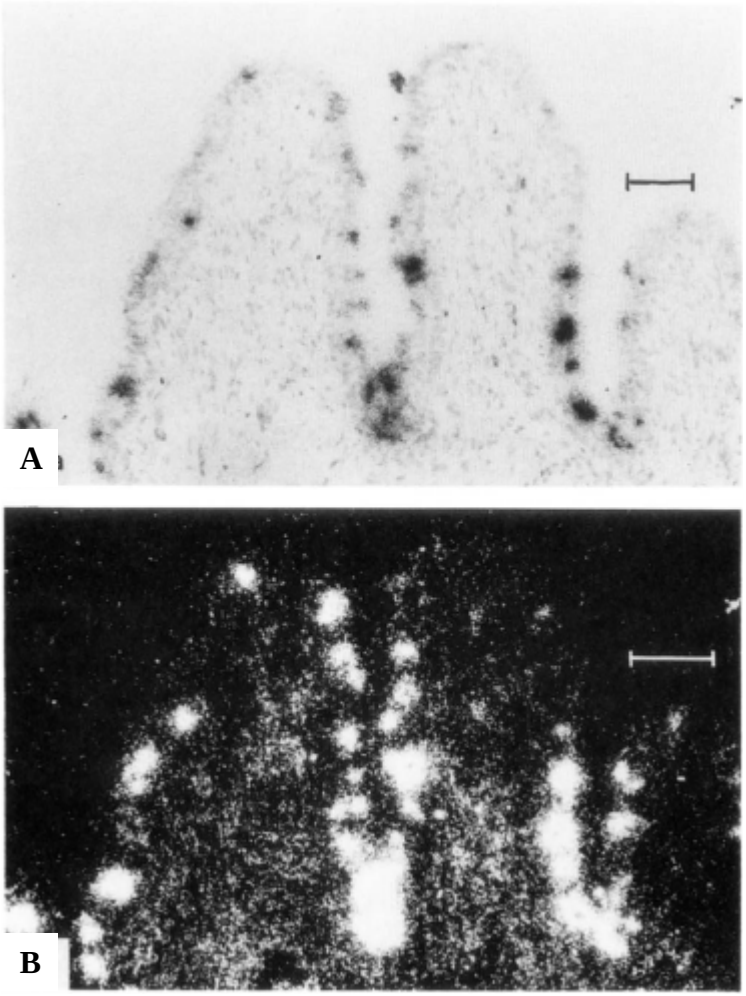

Figure 12. SP-A mRNA in scattered bronchial epithelial cells of an 18-week fetus. Lung tissue was hybridized in situ to an anti-sense SP-A probe and photographed with (A) brightfield and (B) darkfield illumination. Original magnification x 130.

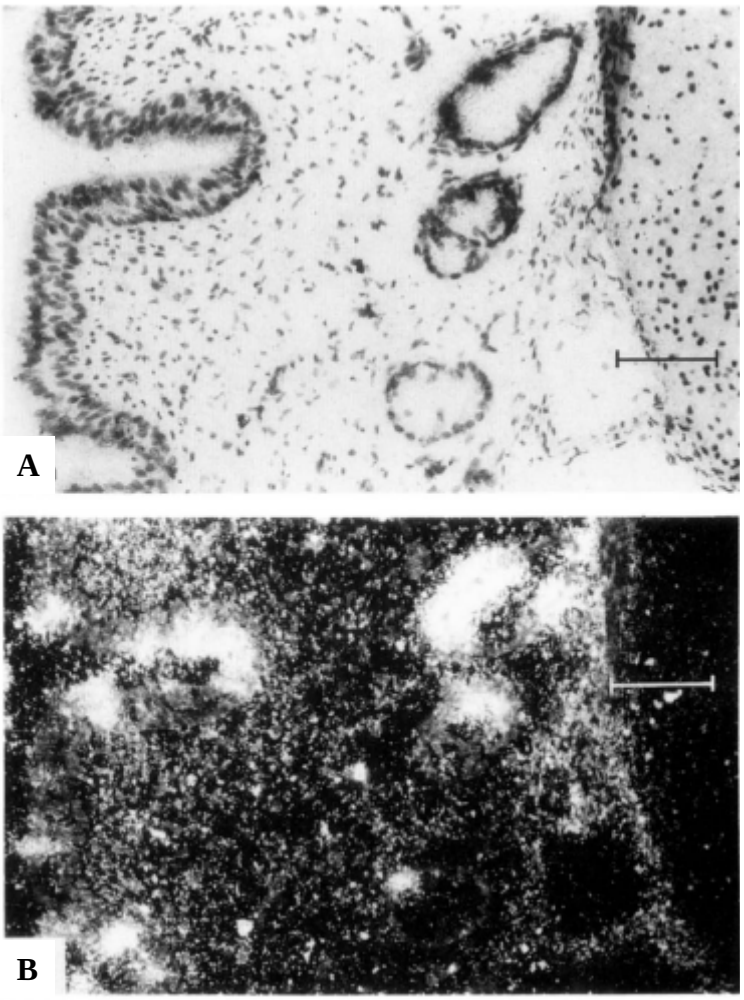

Figure 13. SP-A mRNA in scattered columnar epithelial cells and submucosal glands in the trachea of a 23-week fetus. A section of the trachea was hybridized in situ to an anti-sense SP-A probe and photographed with (A) brightfield and (B) darkfield illumination. Original magnification x 160.

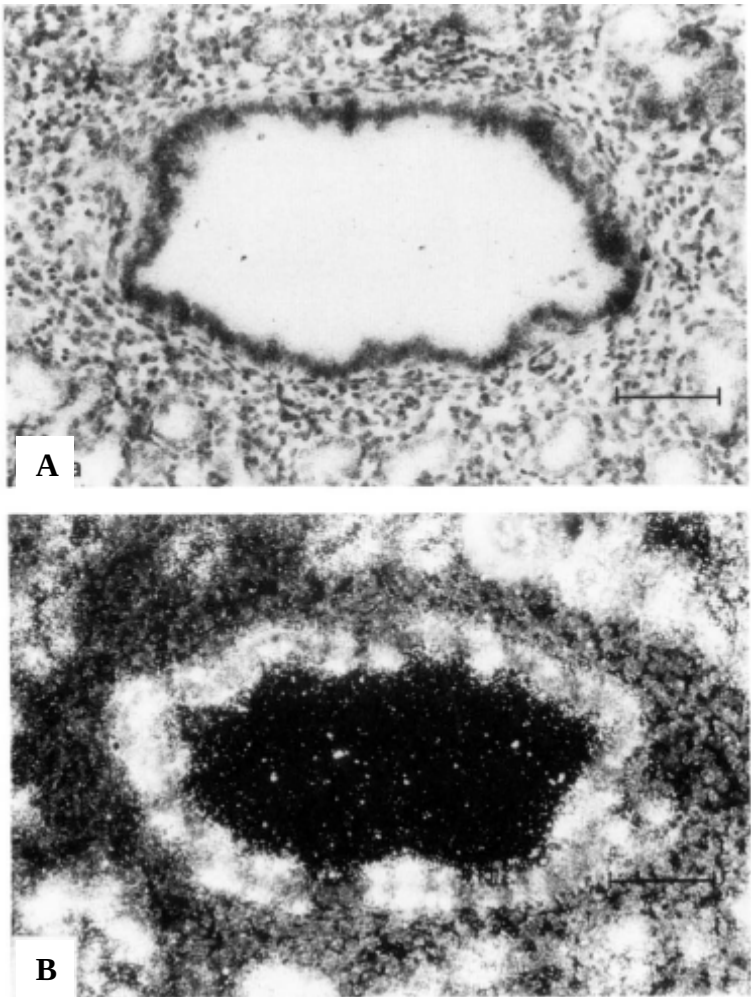

Figure 14. SP-A mRNA in scattered bronchiolar epithelial cells of a 22-week fetus. Lung tissue was hybridized in situ to an anti-sense SP-A probe and photographed with (A) brightfield and (B) darkfield illumination. Original magnification x 160.

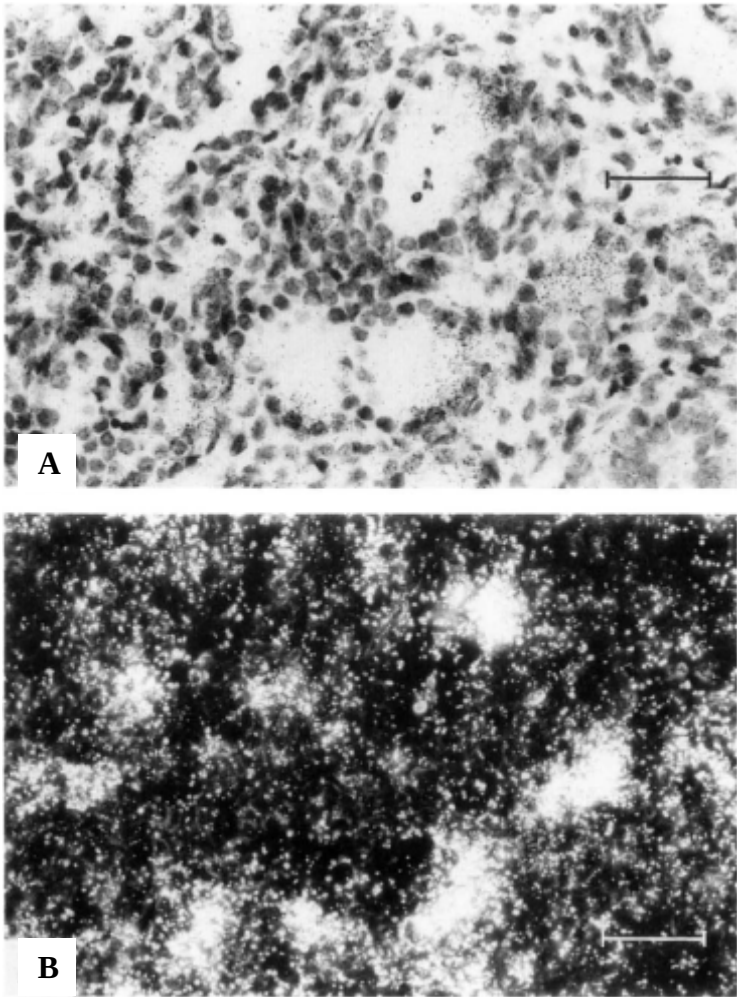

Figure 15. SP-A mRNA-containing cells in terminal airways of a 19-week fetus. Lung tissue was hybridized in situ to an anti-sense SP-A probe and photographed with (A) brightfield and (B) darkfield illumination. Original magnification x 320.

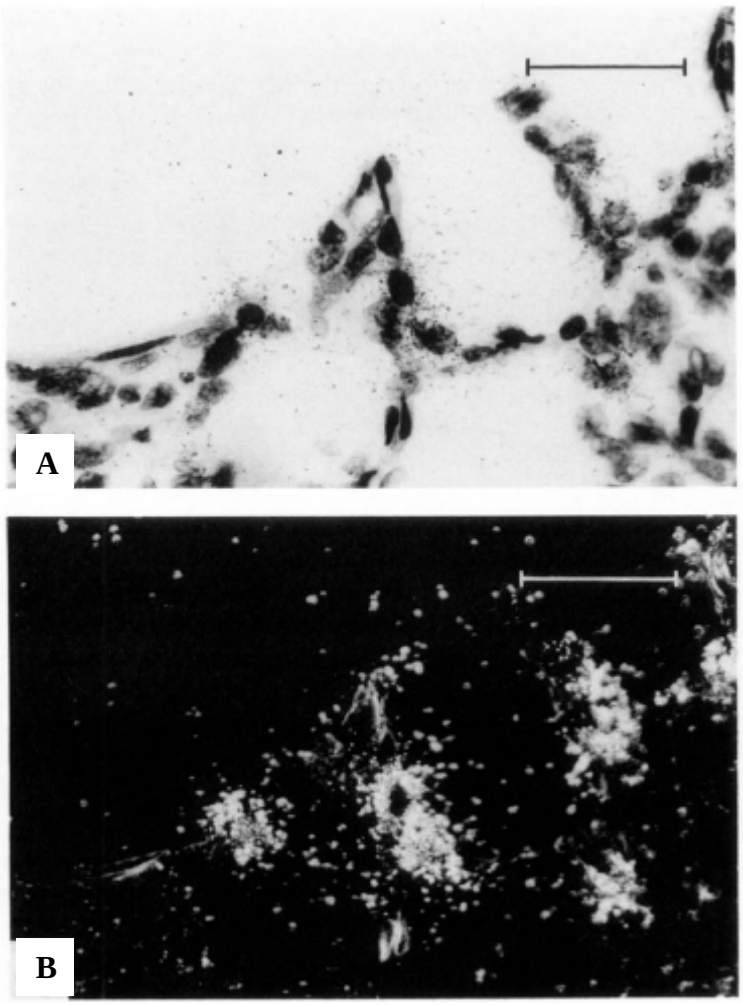

Figure 16. SP-A mRNA in Type II cells in the lung of a term infant. The infant was born at 40 weeks' gestation and died from non-pulmonary causes. Lung tissue was hybridized in situ to an anti-sense SP-A probe and photographed with (A) brightfield and (B) darkfield illumination. Original magnification x 510.

5.2. Expression of pro-SP-B and SP-B mRNA in the developing lung

Immunohistochemistry and in situ hybridization were used to determine the expression of pro-SP-B and SP-B mRNA in the developing lung [51]. Temporal and spatial distribution of pro-SP-B and SP-B mRNA is shown in **Tables 8 and 9** and **Figures 17 and 18**. Pro-SP-B and SP-B mRNA were detected in bronchi and broncbioles by 15 weeks of gestation. After 25 weeks, pro-SP-B and SP-B mRNA were co-localized in Clara cells, cells of the bronchioloalveolar portals, and Type II cells.

Table 8. SP-B mRNA and Immunoreactive Precursor in Fetuses

Gestational age (wk)	Postnatal age	Trachea				Bronchi				Ciliated bronchioles		Cells lining terminal airways	
		Epithelium		Glands		Epithelium		Glands					
		IS	H	IS	H	IS	H	IS	H	IS	H	IS	H
10		–	P	–	0	–	P	–	0	–	P	–	P
11		na	na	na	na	na	0	na	0	na	P	na	P
12		na	na	na	na	na	0	na	0	na	P	na	+
12		–	P	0	0	–	P	0	0	–	P	–	P
13		–	P	–	–	–	0	–	0	–	P	–	+
14		na	na	na	na	0	0	0	0	–	P	–	P
14		na	na	na	na	na	P	na	–	na	P	na	+
14		na	na	na	na	na	0	na	0	na	P	na	P
15		na	P	–	–	na	0	na	0	na	+	na	+
15		na	na	na	na	+	0	0	0	–	P	–	+
16		na	P	na	–	+	+	–	–	+	P	+	+
16		–	+	–	–	+	P	–	0	+	P	+	P
16		–	–	–	–	0	+	0	0	+	P	+	+
17		na	–	na	–	+	P	0	0	+	P	+	+
17		na	na	na	na	0	0	0	0	+	+	+	+
18		–	–	–	–	+	+	–	–	+	+	+	+
18		–	+	–	+	+	+	–	+	–	+	–	+
18		na	na	na	na	na	0	na	0	na	+	na	+
19	SB	–	+	–	+	0	0	0	0	+	+	+	+
19	7 hr	–	+	–	+	0	+	0	–	+	+	+	+
20	1 hr	na	+	na	–	na	+	na	–	–	+	na	+
20	SB	–	–	–	–	0	+	0	–	+	+	+	+
20	SB	na	na	na	na	0	0	0	0	+	+	+	+
20	1 hr	na	na	na	na	na	0	na	0	na	+	na	+
20	SB	–	+	–	+	+	P	–	0	+	+	+	+
20	SB	na	na	na	na	0	+	na	0	na	+	na	+
20	SB	na	na	na	na	na	+	na	0	na	P	na	P
21	SB	na	na	na	na	+	+	–	0	+	+	+	+
21	SB	na	na	na	na	na	+	na	0	na	0	na	+
22	1.5 hr	–	–	–	–	0	+	0	–	+	+	+	+
22	0.5 hr	na	+	na	+	+	+	–	0	+	+	+	+
22	SB	na	+	na	–	na	+	na	+	na	+	na	+
22	1 hr	na	na	na	na	na	0	na	0	na	+	na	+
23	SB	–	+	–	+	+	+	–	–	+	+	+	+
23	SB	na	na	na	na	0	+	0	0	+	+	+	+
23	2 hr	na	na	na	na	+	+	–	–	+	+	+	+
23	2 hr	na	na	na	na	+	+	–	–	+	+	+	+
23	2.7 hr	na	na	na	na	+	+	0	0	+	+	+	+

IS, in situ hybridization; H, immunohistochemistry; P, peripheral staining; SB, stillborn; 0, structure not present in section; na, not available.

Table 9. SP-B mRNA and Immunoreactive Precursor in Neonates

Gestational age (wk)	Postnatal age	Trachea				Bronchi				Ciliated bronchioles		Respiratory bronchioles and B-A portals		Mature type II cells	
		Epithelium		Glands		Epithelium		Glands							
		IS	H	IS	H	IS	H	IS	H	IS	H	IS	H	IS	H
25	15 min	na	na	na	na	na	0	na	0	na	+	na	+	na	+
36	1.5 hr	na	na	na	na	+	+	–	+	+	+	+	+	+	+
37	1 day	na	na	na	na	na	0	na	0	na	+	na	+	na	+
38	24 hr	na	na	na	na	na	+	na	0	na	+	na	+	na	+
38	90 hr	na	na	na	na	na	+	na	+	na	+	na	+	na	+
40	10 hr	na	na	na	na	+	+	0	–	+	+	+	+	+	+
40	10 days	–	–	–	–	+	+	–	–	+	+	+	+	+	+
42	12 days	–	–	–	–	+	+	0	+	+	+	+	+	+	+

IS, in situ hybridization; H, immunohistochemistry: 0, structure not present in section; na, not available.

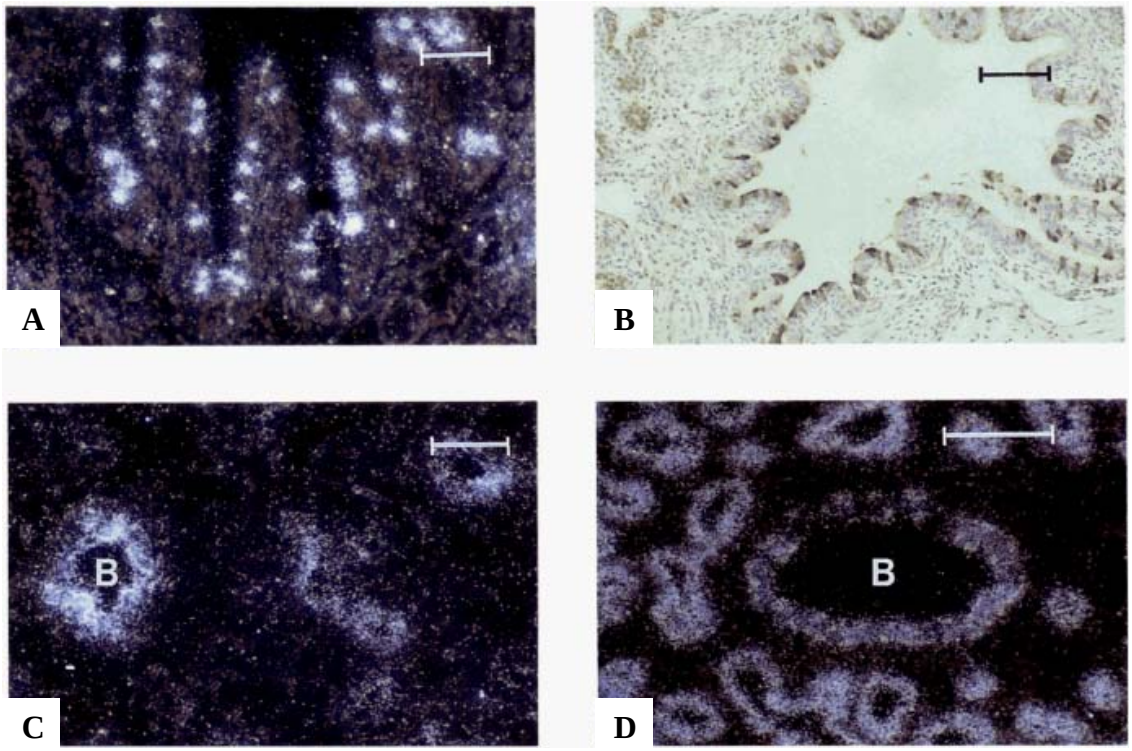

Figure 17. (A) SP-B mRNA is seen in scattered bronchial epithelial cells. Lung tissue from a fetus of 23 weeks' gestation hybridized in situ to an anti-sense SP-B probe and photographed with darkfield illumination. Original magnification x 90. (B) Bronchus from the lung of a fetus of 22 weeks' gestation immunostained for pro-SP-B. Non-ciliated cells in the bronchial epithelium are immunolabeled, as well as cells lining terminal airways. Immunoperoxidase and hematoxylin. Original magnification x 100. (C) SP-B mRNA is detected in terminal airways and the bronchiolar epithelium. Lung of a fetus of 16 weeks' gestation hybridized in situ to an antisense SP-B probe and photographed with darkfield illumination. B, bronchiole. Original magnification x 110. (D) Lung of a fetus of 22 weeks' gestation hybridized in situ to an anti-sense SP-B probe and photographed with darkfield illumination. SP-B mRNA is expressed in both bronchiolar and terminal airway lining cells. B, bronchiole. Original magnification x 150.

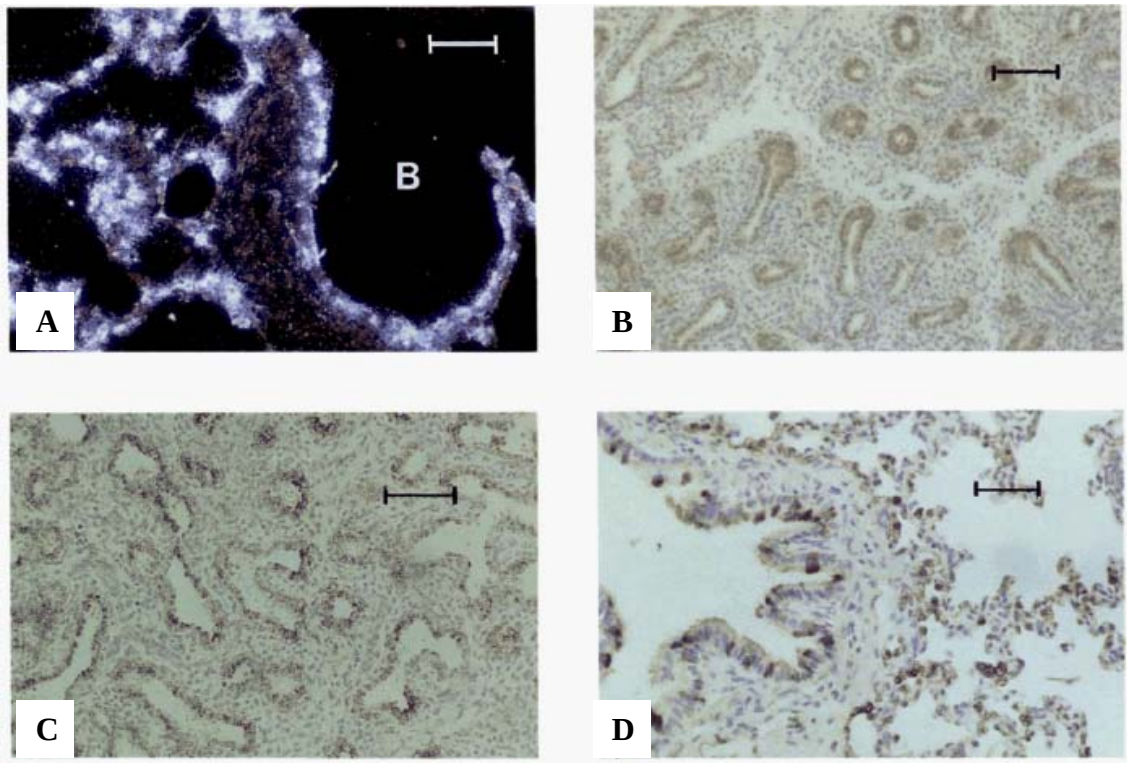

Figure 18. (A) SP-B mRNA is localized in alveolar Type II cells and in bronchiolar epithelial cells, including those of the bronchiolo-alveolar portal. Lung of an infant of 40 weeks' gestation hybridized in situ to an anti-sense SP-B probe and photographed with darkfield illumination. B, bronchiole. Original magnification x 90. (B) Lung of a fetus of 18 weeks'gestation immunostained for pro-SP-B. Immunolabeling is more intense in the distal airways. Immunoperoxidase and hematoxylin. Original magnification x 100. (C) Lung of a fetus of 20 weeks' gestation showing many terminal airways lined with cells immunostained for pro-SP-B. Immunoperoxidase and hematoxylin. Original magnification x 100. (D) Large bronchiole and terminal airways from the lung of a live-born infant of 36 weeks'gestation immunostained for pro-SP-B. There is immunolabeling of non-ciliated bronchiolar cells and of many Type II cells in the terminal airways. Immunoperoxidase and hematoxylin. Original magnification x 175.

5.3. Expression of pro-SP-C and SP-C mRNA in the developing lung

We also determined the temporal and spatial distribution of pro-SP-C and SP-C mRNA in fetal and neonatal lung [51]. The results are shown in **Tables 10 and 11** and **Figures 19 and 20**. Pro-SP-C and SP-C mRNA were detected in cells lining terminal airways from 15 weeks of gestation and thereafter. After 25 weeks, SP-C mRNA and pro-SP-C were detected in epithelial cells of the bronchiolo-alveolar portals and in Type II cells, where expression seemed to increase with advancing gestational age.

Table 10. SP-C mRNA and Immunoreactive Precursor in Fetuses

Gestational age (wk)	Postnatal age	Trachea				Bronchi				Ciliated bronchioles		Cells lining terminal airways	
		Epithelium		Glands		Epithelium		Glands					
		IS	H	IS	H	IS	H	IS	H	IS	H	IS	H
10		–	–	0	–	–	–	0	–	–	P	–	P
11		na	na	na	na	na	0	na	0	na	–	na	–
12		na	na	na	na	na	P	na	0	na	P	na	P
12		–	P	0	0	–	–	0	0	–	P	–	P
13		–	–	–	–	–	0	–	0	–	–	–	–
14		na	na	na	na	0	0	0	0	–	P	–	–
14		na	na	na	na	na	P	na	–	na	P	na	P
14		na	na	na	na	na	0	na	0	na	–	na	–
15		na	–	na	–	na	P	na	0	na	P	na	P
15		na	na	na	na	–	0	0	0	–	–	+	P
16		na	+	na	–	–	–	–	–	–	P	+	P
16		–	–	–	–	–	–	–	0	–	–	+	–
16		–	–	–	–	0	0	0	0	–	–	+	–
17		na	–	na	–	–	–	0	–	–	–	+	–
17		na	na	na	na	0	–	0	–	–	–	+	P
18		–	–	–	–	–	–	–	–	–	–	+	P
18		–	–	–	–	–	–	–	–	–	–	+	P
18		na	na	na	na	na	0	na	0	na	P	na	P
19	SB	–	+	–	+	0	0	0	0	–	P	+	P
19	0.7 hr	–	–	–	–	0	–	0	0	–	–	+	–
20	1 hr	na	–	na	+	na	–	na	+	na	–	na	+
20	SB	–	+	–	+	0	–	0	0	–	–	+	+
20	SB	na	na	na	na	0	0	0	0	–	+	+	+
20	1 hr	na	na	na	na	na	0	na	0	na	–	na	–
20	SB	–	–	–	–	–	0	–	0	–	–	+	P
20	SB	na	na	na	na	na	–	na	–	na	–	na	+
20	SB	na	na	na	na	na	P	na	0	na	P	na	+
21	SB	na	na	na	na	–	–	–	–	–	–	+	P
21	SB	na	na	na	na	na	0	na	0	na	–	na	–
22	1.5 hr	–	–	–	–	0	–	0	–	–	–	+	+
22	0.5 hr	na	na	na	na	–	P	–	–	–	P	+	+
22	SB	na	–	na	+	na	–	na	+	na	–	na	+
22	1 hr	na	na	na	na	0	0	0	0	–	–	+	+
23	SB	–	–	–	+	–	+	–	+	–	–	+	+
23	SB	na	na	na	na	0	0	0	0	–	–	+	+
23	2 hr	na	na	na	na	–	–	–	–	–	–	+	+
23	2 hr	na	na	na	na	–	–	–	–	–	–	+	–
23	2.7 hr	na	na	na	na	–	–	0	0	–	–	+	+

IS, in situ hybridization; H, immunohistochemistry; P, peripheral staining; SB, stillborn; 0, structure not present in section; na, not available.

Table 11. SP-C mRNA and Immunoreactive Precursor in Neonates

Gestational age (wk)	Postnatal age	Trachea				Bronchi				Ciliated bronchioles		Respiratory bronchioles and B-A portals		Mature type II cells	
		Epithelium		Glands		Epithelium		Glands							
		IS	H	IS	H	IS	H	IS	H	IS	H	IS	H	IS	H
25	15 min	na	na	na	na	na	0	na	0	na	–	na	+	na	+
36	1.5 hr	na	na	na	na	–	–	–	–	–	–	+	+	+	+
37	1 day	na	na	na	na	na	–	na	–	na	–	na	–	na	+
38	24 hr	na	na	na	na	na	–	na	0	na	–	na	–	na	+
38	90 hr	na	na	na	na	na	+	na	+	na	–	na	+	na	+
40	10 hr	na	na	na	na	–	0	0	0	–	–	+	+	+	+
40	10 days	–	–	–	–	–	–	–	–	–	–	+	+	+	+
42	12 days	na	na	na	na	–	+	–	+	–	–	+	+	+	+

IS, in situ hybridization; 0, structure not present in section; H, immunohistochemistry; no stained cells identified; na, not available.

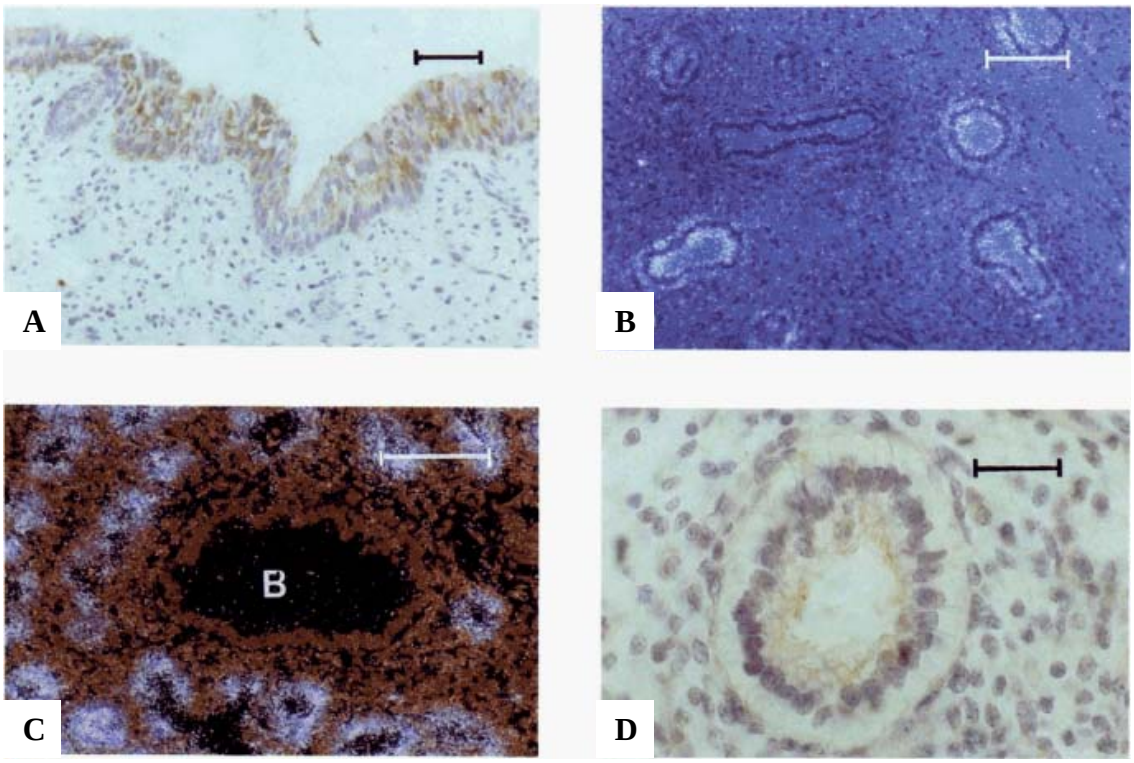

Figure 19. (A) Trachea from a fetus of 16 weeks' gestation immunostained for pro-SP-C. Scattered epithelial cells are immunolabeled. Immunoperoxidase and hematoxylin. Original magnification x 175. (B) Terminal airways from a 15-week fetus express SP-C mRNA. In situ hybridization, darkfield illumination. Original magnification x 110. (C) Lung from a 22-week fetus expresses SP-C mRNA in terminal airways, but not in the bronchiolar epithelium. In situ hybridization, darkfield illumination. Original magnification x 150. B, bronchiole. (D) A terminal airway of a 15-week fetus shows weak immunoreactivity for pro-SP-C. Immunoperoxidase and hematoxylin. Original magnification x 450.

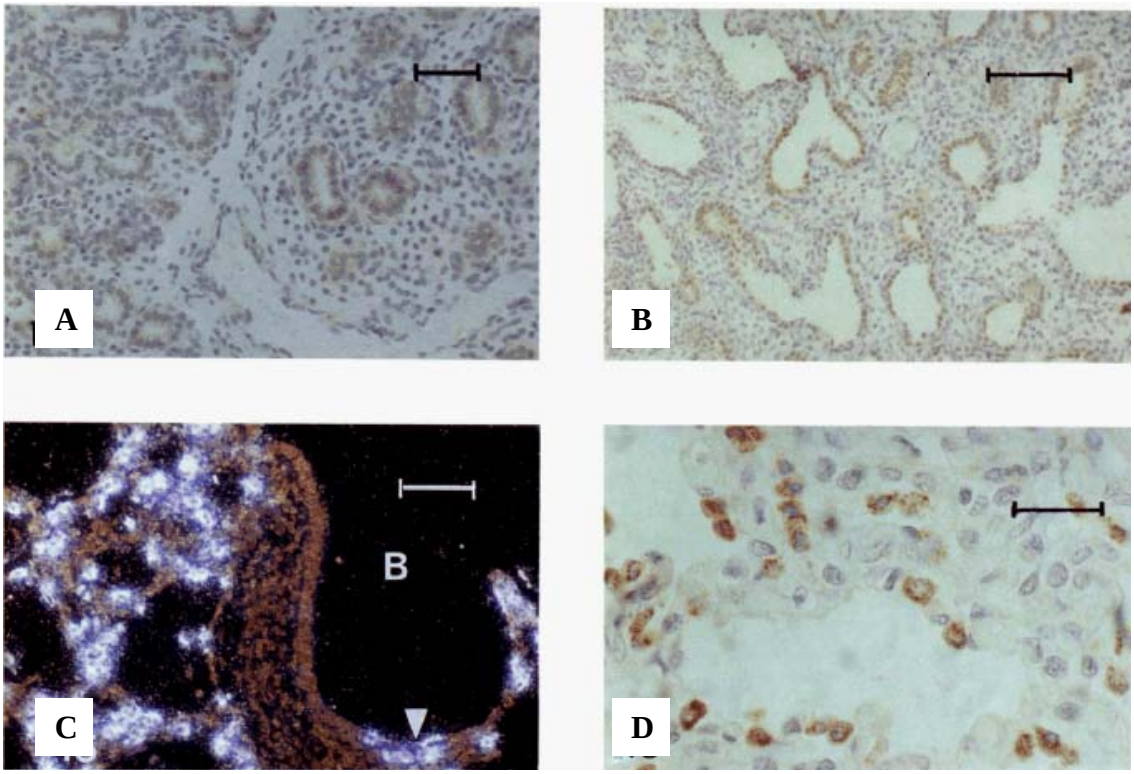

Figure 20. (A) Lung of a fetus of 20 weeks' gestation immunolabeled for pro-SP-C in lining epithelial cells of terminal airways. Immunoperoxidase and hematoxylin. Original magnification x 175. (B) Lung of a fetus of 23 weeks' gestation immunostained for pro-SP-C. Only epithelial cells of the most distal airways are immunolabeled. Immunoperoxidase and hematoxylin. Original magnification x 100. (C) SP-C mRNA is localized to alveolar Type II cells and cells of the bronchiolo-alveolar portal (arrowhead). B, bronchiole. Original magnification x 90. (D) Lung of a term gestation live-born infant immunostained for pro-SP-C. Type II cells in terminal airways are immunolabeled. Immunoperoxidase and hematoxylin. Original magnification x 450.

5.4. Expression of CCSP and CCSP mRNA in the developing lung

We have determined the temporal-spatial distribution of CCSP and its mRNA in the developing human lung and in neonatal lung disease, using immunohistochemistry and in situ hybridization [50]. The results are shown in **Tables 12-14** and **Figures 21-24**.

CCSP immunoreactivity was found in noncitiated bronchiolar epithelial cells from 12 weeks of gestation onward. Tracheal and bronchial epithelia showed positive immunoreactivity after 15 weeks and 14 weeks of gestation, respectively. CCSP mRNA was seen in the bronchial and bronchiolar epithelia from 16 weeks onward and was detected in the trachea from 19 through 23 weeks of gestation. CCSP immunoreactivity and mRNA were present in nonciliated single cells of bronchial and bronchiolar epithelia in fetuses and in infants with and without lung disease. CCSP and CCSP mRNA containing epithelial cells also formed clusters around neuroepithelial bodies, especially at airway branch points.

Table 12. CCSP mRNA and Immunoreactive CCSP in Fetuses

Gest age (weeks)	No. of cases	Tracheas				Bronchi				Bronchioles		NE cells	
		Epithelium		Glands		Epithelium		Glands					
		IS P/A	H P/A	IS P/A	H P/A	IS P/A	H P/A	IS P/A	H P/A	IS P/A	H P/A	C P/A	S P/A
10	2	0/0	0/0	0/0	0/0	0/0	0/0	0/0	0/0	0/0	1/2	1/2	0/2
12	2	0/1	1/1	0/0	0/0	0/1	1/1	0/0	0/0	0/1	2/2	2/2	0/2
13	1	0/1	1/1	0/1	0/0	0/0	0/0	0/0	0/0	0/1	1/1	1/1	0/1
14	3	0/0	0/0	0/0	0/0	0/0	1/1	0/0	0/0	0/1	3/3	3/3	0/3
15	2	0/0	1/1	0/0	0/0	0/1	1/1	0/1	0/0	0/1	2/2	2/2	0/2
16	3	0/2	2/3	0/2	1/3	3/3	3/3	0/2	0/0	3/3	3/3	3/3	0/3
17	2	0/0	1/1	0/0	0/1	1/1	1/1	0/0	0/0	1/1	2/2	2/2	0/2
18	3	0/1	1/1	0/1	1/1	2/2	2/2	0/2	0/0	2/2	3/3	3/3	2/3
19	2	2/2	2/2	0/2	2/2	1/1	1/1	0/0	0/0	2/2	2/2	2/2	1/2
20	9	2/2	2/2	0/2	1/2	1/1	2/2	0/1	0/0	3/3	9/9	7/9	5/9
21	1	0/0	0/0	0/0	0/0	1/1	0/0	0/1	0/0	1/1	1/1	1/1	1/1
22	6	0/0	1/2	0/0	0/2	2/2	3/3	0/1	1/1	3/3	6/6	6/6	4/6
23	5	1/1	1/1	0/1	1/1	4/5	1/1	1/3	1/1	5/5	5/5	5/5	5/5
Total	41	5/10 (50%)	13/15 (87%)	0/9 (0%)	6/12 (50%)	15/16 (94%)	16/16 (100%)	1/11 (9%)	2/2 (100%)	20/24 (83%)	40/40 (100%)	38/41 (93%)	18/41 (44%)

Gest age, gestational age; IS, in situ hybridization; H, immunohistochemistry; P, number of positive cases; A, number of available cases that contain the structure; C, crowns or clusters over neuroepithelial bodies; S, single epithelial cells.

Table 13. CCSP mRNA and Immunoreactive CCSP in Liveborn Infants Who Died of Nonpulmonary Causes

Gest age (weeks)	No. of cases	Bronchi: Epithelium IS P/A	Bronchi: Epithelium H P/A	Bronchi: Glands IS P/A	Bronchi: Glands H P/A	Bronchioles IS P/A	Bronchioles H P/A	NE cells C P/A	NE cells S P/A
25	1	0/0	0/0	0/0	0/0	0/0	1/1	1/1	1/1
27	1	0/0	0/0	0/0	0/0	0/0	1/1	0/1	1/1
29	1	0/0	0/0	0/0	0/0	0/0	1/1	1/1	1/1
36	2	1/1	2/2	0/1	1/2	1/1	2/2	2/2	2/2
37	1	0/0	0/0	0/0	0/0	0/0	1/1	1/1	1/1
38	2	0/0	2/2	0/0	1/1	0/0	2/2	2/2	2/2
40	4	2/2	4/4	0/0	1/1	2/2	4/4	3/4	4/4
42	1	1/1	1/1	0/0	0/0	1/1	1/1	1/1	1/1
Total	13	4/4 (100%)	9/9 (100%)	0/1 (0%)	3/4 (75%)	4/4 (100%)	13/13 (100%)	11/13 (85%)	13/13 (100%)

Gest age, gestational age; IS, in situ hybridization; H, immunohistochemistry; P, number of positive cases; A, number of available cases that contain the structure; C, crowns or clusters over neuroepithelial bodies; S, single epithelial cells.

Table 14. CCSP mRNA and Immunoreactive CCSP in Infants with HMD and BPD

Disease	No. of cases	Bronchi: Epithelium IS P/A	Bronchi: Epithelium H P/A	Bronchi: Glands IS P/A	Bronchi: Glands H P/A	Bronchioles IS P/A	Bronchioles H P/A	NE cells C P/A	NE cells S P/A
HMD, ≤2 days	23	5/9 (56%)	4/4 (100%)	0/9 (0%)	1/1 (100%)	5/9 (56%)	20/23 (87%)	2/23 (9%)	20/23 (87%)
Regenerating HMD	15	3/4 (75%)	8/10 (80%)	0/4 (0%)	2/4 (50%)	3/5 (60%)	13/15 (87%)	1/15 (7%)	13/15 (87%)
Early BPD	15	4/6 (67%)	3/5 (60%)	1/7 (14%)	5/7 (71%)	7/9 (78%)	11/15 (73%)	5/15 (33%)	11/15 (74%)
Late BPD	9	4/4 (100%)	3/3 (100%)	3/3 (100%)	0/0	4/4 (100%)	9/9 (100%)	7/9 (78%)	9/9 (100%)

Gest age, gestational age; IS, in situ hybridization; H, immunohistochemistry; P, number of positive cases; A, number of available cases that contain the structure; C, crowns or clusters over neuroepithelial bodies; S, single epithelial cells.

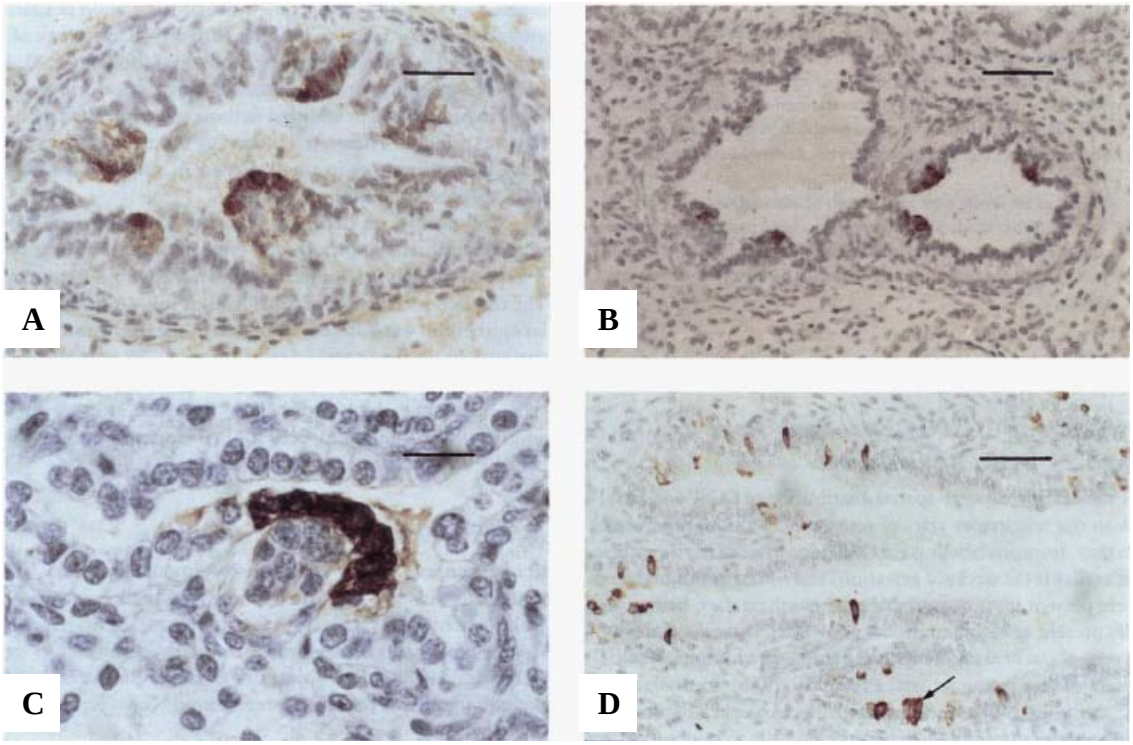

Figure 21. (A) Bronchiole from a fetus of 12 weeks' gestation immunostained for CCSP. Epithelial lining cells surrounding neuroendocrine bodies (NEBs) are immunolabeled. Original magnification x 280. (B) Bronchiole from a fetus of 14 weeks' gestation immunostained for CCSP. NEBs are associated with "crowns" of immunolabeled epithelial lining cells. Original magnification x 180. (C) Small branching bronchiole from a fetus of 18 weeks' gestation immunostained for CCSP. The luminal surface of an egg shaped NEB at a branch point is covered by a "crown" of immunolabeled cuboidal cells. Original magnification x 550. (D) Branching bronchiole from a fetus of 20 weeks' gestation immunostained for CCSP. Many single columnar epithelial cells are immunolabeled. A probable NEB is associated with a small cluster of immunolabeled cells (arrow). Original magnification x 180.

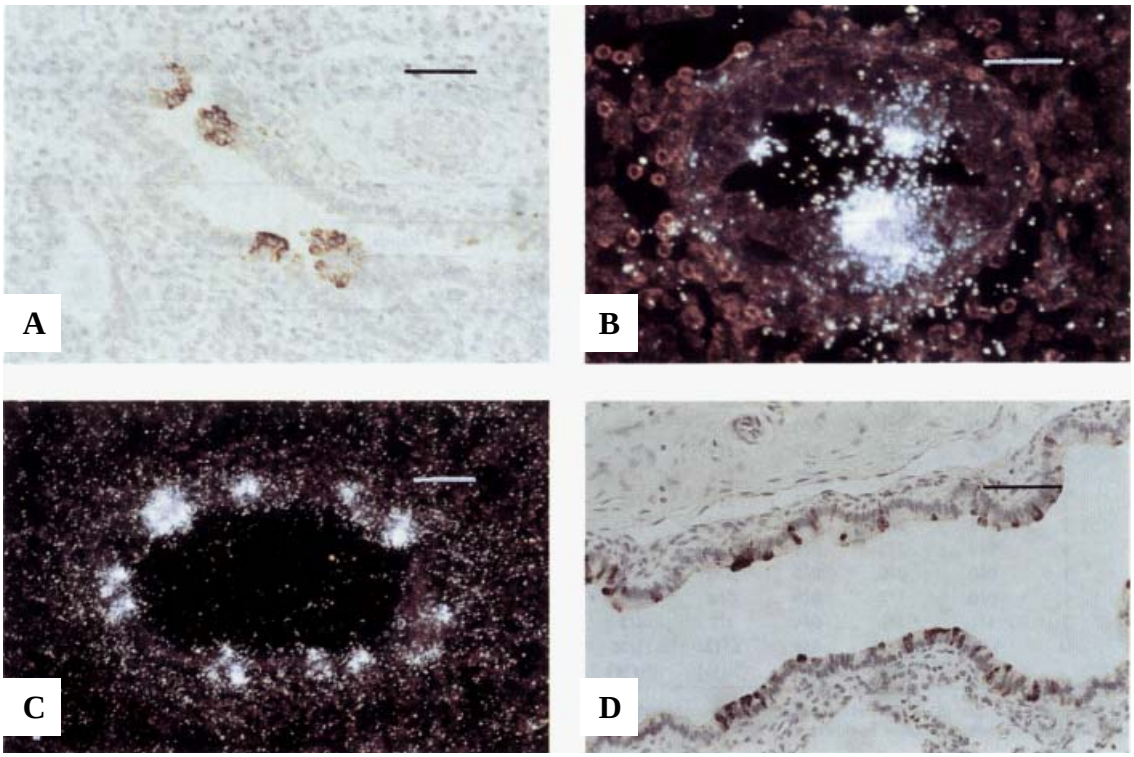

Figure 22. (A) Bronchiole from the lung of the same fetus shown in Figure 21D, immunostained for CCSP. Four NEB, some of which are at branch points, are surrounded by immundabeled epithelial lining cells. Original magnification x 180. (B) Bronchiole from the lung of a fetus of 16 weeks' gestation hybridized in situ to an antisense CCSP probe and photographed with darkfield illumination. CCSP mRNA is expressed in association with NEBs. Original magnification x 440. (C) Bronchiole from the lung of a fetus of 22 weeks' gestation hybridized in situ to an antisense CCSP probe and photographed with darkfield illumination. CCSP mRNA is expressed in scattered epithelial lining cells and in clusters associated with NEBs. Original magnification x 120. (D) Bronchiole from the lung of a newborn infant of 36 weeks' gestation immunostained for CCSP. Many single cells are immunolabeled as well as dusters associated with NEBs. Original magnification x 175.

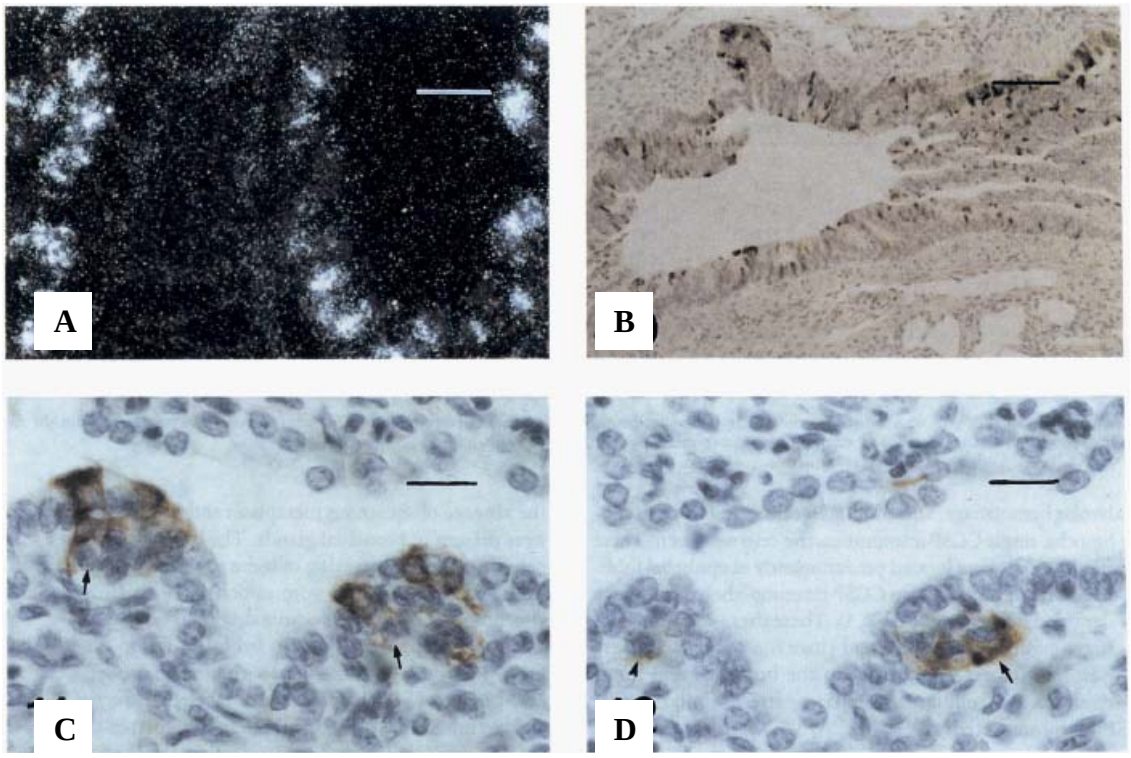

Figure 23. (A) Bronchiole from the lung of an infant of 40 weeks' gestation who survived for 10 days. CCSP mRNA is expressed in many epithelial lining cells. Original magnification x 960. (B) Section of lung taken from an infant of 26 weeks' gestation subjected to lobectomy at 30 postnatal days for lobar emphysema, immunostained for CCSP. Many single epithelial lining cells and a few clusters are immunoreactive. Original magnification x 180. (C) Cuboidal cell-lined bronchiole from the lung of a fetus of 23 weeks' gestation immunostained for CCSP. There are two NEBs at branch points (arrows), which are associated with immunolabeled epithelial lining. Original magnification x 540. (D) Adjacent section of the same lung as seen in (C), immunostained for bombesin. One of the NEBs is immunolabeled for bombesin (arrow). The second NEB shows only a trace of bombesin (arrowhead). Original magnification x 540.

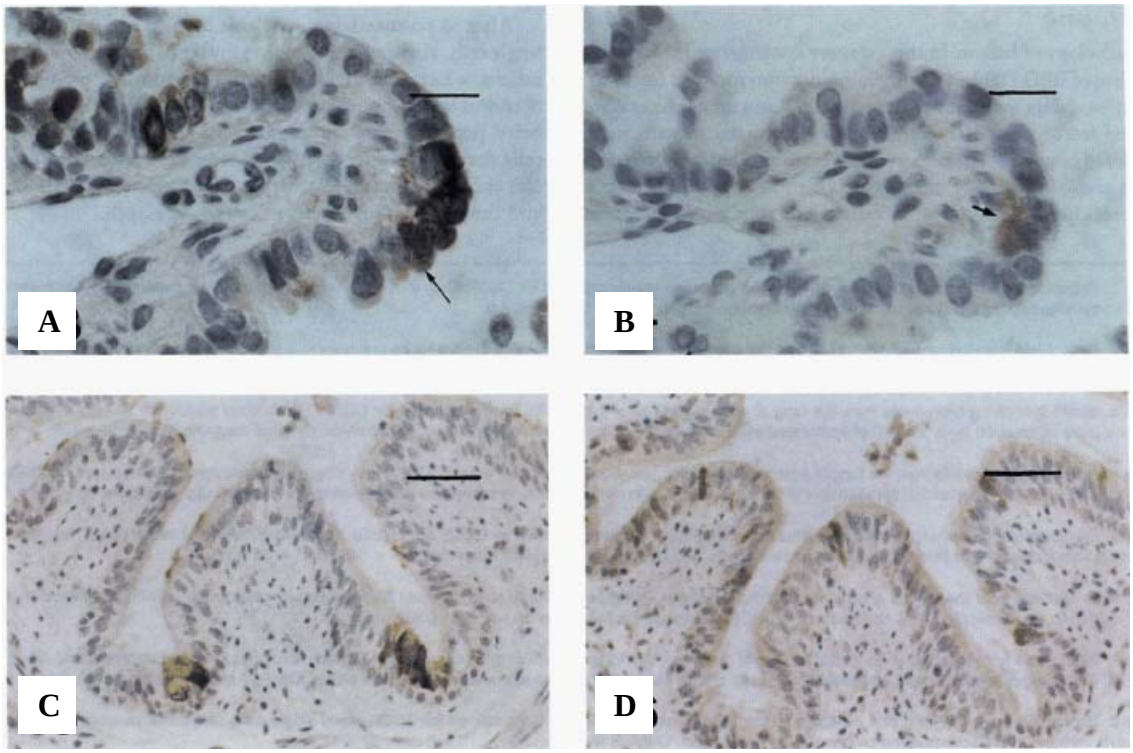

Figure 24. (A) Lung from an infant of 31 weeks' gestation who had a lobectomy at 28 postnatal days is immunostained for CCSP. Immunolabeled cuboidal cells bordering the lumen at a branch point (arrow) overlie a NEB. Isolated single cells are also seen. Immunoperoxidase and hematoxylin. Original magnification x 540. (B) Adjacent serial section of the same lung as seen in Figure A immunostained for calcitonin gene-related peptide (CGRP). The same NEB seen in Figure A is immunolabeled for CGRP (arrow). Immunoperoxidase and hematoxylin. Original magnification x 540. (C) Bronchiole from the lung of a fetus of 23 weeks' gestation immunostained for CCSP. There are clusters of immunolabeled epithelial cells flanking the depths of two deep folds. Immunoperoxidase and hematoxylin. Original magnifiation x 240. (D) Adjacent serial section from the same lung as seen in (C), immunostained for pro-SP-B. Immunolabeled columnar epithelial lining cells are scattered over the surface of folds but are not seen in the flanking regions in the depths of folds. Immunoperoxidase and hematoxylin. Original magnification x 240.

5.5. Differential expression of pro-SP-B and SP-B mRNA in NSCLCs and non-pulmonary adenocarcinomas

Immunostaining for pro-SP-B was evaluated in 35 NSCLCs and 15 nonpulmonary adenocarcinomas [53]. In the non-neoplastic lung, pro-SP-B immunoreactivity was detected in normal and hyperplastic alveolar Type II cells and in some nonciliated bronchiolar epithelial cells. Sixty percent of pulmonary adenocarcinomas showed strong cytoplasmic immunoreactivity for pro-SP-B (**Table 15** and **Figure 25**). In three

cases, staining was diffuse, involving more than 50% of the tumor cells. In the remaining six cases, staining was focal, involving 10 to 50% of the tumor cells. Expression was seen in carcinomas with acinar, papillary, bronchioloalveolar, and solid growth patterns. Squamous cell and large cell carcinomas of the lung did not stain with the pro-SP-B antibody. Adenocarcinomas from other sites, including the colon, prostate, stomach, and esophagus, were also devoid of staining. The sensitivity and specificity of pro-SP-B for adenocarcinomas of the lung were 60% and 100%, respectively.

The same 35 SCLCs and 15 nonpulmonary adenocarcinomas were used for in situ hybridization [53]. In the non-neoplastic lung tissue, in situ hybridization signal was detected in normal and hyperplastic Type II cells and in scattered bronchiolar epithelial cells. Approximately 53% of the pulmonary adenocarcinomas contained SP-B mRNA (**Table 15** and **Figure 26**). The distribution of SP-B mRNA in these tumors was similar to that of pro-SP-B. Similarly to pro-SP-B, SP-B mRNA was detected in adenocarcinomas with acinar, papillary, bronchioloalveolar, and solid growth patterns. Squamous cell and large cell carcinomas of the lung and nonpulmonary adenocarcinomas were devoid of any in situ hybridization signal. The sensitivity and specificity of SP-B mRNA signal for adenocarcinoma of the lung were 53% and 100%, respectively.

Table 15. Pro-SP-B and SP-B mRNA in Carcinomas of the Lung and Non-Pulmonary Adenocarcinomas

Tumor type	Pro-SP-B positive	SP-B mRNA positive
Adenocarcinoma of lung (n=15)	9 (60%)	8 (53%)
Acinar (n=6)	4 (67%)	4 (67%)
Papillary (n=4)	2 (50%)	1 (25%)
Bronchioloalveolar (n=2)	2 (100%)	2 (100%)
Solid (n=3)	1 (33%)	1 (33%)
Squamous cell carcinoma of lung (n=15)	0	0
Large cell carcinoma of lung (n=5)	0	0
Non-pulmonary adenocarcinoma (n=15)	0	0

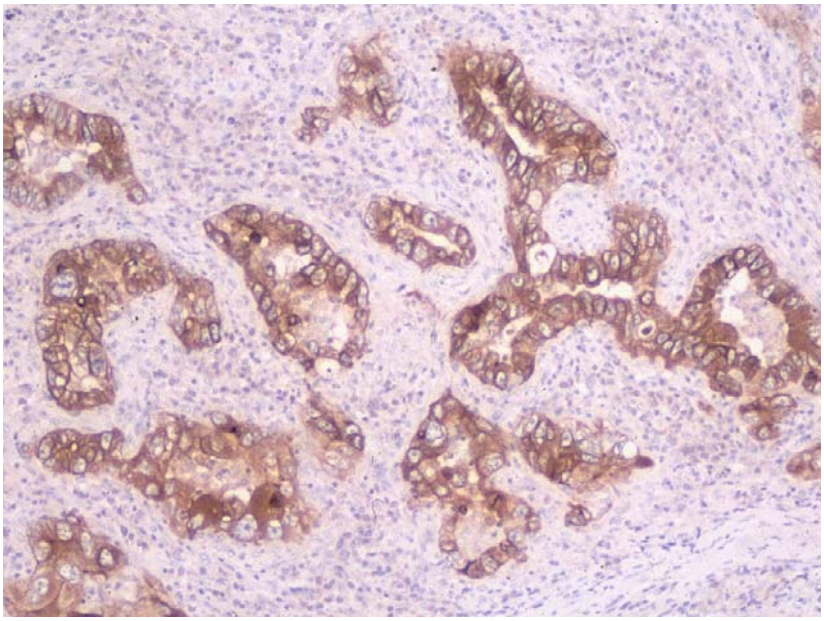

Figure 25. Pro-SP-B immunoreactivity in adenocarcinoma of the lung with acinar growth pattern (biotin-streptavidin technique with DAB chromogen; original magnification, 175X).

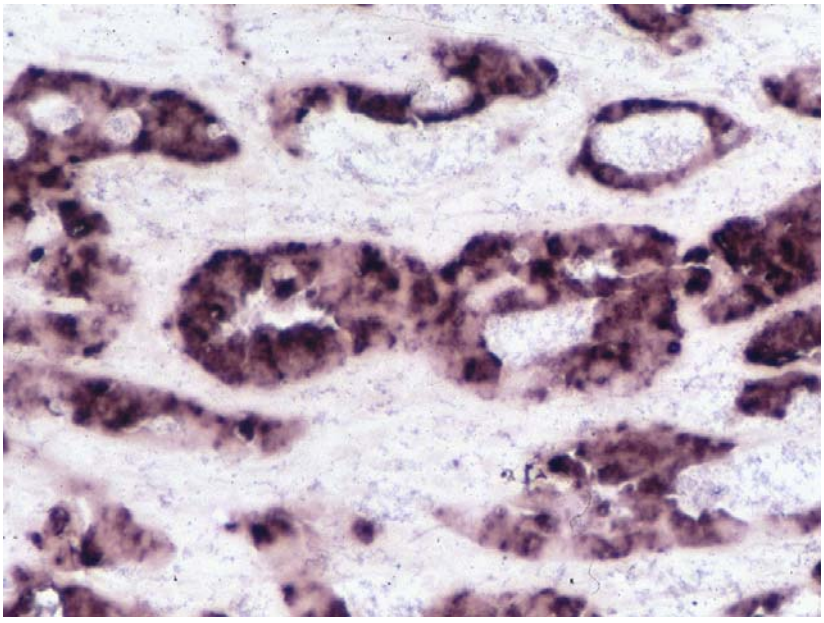

Figure 26. SP-B mRNA in pulmonary adenocarcinoma with acinar growth pattern (nonradioactive in situ hybridization with nitroblue tetrazolium chromogen; original magnification, 175x).

5.6. The utility of pro-SP-B and TTF-1 in differentiating adenocarcinoma of the lung from malignant mesothelioma

Only cytoplasmic staining was considered positive for pro-SP-B. Immunoreactive pro-SP-B was detected in 57% of adenocarcinomas and 20% of large cell carcinomas (**Table 16**) [54]. Immunoreactivity was seen in all subtypes of adenocarcinoma, including acinar, papillary, bronchioloalveolar, and solid (**Figure 27**). Squamous cell carcinomas and malignant mesotheliomas were uniformly negative. The sensitivity and specificity of pro-SP-B for adenocarcinoma of the lung versus malignant mesothelioma were 57% and 100%, respectively.

Only nuclear staining was considered positive for TTF-1. Seventy-six percent of adenocarcinomas and 26% of large cell carcinomas were reactive (**Table 16**) [54]. Immunoreactivity was seen in all subtypes of adenocarcinoma, including acinar, papillary, bronchioloalveolar, and solid (**Figure 28**). Squamous cell carcinomas and malignant mesotheliomas were uniformly negative. The sensitivity and specificity of TTF-1 for adenocarcinoma of the lung versus malignant mesothelioma were 76% and 100%, respectively.

Table 16. Pro-SP-B and TTF-1 in Carcinomas of the Lung and Malignant Mesothelioma

Tumor type	pro-SP-B	TTF-1	TTF-1 or pro-SP-B
Adenocarcinoma (n=208)	119 (57%)	158 (76%)	164 (79%)
Acinar (n=110)	65 (59%)	86 (78%)	89 (81%)
Papillary (n=32)	25 (78%)	27 (84%)	28 (88%)
Bronchioloalveolar (n=29)	21 (72%)	25 (86%)	26 (90%)
Solid (n=37)	8 (22%)	20 (54%)	21 (57%)
Large cell carcinoma (n=61)	12 (20%)	16 (26%)	17 (28%)
Squamous cell carcinoma (n=101)	0	0	0
Malignant mesothelioma (n=95)	0	0	0

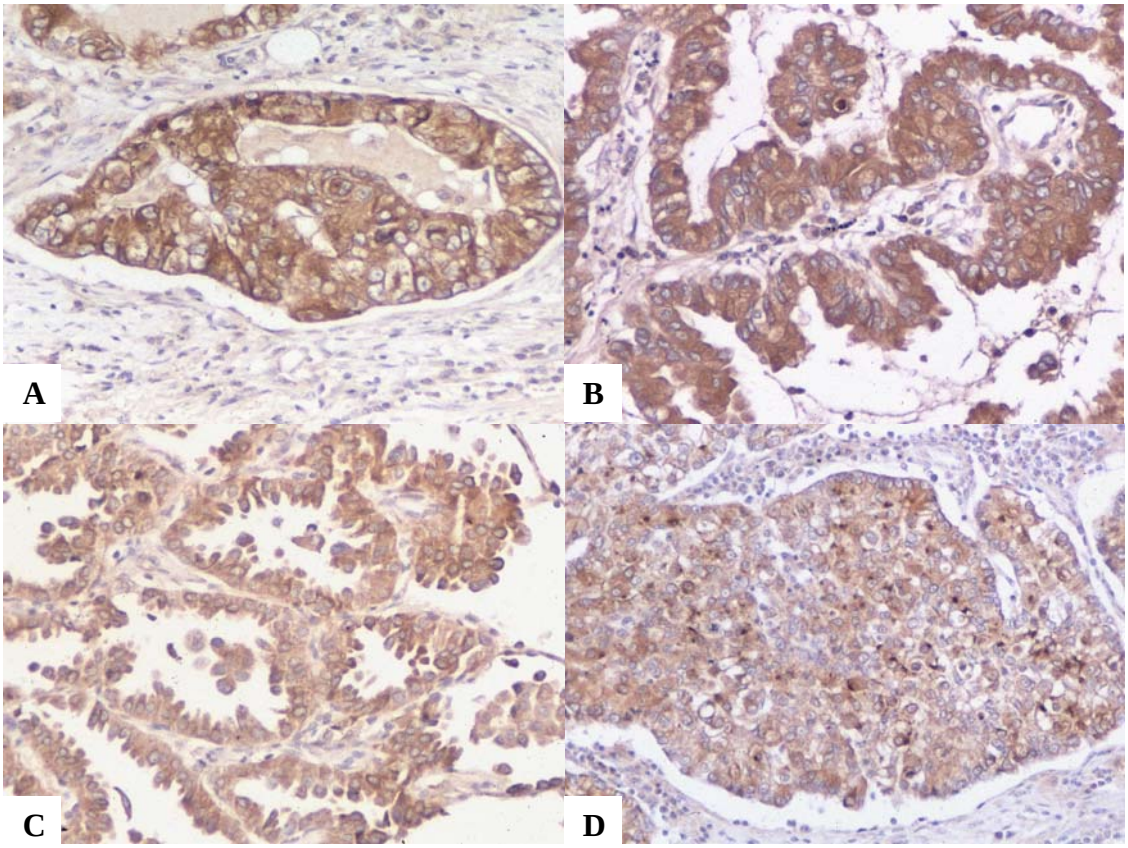

Figure 27. Pro-SP-B immunoreactivity in adenocarcinomas of the lung with different growth patterns. The staining is cytoplasmic (biotin-streptavidin technique, DAB chromogen, and hematoxylin counterstain). (A) Acinar; (B) Papillary; (C) Bronchioloalveolar; (D) Solid.

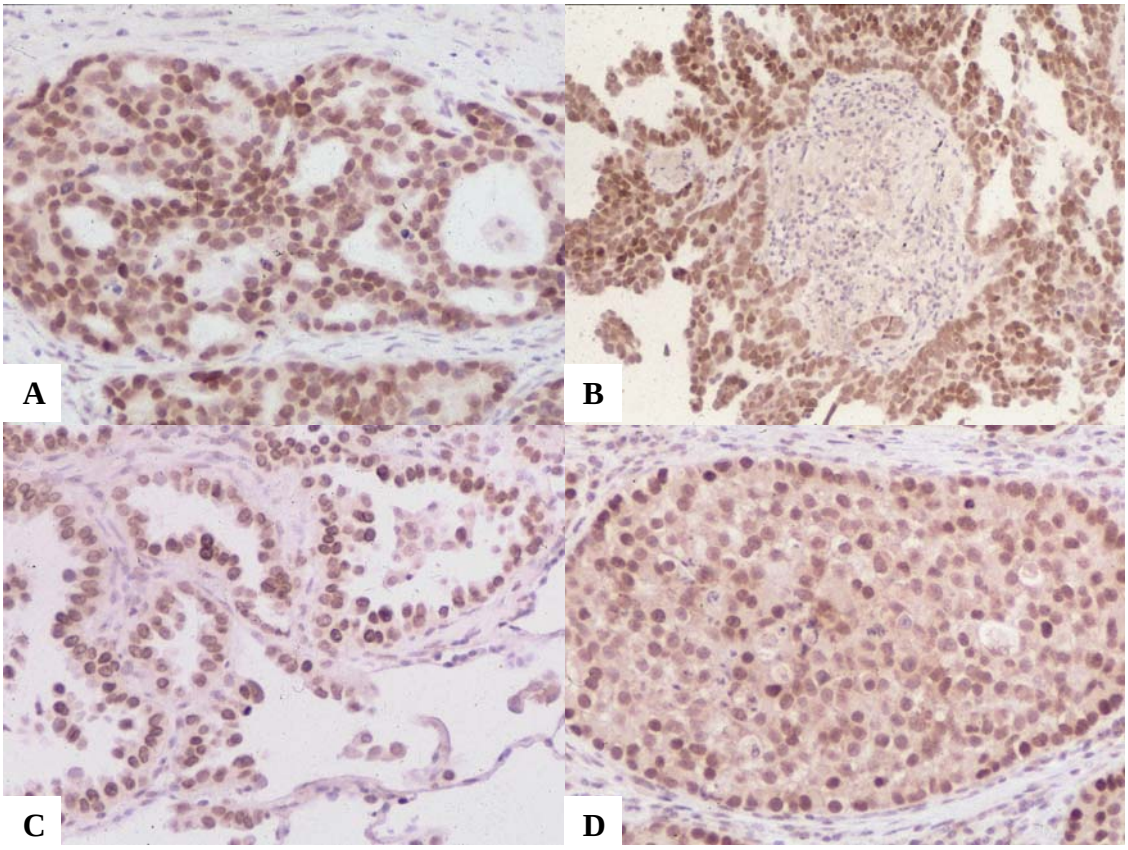

Figure 28. TTF-1 immunoreactivity in adenocarcinomas of the lung with different growth patterns. The staining is nuclear (biotin-streptavidin technique, DAB chromogen, and hematoxylin counterstain). (A) Acinar; (B) Papillary; (C) Bronchioloalveolar; (D) Solid.

5.7. The prognostic value of pro-SP-B and TTF-1 in early stage adenocarcinoma of the lung

Pro-SP-B immunoreactivity was correlated with clinical data in 204 cases of pulmonary adenocarcinoma [82]. One-hundred and eighteen of the 204 cases were positive for pro-SP-B (58%). Actuarial cumulative survival curves for 172 cases of stage I and II adenocarcinomas demonstrated a significantly longer survival period for patients with pro-SP-B positive tumors versus negative tumors (p=0.0310) (**Figure 29**).

TTF-1 immunoreactivity was correlated with clinical data in 189 cases of pulmonary adenocarcinoma [83]. Immunoreactive TTF-1 was present in 145 adenocarcinomas (77%). Survival curves for 160 cases of stage I and II tumors demonstrated a significantly longer survival period for patients with TTF-1 positive tumors versus negative tumors (p=0.0001) (**Figure 30**).

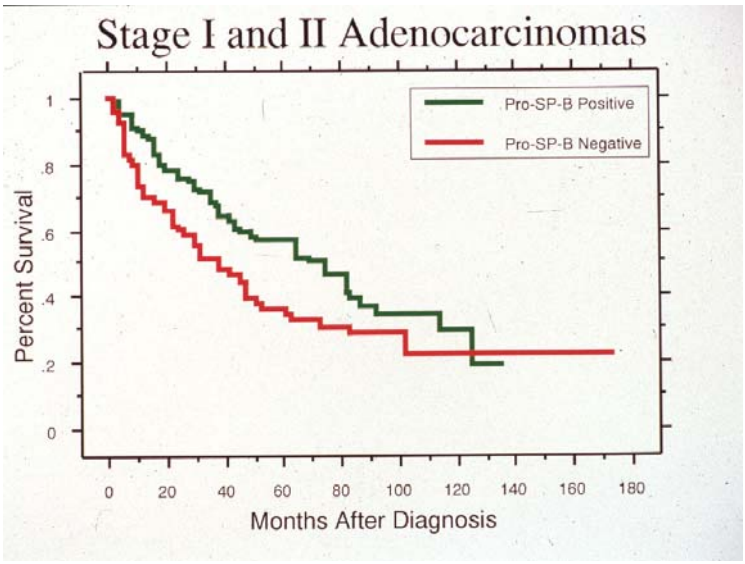

Figure 29. Actuarial cumulative survival curves for 172 patients with stage I and II adenocarcinoma. There is significantly longer survival for patients with pro-SP-B positive tumors versus negative tumors (p=0.0310).

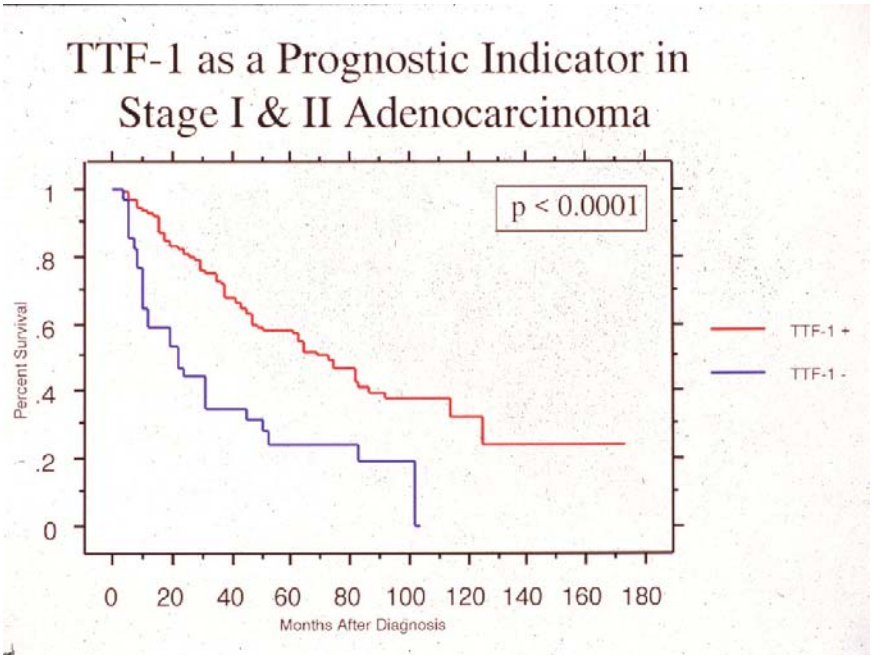

Figure 30. Survival curves for 160 cases of stage I and II pulmonary adenocarcinomas. There is significantly longer survival for patients with TTF-1 positive tumors versus negative tumors (p=0.0001).

5.8. The utility of TTF-1, Cdx2, CK7 and CK20 in determining the primary site for adenocarcinomas metastatic to the brain

Expression of TTF-1, Cdx2, CK7, and CK20 in 38 adenocarcinomas metastatic to the brain and the performance of these immunohistochemical markers in identification of a primary site are summarized in **Tables 17 and 18** [55]. Although it was not a criterion for positivity, all positive cases contained at least 10% immunoreactive tumor cells. The characteristic staining patterns are shown in **Figures 31-33**. The brain parenchyma was devoid of immunostaining for all markers. Fifty-five percent of pulmonary adenocarcinomas expressed TTF-1, while none of the breast or gastrointestinal primaries did. Cdx2 was limited to 83% of gastrointestinal adenocarcinomas and no pulmonary or breast adenocarcinomas. As expected, 100% of pulmonary and breast adenocarcinomas expressed CK7, with only 1 gastrointestinal tumor showing positivity. The opposite pattern was demonstrated for CK20, with staining present in 83% of adenocarcinomas of gastrointestinal origin, 1 pulmonary primary, and no breast tumors.

Table 17. Expression of TTF-1, Cdx2, CK7 and CK20 in 38 Metastatic Adenocarcinomas to the Brain

	Lung (n=22)	Breast (n=10)	GI (n=6)
TTF-1+	12 (55%)	0	0
CDX2	0	0	5 (83%)
CK7+	22 (100%)	10 (100%)	1 (17%)
CK20+	1 (5 %)	0	5 (83%)

Abbreviation: GI indicates gastrointestinal.

Table 18. Performance of Immunohistochemical Markers in Identification of a Primary Site for Metastatic Adenocarcinoma to the Brain

	TP[a]	FP	TN	FN	Sensitivity (%)	Specificity (%)	PV+ (%)	PV- (%)
TTF-1	12	0	16	10	55	100	100	62
Cdx2	5	0	32	1	83	100	100	97
CK7	32	1	5	0	100	83	97	100
CK20	5	1	31	1	83	97	83	97

Abbreviations: TP indicates true positive; FP, false positive; TN, true negative; FN, false negative; PV+, positive predictive value; PV-, negative predictive value. [a]True positives were defined as TTF-1 in lung, CDX2 in gastrointestinal, CK7 in lung or breast, and CK20 in gastrointestinal primaries.

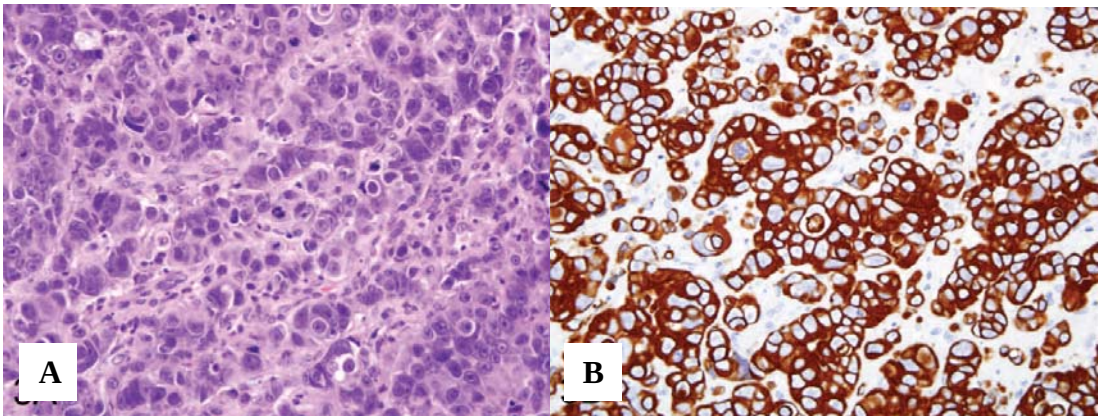

Figure 31. Brain metastasis from a mammary carcinoma, showing immunoreactivity only for CK7; hematoxylin-eosin (A) and CK7 (B); original magnifications x400.

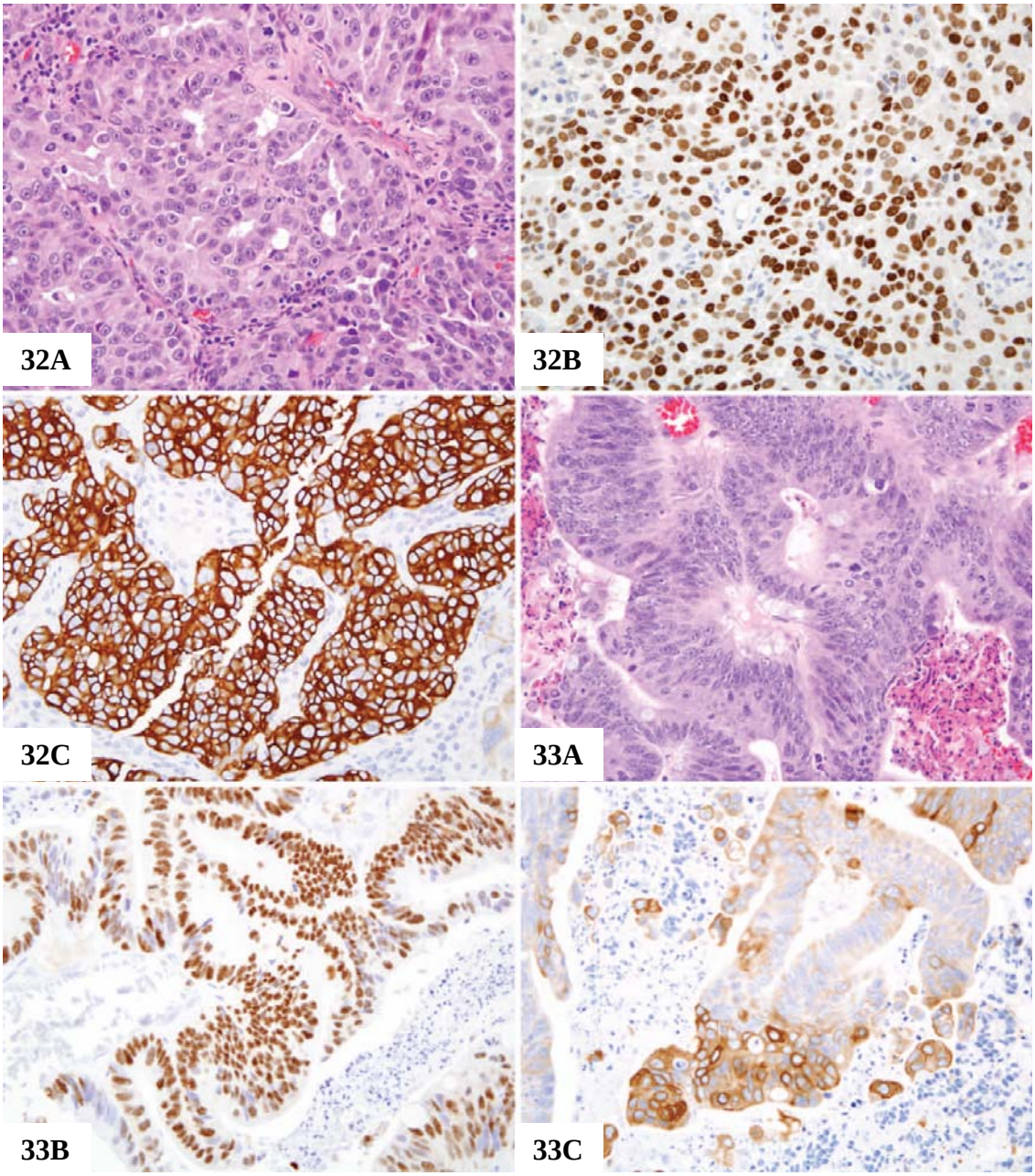

Figure 32. Brain metastasis from a pulmonary adenocarcinoma, showing immunoreactivity for TTF-1 and CK7; hematoxylin-eosin (A), TTF-1 (B), and CK7 (C); original magnifications x400.

Figure 33. Brain metastasis from a colonic adenocarcinoma, showing immunoreactivity for Cdx2 and CK20; hematoxylin-eosin (A), Cdx2 (B), and CK20 (C); original magnifications x400.

5.9. Expression of TTF-1 in malignant pleural effusions

Nuclear immunoreactivity for TTF-1 was detected in 19 (73%) of the 26 metastatic pulmonary adenocarcinomas [56] (**Figure 34** and **Table 19**). Non-pulmonary adenocarcinomas and malignant mesotheliomas were uniformly devoid of any staining. The sensitivity of TTF-1 for adenocarcinoma of the lung was 73% and the specificity of TTF-1 for adenocarcinoma of the lung versus non-pulmonary adenocarcinoma and malignant mesothelioma were 100%.

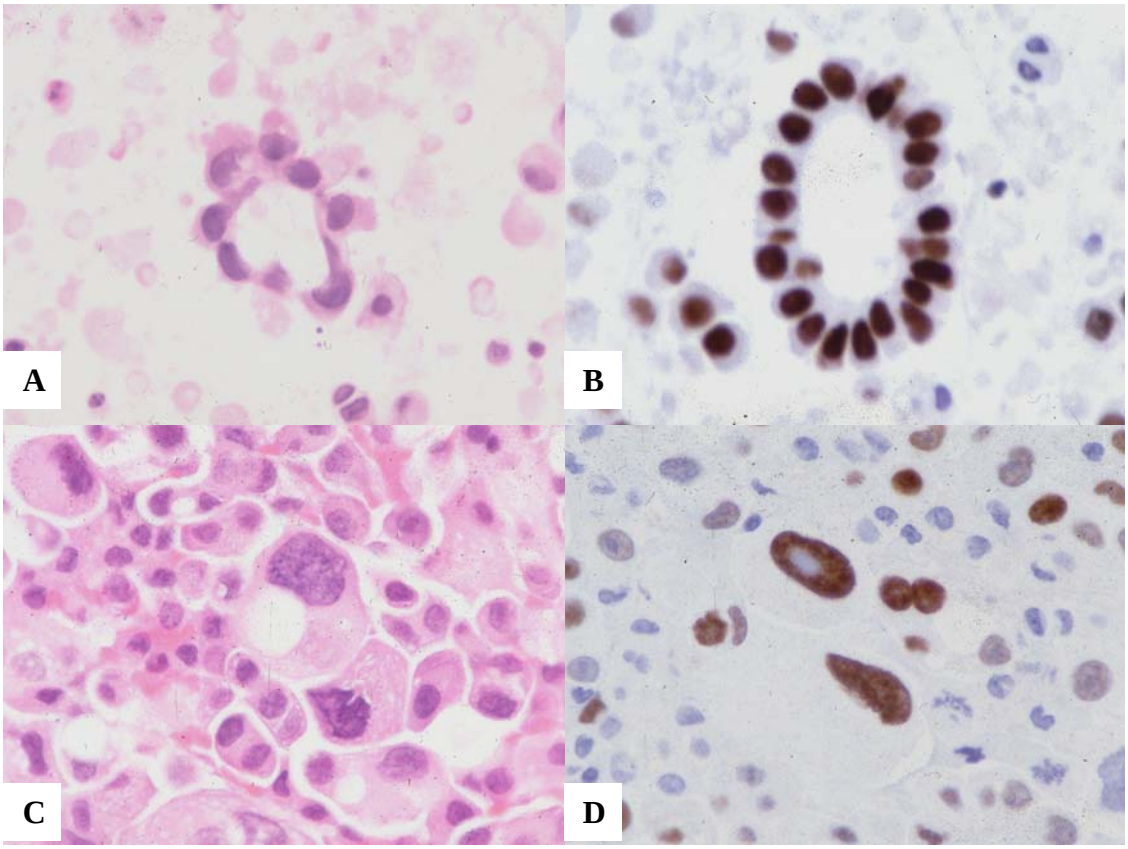

Figure 34. TTF-1 expression in adenocarcinomas of lung origin in pleural effusions (cell block preparations). Low-grade pulmonary adenocarcinoma with H&E stain (A) and nuclear immunoreactivity for TTF-1 (B). High-grade pulmonary adenocarcinoma with H&E stain (C) and nuclear immunoreactivity for TTF-1 (D). Original magnification x600 (a-d).

Table 19. TTF-1 Immunoreactivity in Malignant Pleural Effusions.

Tumor type	TTF-1 positive
Pulmonary adenocarcinoma (n=26)	19 (73%)
Non-pulmonary adenocarcinoma (n=26)	0
Malignant mesothelioma (n=4)	0

5.10. Differential expression of TTF-1 and CK20 in SCLC and Merkel cell tumor

TTF-1 immunoreactivity was detected in 97% of SCLCs, whereas Merkel cell tumors were uniformly negative (**Table 20, Figures 35 and 36**) [58]. In all positive cases, at least 10% of the neoplastic cells were reactive. In 81% of the positive cases, the reactivity involved more than 50% of the neoplastic cells. In the remaining 19% of the positive cases, the reactivity involved 10% to 50% of the neoplastic cells. The sensitivity and specificity of TTF-1 for SCLC were 97% and 100%, respectively.

CK20 immunoreactivity was present in 76% of Merkel cell tumors (**Table 20, Figure 36**). In all positive cases, at least 10% of the neoplastic cells were reactive. In 69% of the positive cases, the reactivity involved more than 50% of the neoplastic cells. In 31% of the positive cases, the reactivity involved 10% to 50% of the neoplastic cells. "Dot-like" paranuclear staining was seen in 63% and diffuse cytoplasmic staining was observed in 37% of positive Merkel cell tumors. One SCLC (3%) showed focal "dot-like" positivity. The sensitivity and specificity of CK20 immunostaining for Merkel cell tumor were 76% and 97%, respectively.

Table 20. TTF-1 and CK20 in SCLC of the Lung and Merkel Cell Tumor

Tumor type	TTF-1 positive	CK20 positive	TTF-1 positive/ CK20 negative	TTF-1 negative/ CK20 positive	TTF-1 positive/ CK20 positive	TTF-1 negative/ CK20 negative
SCLC (n=36)	35 (97%)	1 (3%)	34 (94%)	0 (0%)	1 (3%)	1 (3%)
Merkel cell tumor (n=21)	0 (0%)	16 (76%)	0 (0%)	16 (76%)	0 (0%)	5 (24%)

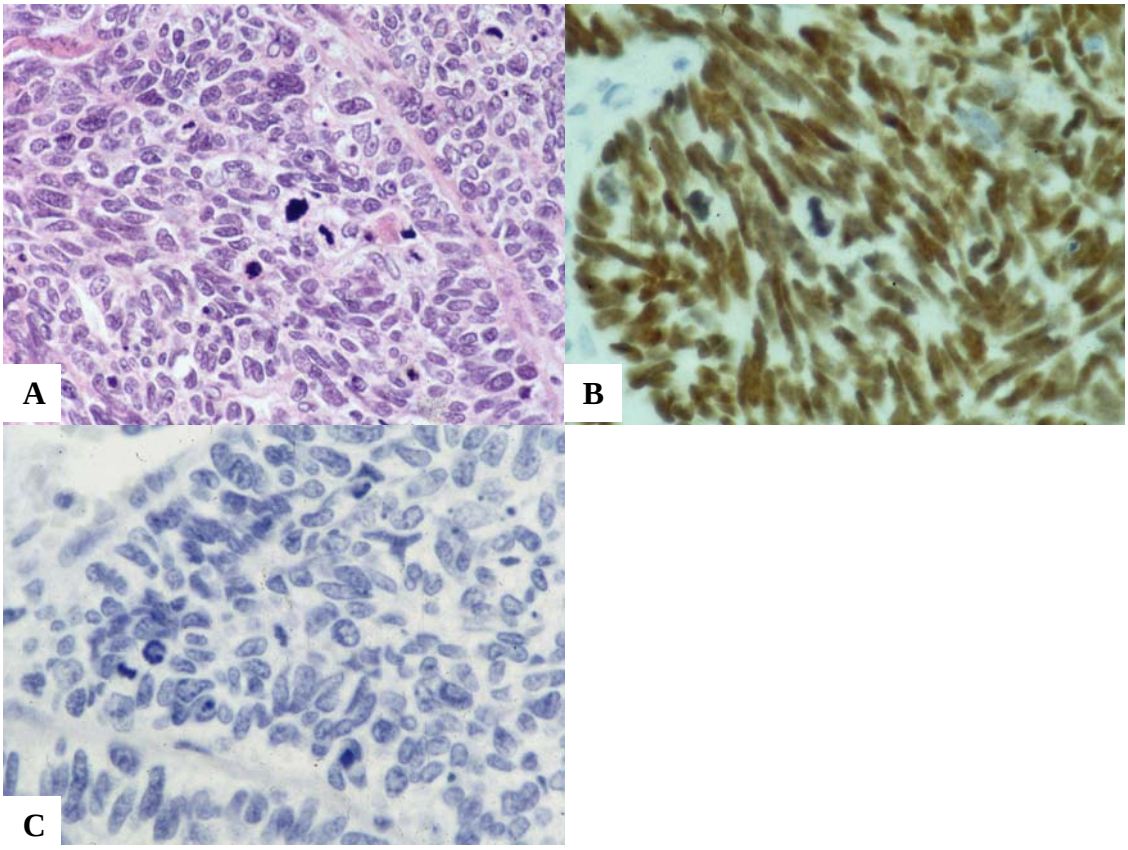

Figure 35. A case of SCLC. (A) The tumor cells show nuclear molding, finely granular chromatin, and scant cytoplasm; mitoses are frequent (H&E, x130). (B) The tumor cells show strong nuclear immunoreactivity for TTF-1 (biotin-streptavidin detection system with DAB and hematoxylin, x190). (C) Immunostaining for CK20 is negative (biotin-streptavidin with DAB and hematoxylin, x190).

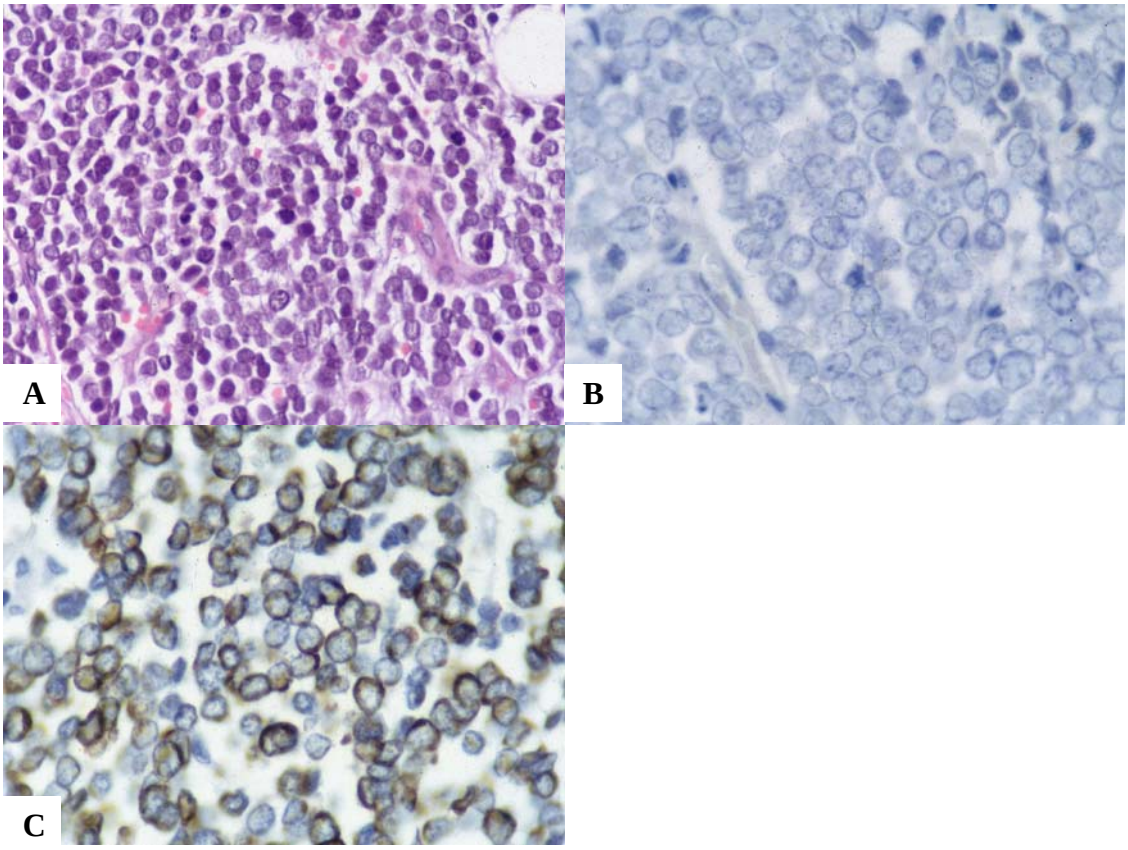

Figure 36. A case of Merkel cell tumor. (A) Histologically, the tumor is similar to a SCLC; the neoplastic cells exhibit occasional nuclear molding, finely granular chromatin, and scant cytoplasm (H&E, x 130). (B) The tumor cells are negative for TTF-1 (biotin-streptavidin detection system with DAB and hematoxylin, x 190). (C) There is strong paranuclear immunoreactivity for CK20 (biotin-streptavidin with DAB and hematoxylin, x 190).

5.11. Expression of Foxa2 in NE lung tumors

Foxa2 immunoreactivity was detected in 76% of typical carcinoids, 100% of atypical carcinoids, 50% of large cell NE carcinomas, 48% of SCLCs, and 5% of adenocarcinomas (**Table 21**, **Figures 37 and 38**) [59]. Reactivity was seen in more than 50% of tumor cells in each positive tumor. Squamous cell carcinomas and (non-NE) large cell carcinomas uniformly lacked Foxa2 staining. In the non-neoplastic lung, nuclear immunoreactivity for Foxa2 was present in Type II cells; other cell types were nonreactive.

Table 21. Expression of Foxa2 Transcription Protein in Lung Tumors

Diagnosis	Foxa2 positive
Typical carcinoid (n=17)	13 (76%)
Atypical carcinoid (n=2)	2 (100%)
Large cell NE carcinoma (n=4)	2 (50%)
SCLC (n=23)	11 (48%)
Adenocarcinoma (n=19)	1 (5%)
Squamous cell carcinoma (n=7)	0
Large cell carcinoma (non-NE) (n=3)	0

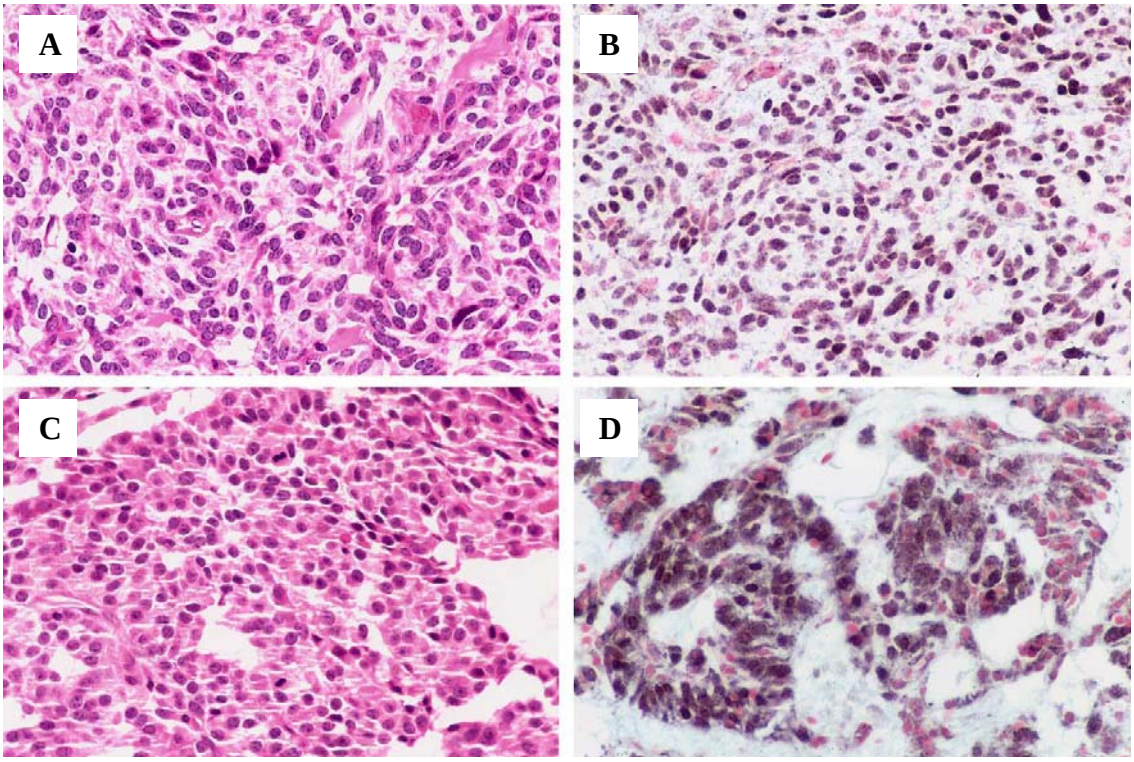

Figure 37. NE lung tumors. (A) Typical carcinoid showing organoid nesting. (B) Foxa2 immunoreactivity in the same typical carcinoid. (Panels A and B, original magnification, x400.) (C) Atypical carcinoid with organoid nesting and increased mitotic rate. (D) Foxa2 immunoreactivity in the same atypical carcinoid. (Panels C and D, original magnification, x400.)

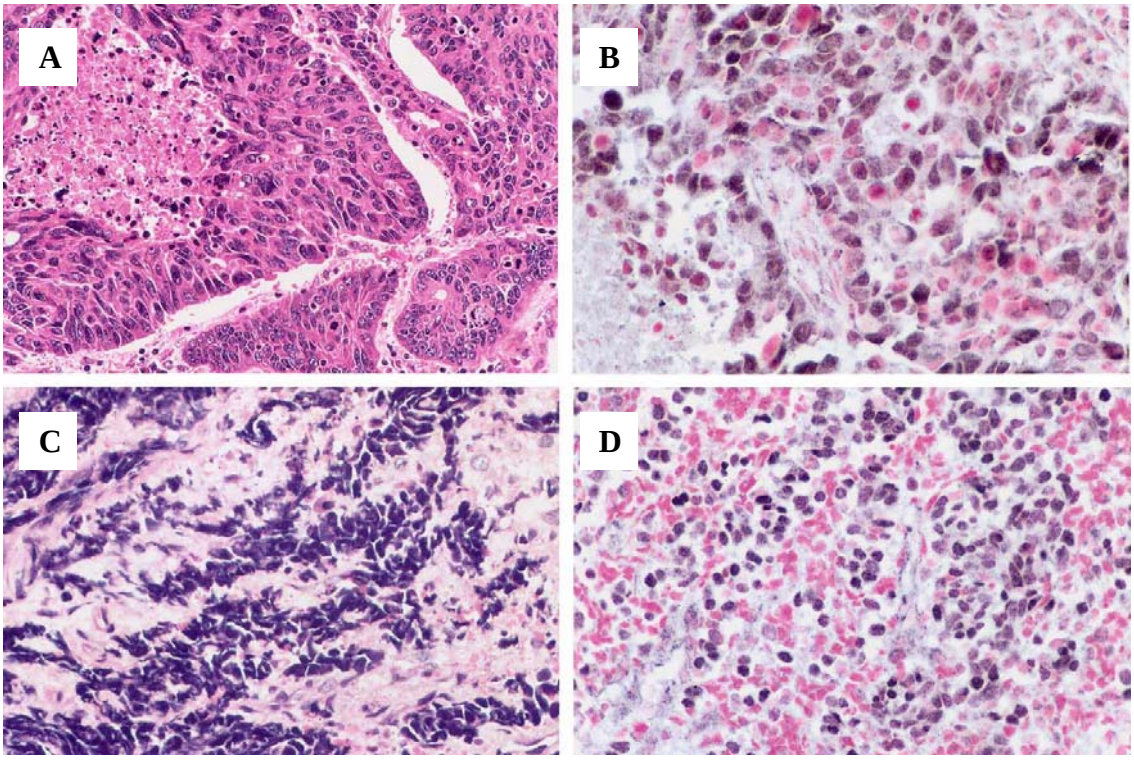

Figure 38. (A) Large cell NE carcinoma with palisading, rosettelike structures, and necrosis. (Original magnification, x250.) (B) Foxa2 immunoreactivity in the same large cell NE carcinoma. (Original magnification, x400.) (C) SCLC with nuclear molding and crush artifact. (D) Foxa2 immunoreactivity in a SCLC. (Panels C and D, original magnification, x400; panels A and C, H&E stain; panels B and D, biotin-streptavidin detection system with DAB chromogen, cobalt chloride enhancement, and nuclear fast red counterstain.)

5.12. Expression of pro-SP-B, pro-SP-C and TTF-1 in alveolar adenoma

Seventeen cases of alveolar adenoma were collected for this study [60]. Low-power magnification showed a well-demarcated, multicystic lesion easily distinguishable from the surrounding lung parenchyma (**Figure 39A**). All tumors were multicystic, with cysts varying in size from large to small. Smaller cysts resembled alveolar spaces (**Figure 39B**). Papillary formations were not seen. In 12 cases, eosinophilic proteinaceous granular material was identified within the cystic spaces. This material was not seen in the adjacent lung parenchyma. Most of the epithelial cells had the appearance of hyperplastic Type II pneumocytes with a cuboidal or hobnailed appearance and eosinophilic, finely vacuolated or foamy cytoplasm. Flattened Type I pneumocytes were present, but ciliated cells or cells with Clara cell morphology were

not seen. The interstitial component varied from a thin layer of connective tissue resembling normal alveolar septa to markedly thickened alveolar walls.

Immunohistochemical results from the 6 cases available for staining are seen in **Table 22**. Positive cytoplasmic staining for pro-SP-B (**Figure 39C**) and pro-SP-C was observed in most of the epithelial cells in all six cases analyzed, confirming the presence of Type II pneumocytes. Type II pneumocytes also showed positive nuclear staining for TTF-1. However, Clara cell marker CCSP was consistently negative (**Figure 39D**).

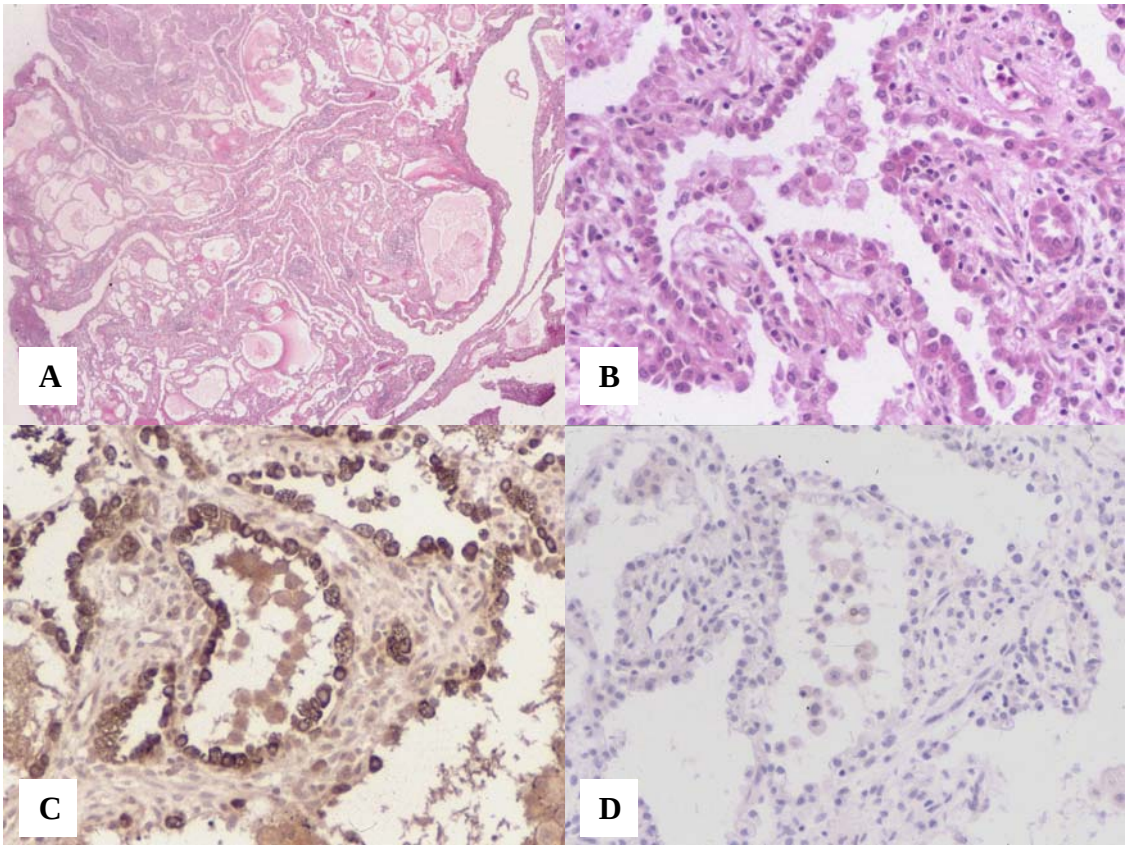

Figure 39. Alveolar adenoma. (A) Low-power magnification shows a well-demarcated, multicystic lesion (H&E stain). (B) At higher magnification, smaller cysts resemble alveolar spaces (H&E stain). (C) Positive cytoplasmic staining for pro-SP-B is seen in most epithelial cells. (D) CCSP stain is negative.

Table 22. Pro-SP-B, Pro-SP-C, CCSP and TTF-1 Immunoreactivity in Lining Cells of Alveolar Adenoma

Case Number	Pro-SP-B	Pro-SP-C	CCSP	TTF-1
1	Positive	Positive	Negative	Positive
6	Positive	Positive	Negative	Positive
10	Positive	Positive	Negative	N/A
11	Positive	Positive	Negative	Positive
16	Positive	Positive	Negative	Positive
17	Positive	Positive	Negative	Positive

N/A = Not assessed.

5.13. Expression of SP-A, pro-SP-B, pro-SP-C and CCSP in mature teratoma of the uterine cervix with pulmonary differentiation

Grossly, the surgical specimen consisted of an irregular, somewhat firm, tan, focally hemorrhagic, 3.5 x 3 x 2 cm mass [63]. Cut sections revealed multiple cysts measuring up to 0.5 cm in diameter and containing mucous fluid. The specimen was sampled extensively for histopathologic evaluation.

Microscopically, the lesion was covered by normal ectocervical and endocervical mucosa. The lesion itself was circumscribed and was composed of mature lung tissue (**Figure 40A**). Bronchial structures lined by pseudostratified, ciliated epithelium could be identified. The bronchial walls contained islands of hyaline cartilage and serous and mucinous glands (**Figure 40B**). Bronchioles and alveoli were also present (**Figure 40C**). The stroma showed numerous lymphoid follicles with prominent germinal centers. Immature components were absent; no placental or decidual elements were seen.

To demonstrate the presence of respiratory epithelial cell diffwerentiation, immunohistochemistry for SP-A, pro-SP-B, pro-SP-C, and CCSP was performed (**Figure 41**). Immunoreactivity for SP-A, pro-SP-B and pro-SP-C was detected in cuboidal terminal airway cells, confirming alveolar Type II cell differentiation. Similar to normal lung, immunoreactive SP-A and pro-SP-B were present in scattered bronchial and bronchiolar epithelial cells. Clara cell differentiation in these cells was confirmed by CCSP immunoreactivity.

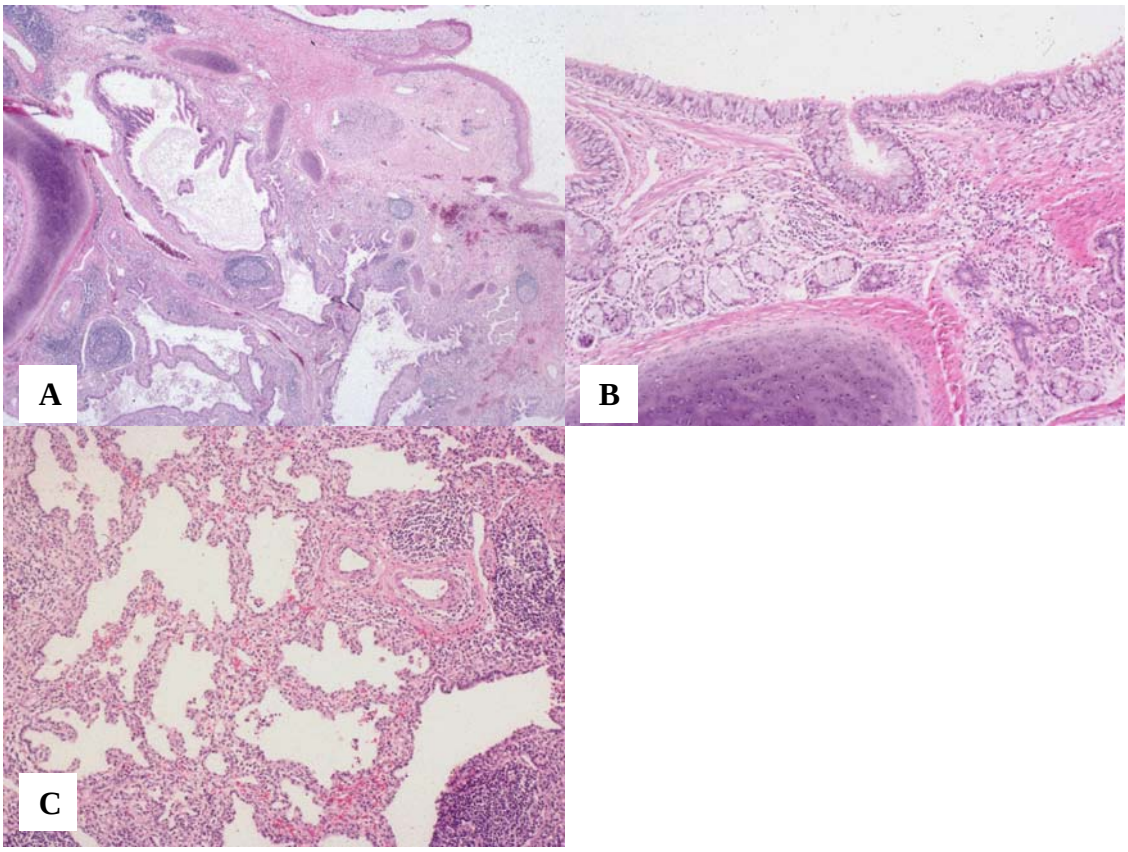

Figure 40. Mature teratoma of the uterine cervix with pulmonary differentiation (H&E stain). (A) Lower power view. (B) Bronchial wall with cartilage and submucosal glands. (C) Bronchioles and thick walled alveolar structures.

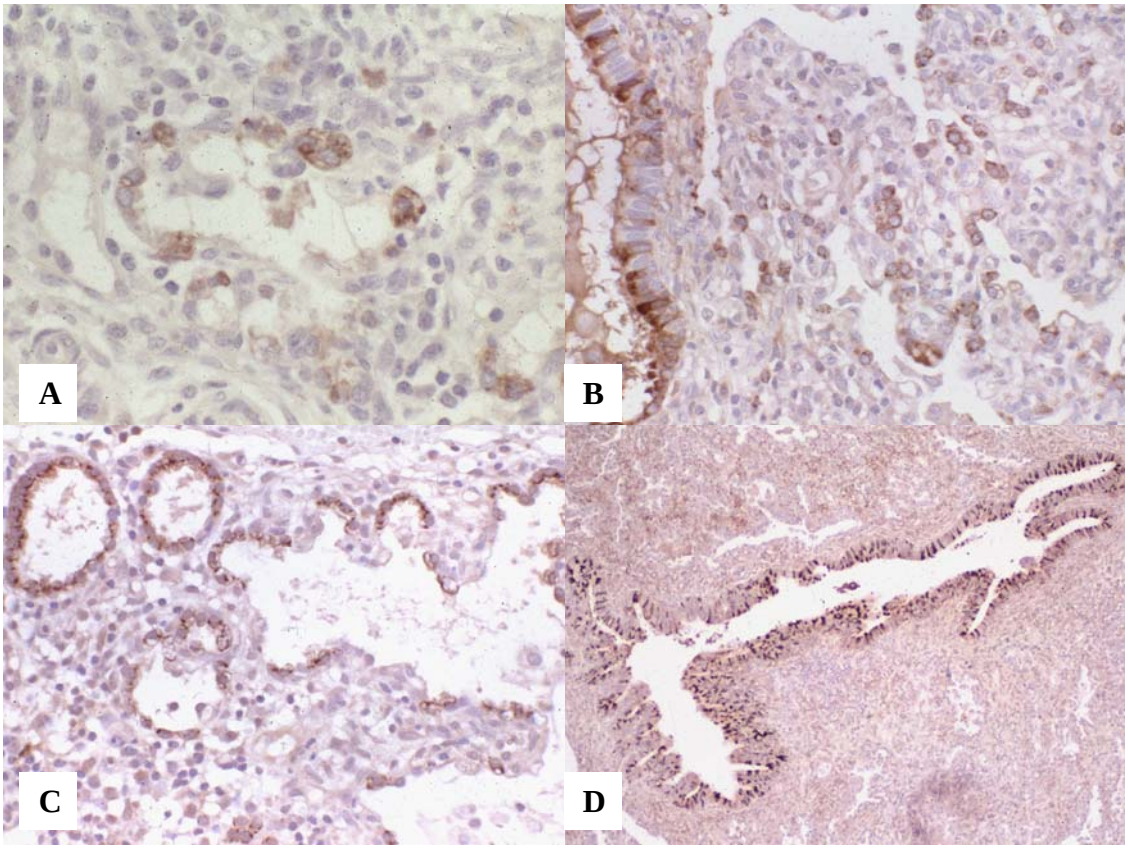

Figure 41. Mature teratoma of the uterine cervix with pulmonary differentiation. The teratoma reduplicates the distribution of surfactant proteins and CCSP in normal airways. (A), SP-A; (B), pro-SP-B; (C) pro-SP-C; and (D), CCSP immunostain.

6. Discussion

Expression of SP-A and SP-A mRNA in the developing lung

We performed immunohistochemistry and in situ hybridization to determine the temporal and spatial distribution of SP-A and SP-A mRNA in the respiratory tract of human fetuses and newborn infants without pulmonary pathology [49]. Immunoreactive SP-A was first detected in the tracheal epithelium at 13 weeks of gestation. Between 13 and 18 weeks of gestation, expression of SP-A and SP-A mRNA was limited to the tracheal and bronchial epithelium and glands. SP-A and SP-A mRNA was detected in terminal airways from 19 weeks of gestation onward. In liveborn infants, tracheal and bronchial epithelial cells and glands, non-ciliated bronchiolar epithelial (Clara) cells, cells of the bronchioloalveolar portals, and alveolar Type II cells contained SP-A and SP-A mRNA (**Table 23**).

Table 23. Expression of Airway Cell Specific Secretory Proteins and Transcription Factors in the Normal Respiratory Epithelium

	Bronchial epithelium/glands	Clara cells	Bronchioloalveolar portals	Type II cells
SP-A mRNA	+	+	+	+
SP-A	+	+	+	+
SP-B mRNA	+	+	+	+
Pro-SP-B	+	+	+	+
SP-B[a]	-	-	+	+
SP-C mRNA	-	-	+	+
Pro-SP-C	-	-	+	+
CCSP mRNA	+	+	-	-
CCSP	+	+	-	-
TTF-1[b]	-	+/-	+	+
Soxa2[c]	-	+/-	+	+

[a]Data from Stahlman et al., 1992 [84]; [b]data from Stahlman et al., 1996 [85]; [c]data from Stahlman et al., 1998 [86].

Detection of immunoreactive SP-A in both conducting and terminal airways is in agreement with a previous observation by Endo and Oka [87]**.** Using a monoclonal SP-A antibody (PE10), these authors have also demonstrated the presence of immunoreactive SP-A in the bronchial epithelium and, in two fetuses, bronchial glands.

Expression of SP-A in Type II cells is consistent with the role SP-A plays in tubular myelin formation [18, 19]. However, expression of SP-A in the tracheal and bronchial epithelium and glands raises the question if these localizations have any functional significance. It has been shown that SP-A is a mannose-binding protein (mannan-binding lectin) that specifically binds certain organisms, such as Group B beta-hemolytic streptococci and Pneumocystis jiroveci [23-26]. Furthermore, it has been demonstrated that SP-A potentiates the antibacterial functions of alveolar macrophages [23-26]. Taken together, these data support the concept that SP-A, through its lectin-like properties, contributes to host-defense mechanisms of the lung.

Expression of SP-B and SP-C proteins and mRNAs in the developing lung

We also investigated the ontogeny and distribution of SP-B and SP-C mRNAs and pro-proteins in the developing human lung [51]. SP-B mRNA, pro-SP-B, SP-C mRNA and pro-SP-C were detected as early as 15 weeks of gestation in both the conducting and terminal airways. Expression of SP-B mRNA and SP-C mRNA at 15 weeks of gestation is in agreement with previous Northern blot analysis data showing that SP-B mRNA and SP-C mRNA appear in the human lung between 13 and 16 weeks of gestation [77, 88]. Interestingly, SP-A mRNA and lamellar bodies have not been detected in pre-Type II cells of terminal airways until 19 weeks of gestation in the same fetal lungs used in the current study [49].

In newborn infants, SP-B and SP-C showed divergent expression patterns (**Table 23)**. Whereas SP-B mRNA and pro-SP-B were expressed in both conducting and terminal airways, expression of SP-C mRNA and pro-SP-C was limited to Type II cells and cells of the bronchioloalveolar portals. These findings suggest that transcription of SP-B and SP-C genes is regulated by different, cell type dependent mechanisms. In addition, divergent cellular patterns of staining for pro-SP-B and the active SP-B peptide (**Table 23)** [84] suggests that proteolytic processing or cellular routing of pro-SP-B is also influenced by cell type.

The localization of SP-B and SP-C gene products to Type II cells is consistent with the important roles these two low-molecular weight, hydrophobic surfactant proteins play in surfactant function and homeostasis [18, 19, 22].

Expression of CCSP and CCSP mRNA in the developing lung

We examined the temporal-spatial distribution of CCSP and its mRNA in the developing human lung, using immunohistochemistry and in situ hybridization [50]. Immunoreactive CCSP and CCSP mRNA were found in noncitiated epithelial cells of the trachea, bronchi, and bronchioles (**Table 23**). These findings are in agreement with reports by Singh et al. [30] and Broers et al. [89].

We described a close spatial relationship between Clara cells and neuroepithelial bodies. In fetuses, nonciliated bronchiolar epithelial cells immunolabeled for CCSP or containing CCSP mRNA formed clusters around neuroepithelial bodies, especially at airway branching points. Several studies suggest a role for peptides secreted by pulmonary NE cells and neuroepithelial bodies in regulating airway epithelial cell growth. The expression of bombesin-like peptides by pulmonary NE cells is transiently upregulated during mouse lung development [90]. Mammalian bombesin (gastrin releasing peptide) stimulates growth of human bronchial epithelial cells in colony-forming assays [91]. In an in vitro model using lung buds, treatments with bombesin resulted in increasing branching morphogenesis [92]. Taken together, these data suggest that NE cells and Clara cells may interact during lung development, affecting proliferation or differentiation.

Differential expression of pro-SP-B and SP-B mRNA in NSCLCs and non-pulmonary adenocarcinomas

Ours was the first study to establish the presence of pro-SP-B and SP-B mRNA in adenocarcinoma of the lung [53]. Pro-SP-B and SP-B mRNA were detected in all major pulmonary adenocarcinoma subtypes, including acinar, papillary, bronchioloalveolar and solid. Similar to our work and in contrast to a previous study [93], Linnoila et al. have demonstrated that expression of SP-A is not limited to papillary or bronchioloalveolar adenocarcinomas [94].

The sensitivity and specificity of pro-SP-B and SP-B mRNA for adenocarcinomas of the lung were 60% and 100%, and 53% and 100%, respectively [53]. The slight difference between the sensitivity of pro-SP-B and SP-B mRNA was

probably due to RNA degradation in a single case. Alternatively, the discrepancy may reflect inherent differences between sensitivities of the two techniques.

As compared to pro-SP-B (60%), the sensitivity of immunoreactive SP-A for adenocarcinomas of the lung is generally lower, in most studies between 19% and 48% [94-96]. However, the sensitivity of a monoclonal SP-A antibody (PE-10) has been reported as high as 62% [97]. As far as specificity is concerned, 23 nonpulmonary adenocarcinomas were negative for SP-A in a study by Mizutani et al. [95] and only 2 of 75 nonpulmonary adenocarcinomas stained in a study by Linnoila et al [94]. Taken together, these data indicate that the sensitivity and specificity of pro-SP-B are similar to those of a better SP-A antibody (PE-10) and suggest that pro-SP-B may be useful in separating adenocarcinomas of pulmonary and nonpulmonary origin.

The utility of pro-SP-B and TTF-1 in differentiating adenocarcinoma of the lung from malignant mesothelioma

We evaluated the utility of pro-SP-B and TTF-1 in differentiating adenocarcinoma of the lung from malignant mesothelioma. The sensitivity and specificity of pro-SP-B immunoreactivity for adenocarcinoma of the lung versus malignant mesothelioma were 57% and 100%, respectively. The sensitivity and specificity of TTF-1 for adenocarcinoma of the lung versus malignant mesothelioma were 76% and 100%, respectively.

The presence of immunoreactive pro-SP-B in 57% of pulmonary adenocarcinomas is in agreement with our previous study, in which 60% of pulmonary adenocarcinomas have been reactive with this antibody [53]. The sensitivity of pro-SP-B for adenocarcinoma of the lung is similar to that of SP-B mRNA [53], active SP-B [98], and SP-A (PE-10 antibody) [97].

In two previous studies, TTF-1 was detected in 75% and 57.5% of pulmonary adenocarcinomas, respectively [98, 99]. Since similar evaluation criteria have been applied, the reason for this discrepancy is unclear. Our study, using a large number of cases, supports the observation that TTF-1 is present in approximately 76% of pulmonary adenocarcinomas. Negative staining for TTF-1 in all of our 95 mesothelioma cases is concordant with a single previous study, in which none of 24 malignant mesotheliomas have been positive [99].

Taken together, our data indicate that immunostaining for pro-SP-B and/or TTF-1 may be helpful in differentiating adenocarcinoma of the lung from malignant

mesothelioma. Whereas both pro-SP-B and TTF-1 were very specific for adenocarcinomas of the lung in our study, the sensitivity of TTF-1 exceeds that of pro-SP-B. Furthermore, the combined sensitivity of pro-SP-B and TTF-1 is only slightly higher than that of TTF-1 alone. Therefore, inclusion of TTF-1 into the "adenocarcinoma versus malignant mesothelioma" antibody panel seems to be especially beneficial.

The differential diagnosis between adenocarcinoma and epithelioid malignant mesothelioma often requires the use of ancillary techniques such as electron microscopy or immunohistochemistry. By demonstrating the long, complex microvilli characteristic of epithelioid malignant mesothelioma, electron microscopy is effective in a large proportion of cases. However, it has several drawbacks, including relatively high costs and a relatively long period of time required for processing and analysis [100, 101]. Currently, immunohistochemical markers are available for both adenocarcinoma and malignant mesothelioma [102]. Popular mesothelial markers include calretinin, keratin 5/6, WT-1 protein, and podoplanin (D2-40). Commonly used, general adenocarcinoma markers include MOC-31, BG8 ($Lewis^Y$), CEA, B72.3, and Ber-EP4. Because of its specificity for pulmonary adenocarcinoma, it is useful to add TTF-1 to this panel.

TTF-1, a member of the homeodomain-containing transcription factor family, activates the expression of select genes in the thyroid, lung and restricted regions of the brain [34, 35]. Homeodomain containing transcriptional factors play key roles in the control of embryonic development and differentiation [36]. TTF-1 is required for branching morphogenesis and epithelial cell differentiation during lung development [103]. Recent reports have suggested that amplification and resultant overexpression of the TTF-1 gene contribute to increased proliferation and survival of lung cancer cells [104, 105]. Therefore, TTF-1 is now considered as a lung cancer-specific oncogene [105].

The prognostic value of pro-SP-B and TTF-1 in early stage adenocarcinoma of the lung

Actuarial cumulative survival curves for 172 cases of stage I and II adenocarcinomas demonstrated a significantly longer survival period for patients with pro-SP-B positive tumors versus negative tumors ($p=0.0310$) [82]. Also, survival curves for 160 cases of stage I and II adenocarcinomas demonstrated a significantly longer survival period for

patients with TTF-1 positive tumors versus negative tumors (p=0.0001) [83]. These data suggest that both pro-SP-B and TTF-1 are positive survival indicators in patients with early stage adenocarcinoma of the lung.

The utility of TTF-1, Cdx2, CK7 and CK20 in determining the primary site for adenocarcinomas metastatic to the brain

The most common source of adenocarcinoma metastatic to the brain in our study was lung (58%), followed by breast (26%), and gastrointestinal tract (16%) [55], in keeping with numerous reported frequencies in the literature from around the world spanning the last 10 to 15 years [106] with an overall average of 53% for the frequency of lung primaries among metastatic carcinomas to the brain.

In our study, TTF-1 was expressed with 100% specificity in adenocarcinomas of pulmonary origin. Several others have described the same results with some exception. Although most determine the specificity of TTF-1 for adenocarcinomas of pulmonary origin to be at or near 100% [107, 108], rare unexpected staining of colorectal adenocarcinomas with TTF-1 has been reported. Nuclear staining with the SPT24 clone (Novocastra) in metastatic colorectal adenocarcinomas is reportedly as high as 5% [109]. In the same study by Comperat et al., another TTF-1 clone, 8G7G3/1 (Dako), did not show this pattern. Using clone 8G7G3/1, we had no false-positive staining. This is in agreement with recent studies showing higher specificity for the 8G7G3/1 TTF-1 clone [110, 111].

The sensitivity of TTF-1 in our study was 55% for primary pulmonary adenocarcinomas metastatic to the brain. Sensitivities reported in the literature range from 59% to 100% [107, 108]. Our sensitivity is lower, likely due to the number of poorly differentiated adenocarcinomas in our series.

To our knowledge, expression of Cdx2 in adenocarcinomas metastatic to the brain has not previously been investigated. The specificity of Cdx2 for gastrointestinal adenocarcinomas in our study was 100%, with 83% sensitivity. This is echoed in a report by Levine et al. [112] in which Cdx2 staining in cytologic cell block material had a sensitivity and specificity of 75% and 100% for colorectal adenocarcinomas metastatic to the lung.

Our data for CK7 and CK20 are similar to those reported in the literature. CK7 was 100% sensitive and 83% specific for breast and lung primaries, with 100% of both tumor types expressing this CK. Large series have shown that 90% to 100% of primary

lung adenocarcinomas are positive for CK7 [106, 113] and 96% to 98% of primary breast adenocarcinomas express CK7 [106, 113], with an overall specificity of 78% [106]. Interestingly, several reports have described the presence of frequent CK7 expression in rectal adenocarcinomas, as great a frequency as 74% [106, 113].

In our study, positivity for CK20 had a sensitivity and specificity of 83% and 97% for adenocarcinomas of gastrointestinal origin. Again, large series have shown that 85% to 97% of similar cases express CK20 in colorectal adenocarcinomas overall [106, 113] with a reported 94% sensitivity and specificity [106].

Expression of TTF-1 in malignant pleural effusions

We analyzed the expression of TTF-1 in malignant pleural effusions caused by pulmonary and non-pulmonary adenocarcinomas and malignant mesotheliomas [56]. Adenocarcinomas are known to be the largest group of malignant pleural effusions. In 1985, Johnston published a review of 584 consecutive malignant pleural effusions; adenocarcinomas comprised 47.4% of the cases [114]. In Johnston's study, the most frequent primary organ site among males was the lung, followed by the gastrointestinal and genitourinary tracts. Among female patients, the order of frequency was breast, female genital tract (usually ovary), lung, and gastrointestinal tract. In our study, the lung was the single most common primary site among not only men, but also women. The reason for this minor discrepancy is not entirely clear. It may be the consequence of local practice variations such as differences in populations served by the two medical centers. Alternatively, it may reflect recent increases in lung cancer among women [5].

The utility of TTF-1 as a pulmonary adenocarcinoma marker is now well established in surgical pathology [54, 55, 98, 115]. On the other hand, the current report is one of the few studies that have evaluated the role of TTF-1 in the field of cytology [116-118]. In the previous cytology studies, immunoreactive TTF-1 has been detected in 79-89% of pulmonary adenocarcinomas [116-118]. These reports do not offer any explanation for the higher expression of TTF-1 in cytology versus surgical samples. In the current study, 73% of pulmonary adenocarcinomas expressed immunoreactive TTF-1. Our results seem to be more in line with results of the surgical pathology studies and are more likely to be reproducible in routine cytology practice.

In the context of separating adenocarcinomas of the lung from non-pulmonary adenocarcinomas and malignant mesotheliomas in surgical specimens, TTF-1 has demonstrated outstanding specificity for lung primaries. As far as cytology

publications are concerned, Hecht et al. have noted a single case of metastatic ovarian carcinoma with focal weak TTF-1 immunoreactivity in 50 metastatic carcinomas of non-pulmonary origin [117]. No TTF-1 staining has been observed in non-pulmonary adenocarcinomas or malignant mesotheliomas by Afify et al. and Ng et al [116]. Likewise, no TTF-1 immunoreactivity was detected in non-pulmonary adenocarcinomas or malignant mesotheliomas in our study. These findings suggest that TTF-1 is highly specific for adenocarcinomas of the lung not only in surgical specimens, but also in cytology preparations.

Differential expression of TTF-1 and CK20 in SCLC and Merkel cell tumor

This was the first study to investigate the utility of TTF-1 in separating SCLC and Merkel cell tumor. SCLC metastasizes to the skin relatively often and the differential diagnosis between metastatic SCLC and Merkel cell tumor of the skin may be difficult. Chan et al. [119] have recommended the use of CK20 immunostaining to solve this dilemma. In their study, CK20 immunoreactivity was observed in 97.1% of Merkel cell tumors and 2.7% of SCLCs. We also evaluated CK20 immunostaining, which was present in 76% of Merkel cell tumors and 3% of SCLCs. The reason for this discrepancy in CK20 sensitivity is unclear. Similar to the study of Chan et al. [119], all tumors included in our study were reactive for broad-spectrum keratin. This finding excluded the possibility of unsatisfactory antigen preservation. The same monoclonal CK20 antibody was used in both studies. Furthermore, we optimized the pretreatment procedure in a preliminary study. The discrepancy, therefore, is unlikely to reflect methodological variations and may be due to other factors such as different study populations.

The sensitivity and specificity of TTF-1 for SCLC versus Merkel cell tumor were 97% and 100%, respectively. Expression of TTF-1 in 97% of SCLCs is in agreement with other studies, in which TTF-1 was detected in 92.7% to 100% of similar tumors [120, 121]. As far as specificity is concerned, this is the first study to investigate the expression of TTF-1 in Merkel cell tumors. Twenty-one cases were stained and all of the cases were negative. In our laboratory, the sensitivity (97%) and specificity (100%) of TTF-1 for SCLC were higher than the sensitivity (76%) and specificity (97%) of CK20 for Merkel cell tumor. These data indicate that it may be

useful to add TTF-1 to the panel of antibodies that are used to differentiate between SCLC and Merkel cell tumor.

Expression of Foxa2 in NE lung tumors

To our knowledge, this was the first study to analyze the expression of Foxa2 in lung tumors [59]. In the nonneoplastic lung, immunoreactivity for Foxa2 was detected in alveolar Type II cells. This is in agreement with a previous study by Stahlman et al [86]. Expression of Foxa2 in Type II cells is consistent with its role in the expression of SP-B and TTF-1 [42, 48].

Foxa2 immunoreactivity was detected in various NE lung tumors and a single case of pulmonary adenocarcinoma. The spectrum of NE lung tumors ranges from low-grade typical carcinoid, to intermediate-grade atypical carcinoid, and to high-grade large cell NE carcinoma and SCLC [5]. Histological characteristics of NE lung tumors include the presence of some NE morphological features such as organoid nesting, palisading, rosette-like structures, or trabecular architecture. They express NE markers by immunohistochemistry (e.g. chromogranin, synaptophysin or CD56) and exhibit NE granules at electron microscopic level [5]. Both genetic similarities and nonrandom differences have been described in these tumors [122]. Although some investigators believe that the differences are more significant than the similarities and that various NE lung tumors belong to different cell lineages [122], Folpe et al. [121] have shown that TTF-1 is expressed in all types of NE lung tumors. Similarly, Foxa2 immunoreactivity was detected in the entire spectrum of NE lung tumors and was rarely seen in other tumor types in the present study. The presence of Foxa2, along with that of TTF-1, in the entire spectrum of NE lung tumors and its absence from the majority of other tumor types support the hypothesis that typical and atypical carcinoids, large cell NE carcinomas, and SCLCs are closely related.

Expression of airway epithelial cell markers in alveolar adenoma

Alveolar adenoma is a rare benign neoplasm with distinctive gross and microscopic features. For many years, alveolar adenomas were thought to be lymphangiomas because of their multicystic appearance, the thin-walled nature of many of the cysts, and the sometimes flat lining cells resembling endothelial cells [123, 124]. The presence, however, of keratin-positive and factor VIII-negative cells lining the cystic spaces confirms its epithelial rather than vascular origin. Furthermore, our

immunohistochemical studies demonstrated that the cystic spaces of alveolar adenomas are lined mostly by alveolar Type II cells, with fewer Type I cells and no Clara cells. More specifically, most of the lining cells were immunoreactive for Type II cell markers pro-SP-B, pro-SP-B and TTF-1 and there was no staining for Clara cell marker CCSP.

Expression of airway epithelial cell markers in mature teratoma of the uterine cervix with pulmonary differentiation

We reported a case of a 33-year-old woman who had presented with heavy vaginal bleeding and a polypoid mass of the uterine cervix. The cervical lesion was composed entirely of mature lung tissue, including bronchial, bronchiolar, and alveolar structures. The presence of well-differentiated respiratory epithelial cells, i.e., Clara cells and alveolar Type II cells was confirmed by immunohistochemistry. Since this was a newly developed mass in an adult individual, we favored a neoplastic process over heterotopia and interpreted the lesion as unilateral lung development in an extragonadal mature teratoma.

Although respiratory epithelium is a relatively frequent constituent of teratomas, the presence of mature lung tissue is an exceptional finding. The present study was the first report of unilateral lung development in a uterine teratoma. This is also the first demonstration of cell specific protein production, including SP-A, pro-SP-B, pro-SP-C and CCSP, by respiratory epithelial cells in a teratoma.

7. Conclusions

Expression of airway cell specific secretory proteins and their mRNAs in the developing human lung

1. Surfactant proteins (SP-A, SP-B and SP-C) show somewhat diverse cellular distribution in the human lung.
2. All surfactant proteins are expressed in Type II cells. Their expression in this cell type facilitates their pivotal roles in the surfactant system.
3. Expression of SP-A in the tracheobronchial epithelium supports the concept that SP-A also has a role outside the surfactant system, perhaps in host-defense.
4. The close spatial relationship between Clara cells and neuroepithelial bodies in fetuses suggests that NE cells and Clara cells may interact during lung development, affecting proliferation or differentiation.

Expression of pro-SP-B, SP-B mRNA and TTF-1 in NSCLC

1. Expression of pro-SP-B (up to 60%), SP-B mRNA (53%) and TTF-1 (76%) in adenocarcinomas of the lung and their lack of expression in nonpulmonary adenocarcinomas and malignant mesotheliomas suggest that pro-SP-B, SP-B mRNA and TTF-1 can be used to separate these neoplasms.
2. Our actuarial cumulative survival curves suggest that pro-SP-B and TTF-1 are positive survival indicators in patients with early stage adenocarcinoma of the lung.
3. TTF-1 (with Cdx2, CK7 and CK20) is helpful in determining the primary site for metastatic adenocarcinomas to the brain.
4. TTF-1 is also useful in identifying metastatic adenocarcinomas of pulmonary origin in cell block preparations of malignant pleural effusions.

Expression of airway cell specific transcription factors in NE lung tumors

1. TTF-1 is also expressed in SCLCs (97%) and is helpful in separating SCLC from Merkel cell tumor.
2. Widespread expression of Foxa2 in NE lung tumors and its lack of expression in most NSCLCs support the hypothesis that carcinoid tumors (typical and atypical), large cell NE carcinoma and SCLC are closely related.

Expression of airway cell specific secretory proteins and TTF-1 in miscellaneous neoplasms

1. Expression of pro-SP-B, pro-SP-C and TTF-1 in lining cells of alveolar adenoma confirms its differentiation toward Type II cells.
2. Expression of SP-A, pro-SP-B, pro-SP-C and CCSP in mature teratoma of the uterine cervix with pulmonary differentiation confirms this diagnosis.

8. References

1. Colby TV, Koss MN, Travis WD (1995) Tumors of the Lower Respiratory Tract. Armed Forces Institute of Pathology, Washington.

2. Gilliland FD, Samet JM (1994) Lung cancer. Cancer Surv. 19-20:175-195.

3. Travis WD, Lubin J, Ries L, Devesa S (1996) United States lung carcinoma incidence trends: declining for most histologic types among males, increasing among females. Cancer. 77:2464-2470.

4. Brundage MD, Davies D, Mackillop WJ (2002) Prognostic factors in non-small cell lung cancer: a decade of progress. Chest. 122:1037-1057.

5. Travis WD, Brambilla E, Muller-Hermelink HK, Harris CC (2004) Pathology and Genetics of Tumours of the Lung, Pleura, Thymus and Heart. In: Kleihues P, Sobin LH, (eds) World Health Organization Classification of Tumours. IARC*Press*, Lyon.

6. Motoi N, Szoke J, Riely GJ, Seshan VE, Kris MG, Rusch VW, Gerald WL, Travis WD (2008) Lung adenocarcinoma: modification of the 2004 WHO mixed subtype to include the major histologic subtype suggests correlations between papillary and micropapillary adenocarcinoma subtypes, EGFR mutations and gene expression analysis. Am J Surg Pathol. 32:810-827.

7. Travis WD, Brambilla E, Noguchi M, Nicholson AG, Geisinger KR, Yatabe Y, Beer DG, Powell CA, Riely GJ, Van Schil PE, Garg K, Austin JH, Asamura H, Rusch VW, Hirsch FR, Scagliotti G, Mitsudomi T, Huber RM, Ishikawa Y, Jett J, Sanchez-Cespedes M, Sculier JP, Takahashi T, Tsuboi M, Vansteenkiste J, Wistuba I, Yang PC, Aberle D, Brambilla C, Flieder D, Franklin W, Gazdar A, Gould M, Hasleton P, Henderson D, Johnson B, Johnson D, Kerr K, Kuriyama K, Lee JS, Miller VA, Petersen I, Roggli V, Rosell R, Saijo N, Thunnissen E, Tsao M, Yankelewitz D (2011) International association for the study of lung cancer/american thoracic society/european respiratory society international multidisciplinary classification of lung adenocarcinoma. J Thorac Oncol. 6:244-285.

8. Koss M, Travis W, Moran C, Hochholzer L (1992) Pseudomesotheliomatous adenocarcinoma: a reappraisal. Semin Diagn Pathol. 9:117-123.

9. Kondo T, Yamada K, Noda K, Nakayama H, Kameda Y (2002) Radiologic-prognostic correlation in patients with small pulmonary adenocarcinomas. Lung Cancer. 36:49-57.

10. Takashima S, Maruyama Y, Hasegawa M, Saito A, Haniuda M, Kadoya M (2003) High-resolution CT features: prognostic significance in peripheral lung adenocarcinoma with bronchioloalveolar carcinoma components. Respiration. 70:36-42.

11. Kodama K, Higashiyama M, Yokouchi H, Takami K, Kuriyama K, Mano M, Nakayama T (2001) Prognostic value of ground-glass opacity found in small lung adenocarcinoma on high-resolution CT scanning. Lung Cancer. 33:17-25.

12. Travis WD, Rush W, Flieder DB, Falk R, Fleming MV, Gal AA, Koss MN (1998) Survival analysis of 200 pulmonary neuroendocrine tumors with clarification of criteria for atypical carcinoid and its separation from typical carcinoid. Am J Surg Pathol. 22:934-944.

13. Soga J, Yakuwa Y (1999) Bronchopulmonary carcinoids: An analysis of 1,875 reported cases with special reference to a comparison between typical carcinoids and atypical varieties. Ann Thorac Cardiovasc Surg. 5:211-219.

14. Travis WD, Linnoila RI, Tsokos MG, Hitchcock CL, Cutler GB, Jr., Nieman L, Chrousos G, Pass H, Doppman J (1991) Neuroendocrine tumors of the lung with proposed criteria for large-cell neuroendocrine carcinoma. An ultrastructural, immunohistochemical, and flow cytometric study of 35 cases. Am J Surg Pathol. 15:529-553.

15. Pelosi G, Pasini F, Sonzogni A, Maffini F, Maisonneuve P, Iannucci A, Terzi A, De Manzoni G, Bresaola E, Viale G (2003) Prognostic implications of neuroendocrine differentiation and hormone production in patients with Stage I nonsmall cell lung carcinoma. Cancer. 97:2487-2497.

16. Hiroshima K, Iyoda A, Shibuya K, Toyozaki T, Haga Y, Fujisawa T, Ohwada H (2002) Prognostic significance of neuroendocrine differentiation in adenocarcinoma of the lung. Ann Thorac Surg. 73:1732-1735.

17. Nicholson SA, Beasley MB, Brambilla E, Hasleton PS, Colby TV, Sheppard MN, Falk R, Travis WD (2002) Small cell lung carcinoma (SCLC): a clinicopathologic study of 100 cases with surgical specimens. Am J Surg Pathol. 26:1184-1197.

18. Perez-Gil J (2008) Structure of pulmonary surfactant membranes and films: the role of proteins and lipid-protein interactions. Biochim Biophys Acta. 1778:1676-1695.

19. Whitsett JA, Wert SE, Weaver TE (2010) Alveolar surfactant homeostasis and the pathogenesis of pulmonary disease. Annu Rev Med. 61:105-119.

20. Weaver TE, Whitsett JA (1991) Function and regulation of expression of pulmonary surfactant-associated proteins. Biochem J. 273(Pt 2):249-264.

21. Hawgood S (1989) Pulmonary surfactant apoproteins: a review of protein and genomic structure. Am J Physiol. 257:L13-22.

22. Whitsett JA, Weaver TE (2002) Hydrophobic surfactant proteins in lung function and disease. N Engl J Med. 347:2141-2148.

23. Kingma PS, Whitsett JA (2006) In defense of the lung: surfactant protein A and surfactant protein D. Curr Opin Pharmacol. 6:277-283.

24. Korfhagen TR, Bruno MD, Ross GF, Huelsman KM, Ikegami M, Jobe AH, Wert SE, Stripp BR, Morris RE, Glasser SW, Bachurski CJ, Iwamoto HS, Whitsett JA (1996) Altered surfactant function and structure in SP-A gene targeted mice. Proc Natl Acad Sci U S A. 93:9594-9599.

25. Whitsett JA (2005) Surfactant proteins in innate host defense of the lung. Biol Neonate. 88:175-180.

26. Wright JR (2005) Immunoregulatory functions of surfactant proteins. Nat Rev Immunol. 5:58-68.

27. Korfhagen TR, Sheftelyevich V, Burhans MS, Bruno MD, Ross GF, Wert SE, Stahlman MT, Jobe AH, Ikegami M, Whitsett JA, Fisher JH (1998) Surfactant protein-D regulates surfactant phospholipid homeostasis in vivo. J Biol Chem. 273:28438-28443.

28. Ikegami M, Whitsett JA, Jobe A, Ross G, Fisher J, Korfhagen T (2000) Surfactant metabolism in SP-D gene-targeted mice. Am J Physiol Lung Cell Mol Physiol. 279:L468-476.

29. Ikegami M, Na CL, Korfhagen TR, Whitsett JA (2005) Surfactant protein D influences surfactant ultrastructure and uptake by alveolar type II cells. Am J Physiol Lung Cell Mol Physiol. 288:L552-561.

30. Singh G, Singh J, Katyal SL, Brown WE, Kramps JA, Paradis IL, Dauber JH, Macpherson TA, Squeglia N (1988) Identification, cellular localization,

isolation, and characterization of human Clara cell-specific 10 KD protein. J Histochem Cytochem. 36:73-80.

31. Singh G, Katyal SL (2000) Clara cell proteins. Ann N Y Acad Sci. 923:43-58.

32. Singh G, Katyal SL, Brown WE, Kennedy AL, Singh U, Wong-Chong ML (1990) Clara cell 10 kDa protein (CC10): comparison of structure and function to uteroglobin. Biochim Biophys Acta. 1039:348-355.

33. Mukherjee AB, Kundu GC, Mantile-Selvaggi G, Yuan CJ, Mandal AK, Chattopadhyay S, Zheng F, Pattabiraman N, Zhang Z (1999) Uteroglobin: a novel cytokine? Cell Mol Life Sci. 55:771-787.

34. Lazzaro D, Price M, de Felice M, Di Lauro R (1991) The transcription factor TTF-1 is expressed at the onset of thyroid and lung morphogenesis and in restricted regions of the foetal brain. Development. 113:1093-1104.

35. Boggaram V (2009) Thyroid transcription factor-1 (TTF-1/Nkx2.1/TITF1) gene regulation in the lung. Clin Sci (Lond). 116:27-35.

36. Gehring WJ (1987) Homeo boxes in the study of development. Science. 236:1245-1252.

37. Civitareale D, Lonigro R, Sinclair AJ, Di Lauro R (1989) A thyroid-specific nuclear protein essential for tissue-specific expression of the thyroglobulin promoter. EMBO J. 8:2537-2542.

38. Mizuno K, Gonzalez FJ, Kimura S (1991) Thyroid-specific enhancer-binding protein (T/EBP): cDNA cloning, functional characterization, and structural identity with thyroid transcription factor TTF-1. Mol Cell Biol. 11:4927-4933.

39. Civitareale D, Castelli MP, Falasca P, Saiardi A (1993) Thyroid transcription factor 1 activates the promoter of the thyrotropin receptor gene. Mol Endocrinol. 7:1589-1595.

40. Endo T, Kaneshige M, Nakazato M, Ohmori M, Harii N, Onaya T (1997) Thyroid transcription factor-1 activates the promoter activity of rat thyroid Na+/I- symporter gene. Mol Endocrinol. 11:1747-1755.

41. Bruno MD, Bohinski RJ, Huelsman KM, Whitsett JA, Korfhagen TR (1995) Lung cell-specific expression of the murine surfactant protein A (SP-A) gene is mediated by interactions between the SP-A promoter and thyroid transcription factor-1. J Biol Chem. 270:6531-6536.

42. Bohinski RJ, Di Lauro R, Whitsett JA (1994) The lung-specific surfactant protein B gene promoter is a target for thyroid transcription factor 1 and

hepatocyte nuclear factor 3, indicating common factors for organ-specific gene expression along the foregut axis. Mol Cell Biol. 14:5671-5681.

43. Liu C, Glasser SW, Wan H, Whitsett JA (2002) GATA-6 and thyroid transcription factor-1 directly interact and regulate surfactant protein-C gene expression. J Biol Chem. 277:4519-4525.

44. Zhang L, Whitsett JA, Stripp BR (1997) Regulation of Clara cell secretory protein gene transcription by thyroid transcription factor-1. Biochim Biophys Acta. 1350:359-367.

45. Besnard V, Xu Y, Whitsett JA (2007) Sterol response element binding protein and thyroid transcription factor-1 (Nkx2.1) regulate Abca3 gene expression. Am J Physiol Lung Cell Mol Physiol. 293:L1395-1405.

46. Friedman JR, Kaestner KH (2006) The Foxa family of transcription factors in development and metabolism. Cell Mol Life Sci. 63:2317-2328.

47. Kaestner KH, Knochel W, Martinez DE (2000) Unified nomenclature for the winged helix/forkhead transcription factors. Genes Dev. 14:142-146.

48. Whitsett JA, Nogee LM, Weaver TE, Horowitz AD (1995) Human surfactant protein B: structure, function, regulation, and genetic disease. Physiol Rev. 75:749-757.

49. Khoor A, Gray ME, Hull WM, Whitsett JA, Stahlman MT (1993) Developmental expression of SP-A and SP-A mRNA in the proximal and distal respiratory epithelium in the human fetus and newborn. J Histochem Cytochem. 41:1311-1319.

50. Khoor A, Gray ME, Singh G, Stahlman MT (1996) Ontogeny of Clara cell-specific protein and its mRNA: their association with neuroepithelial bodies in human fetal lung and in bronchopulmonary dysplasia. J Histochem Cytochem. 44:1429-1438.

51. Khoor A, Stahlman MT, Gray ME, Whitsett JA (1994) Temporal-spatial distribution of SP-B and SP-C proteins and mRNAs in developing respiratory epithelium of human lung. J Histochem Cytochem. 42:1187-1199.

52. Floros J, Phelps DS, deMello DE, Longmate J, Harding H, Benson B, White T (1991) The utility of postmortem lung for RNA studies; variability and correlation of the expression of surfactant proteins in human lung. Exp Lung Res. 17:91-104.

53. Khoor A, Whitsett JA, Stahlman MT, Halter SA (1997) Expression of surfactant protein B precursor and surfactant protein B mRNA in adenocarcinoma of the lung. Mod Pathol. 10:62-67.

54. Khoor A, Whitsett JA, Stahlman MT, Olson SJ, Cagle PT (1999) Utility of surfactant protein B precursor and thyroid transcription factor 1 in differentiating adenocarcinoma of the lung from malignant mesothelioma. Hum Pathol. 30:695-700.

55. Strickland-Marmol LB, Khoor A, Livingston SK, Rojiani A (2007) Utility of tissue-specific transcription factors thyroid transcription factor 1 and Cdx2 in determining the primary site of metastatic adenocarcinomas to the brain. Arch Pathol Lab Med. 131:1686-1690.

56. Khoor A, Byrd-Gloster AL, Nicosia SV (2010) Expression of Thyroid Transcription Factor-1 in Malignant Pleural Effusions. Pathol Oncol Res.

57. Yang GC, Wan LS, Papellas J, Waisman J (1998) Compact cell blocks. Use for body fluids, fine needle aspirations and endometrial brush biopsies. Acta Cytol. 42:703-706.

58. Byrd-Gloster AL, Khoor A, Glass LF, Messina JL, Whitsett JA, Livingston SK, Cagle PT (2000) Differential expression of thyroid transcription factor 1 in small cell lung carcinoma and Merkel cell tumor. Hum Pathol. 31:58-62.

59. Khoor A, Stahlman MT, Johnson JM, Olson SJ, Whitsett JA (2004) Forkhead box A2 transcription factor is expressed in all types of neuroendocrine lung tumors. Hum Pathol. 35:560-564.

60. Burke LM, Rush WI, Khoor A, Mackay B, Oliveira P, Whitsett JA, Singh G, Turnicky R, Fleming MV, Koss MN, Travis WD (1999) Alveolar adenoma: a histochemical, immunohistochemical, and ultrastructural analysis of 17 cases. Hum Pathol. 30:158-167.

61. Oliveira P, Moura Nunes JF, Clode AL, da Costa JD, Almeida MO (1996) Alveolar adenoma of the lung: further characterization of this uncommon tumour. Virchows Arch. 429:101-108.

62. Roque L, Oliveira P, Martins C, Carvalho C, Serpa A, Soares J (1996) A nonbalanced translocation (10;16) demonstrated by FISH analysis in a case of alveolar adenoma of the lung. Cancer Genet Cytogenet. 89:34-37.

63. Khoor A, Fleming MV, Purcell CA, Seidman JD, Ashton AH, Weaver DL (1995) Mature teratoma of the uterine cervix with pulmonary differentiation. Arch Pathol Lab Med. 119:848-850.

64. Lowry OH, Rosebrough NJ, Farr AL, Randall RJ (1951) Protein measurement with the Folin phenol reagent. J Biol Chem. 193:265-275.

65. O'Reilly MA, Gazdar AF, Clark JC, Pilot-Matias TJ, Wert SE, Hull WM, Whitsett JA (1989) Glucocorticoids regulate surfactant protein synthesis in a pulmonary adenocarcinoma cell line. Am J Physiol. 257:L385-392.

66. Voorhout WF, Veenendaal T, Haagsman HP, Weaver TE, Whitsett JA, van Golde LM, Geuze HJ (1992) Intracellular processing of pulmonary surfactant protein B in an endosomal/lysosomal compartment. Am J Physiol. 263:L479-486.

67. Vorbroker DK, Dey C, Weaver TE, Whitsett JA (1992) Surfactant protein C precursor is palmitoylated and associates with subcellular membranes. Biochim Biophys Acta. 1105:161-169.

68. Wikenheiser KA, Vorbroker DK, Rice WR, Clark JC, Bachurski CJ, Oie HK, Whitsett JA (1993) Production of immortalized distal respiratory epithelial cell lines from surfactant protein C/simian virus 40 large tumor antigen transgenic mice. Proc Natl Acad Sci U S A. 90:11029-11033.

69. Holzinger A, Dingle S, Bejarano PA, Miller MA, Weaver TE, DiLauro R, Whitsett JA (1996) Monoclonal antibody to thyroid transcription factor-1: production, characterization, and usefulness in tumor diagnosis. Hybridoma. 15:49-53.

70. Zhou L, Lim L, Costa RH, Whitsett JA (1996) Thyroid transcription factor-1, hepatocyte nuclear factor-3beta, surfactant protein B, C, and Clara cell secretory protein in developing mouse lung. J Histochem Cytochem. 44:1183-1193.

71. Sternberger LA, Hardy PH, Jr., Cuculis JJ, Meyer HG (1970) The unlabeled antibody enzyme method of immunohistochemistry: preparation and properties of soluble antigen-antibody complex (horseradish peroxidase-antihorseradish peroxidase) and its use in identification of spirochetes. J Histochem Cytochem. 18:315-333.

72. Hsu SM, Raine L, Fanger H (1981) Use of avidin-biotin-peroxidase complex (ABC) in immunoperoxidase techniques: a comparison between ABC and unlabeled antibody (PAP) procedures. J Histochem Cytochem. 29:577-580.

73. Chilosi M, Lestani M, Pedron S, Montagna L, Benedetti A, Pizzolo G, Menestrina F (1994) A rapid immunostaining method for frozen sections. Biotech Histochem. 69:235-239.

74. Sabattini E, Bisgaard K, Ascani S, Poggi S, Piccioli M, Ceccarelli C, Pieri F, Fraternali-Orcioni G, Pileri SA (1998) The EnVision++ system: a new immunohistochemical method for diagnostics and research. Critical comparison with the APAAP, ChemMate, CSA, LABC, and SABC techniques. J Clin Pathol. 51:506-511.

75. Whitsett JA, Weaver TE, Lieberman MA, Clark JC, Daugherty C (1987) Differential effects of epidermal growth factor and transforming growth factor-beta on synthesis of Mr = 35,000 surfactant-associated protein in fetal lung. J Biol Chem. 262:7908-7913.

76. Cox KH, DeLeon DV, Angerer LM, Angerer RC (1984) Detection of mrnas in sea urchin embryos by in situ hybridization using asymmetric RNA probes. Dev Biol. 101:485-502.

77. Whitsett JA, Weaver TE, Clark JC, Sawtell N, Glasser SW, Korfhagen TR, Hull WM (1987) Glucocorticoid enhances surfactant proteolipid Phe and pVal synthesis and RNA in fetal lung. J Biol Chem. 262:15618-15623.

78. Singh G, Katyal SL, Brown WE, Phillips S, Kennedy AL, Anthony J, Squeglia N (1988) Amino-acid and cDNA nucleotide sequences of human Clara cell 10 kDa protein. Biochim Biophys Acta. 950:329-337.

79. Pelton RW, Johnson MD, Perkett EA, Gold LI, Moses HL (1991) Expression of transforming growth factor-beta 1, -beta 2, and -beta 3 mRNA and protein in the murine lung. Am J Respir Cell Mol Biol. 5:522-530.

80. Springer JE, Robbins E, Gwag BJ, Lewis ME, Baldino F, Jr. (1991) Non-radioactive detection of nerve growth factor receptor (NGFR) mRNA in rat brain using in situ hybridization histochemistry. J Histochem Cytochem. 39:231-234.

81. Elston RC, Johnson W (2008) Basic Biostatistics for Geneticists and Epidemiologists: A Practical Approach. Wiley, Chichester.

82. Khoor A, Whitsett JA, Stephenson M, Cagle PT (1996) Correlation between immunoreactivity for surfactant protein B precursor and better prognosis in early stage adenocarcinoma of lung. Mod Pathol. 9:158A.

83. Khoor A, Whitsett JA, Stahlman MT, Stephenson M, Cagle PT (1997) Immunoreactivity for thyroid transcription factor-1 (TTF-1) correlates with better prognosis in early stage adenocarcinoma of the lung. Am J Respir Crit Care Med. 155:A36.

84. Stahlman MT, Gray ME, Whitsett JA (1992) The ontogeny and distribution of surfactant protein B in human fetuses and newborns. J Histochem Cytochem. 40:1471-1480.

85. Stahlman MT, Gray ME, Whitsett JA (1996) Expression of thyroid transcription factor-1(TTF-1) in fetal and neonatal human lung. J Histochem Cytochem. 44:673-678.

86. Stahlman MT, Gray ME, Whitsett JA (1998) Temporal-spatial distribution of hepatocyte nuclear factor-3beta in developing human lung and other foregut derivatives. J Histochem Cytochem. 46:955-962.

87. Endo H, Oka T (1991) An immunohistochemical study of bronchial cells producing surfactant protein A in the developing human fetal lung. Early Hum Dev. 25:149-156.

88. Liley HG, White RT, Warr RG, Benson BJ, Hawgood S, Ballard PL (1989) Regulation of messenger RNAs for the hydrophobic surfactant proteins in human lung. J Clin Invest. 83:1191-1197.

89. Broers JL, Jensen SM, Travis WD, Pass H, Whitsett JA, Singh G, Katyal SL, Gazdar AF, Minna JD, Linnoila RI (1992) Expression of surfactant associated protein-A and Clara cell 10 kilodalton mRNA in neoplastic and non-neoplastic human lung tissue as detected by in situ hybridization. Lab Invest. 66:337-346.

90. Sunday ME, Hua J, Dai HB, Nusrat A, Torday JS (1990) Bombesin increases fetal lung growth and maturation in utero and in organ culture. Am J Respir Cell Mol Biol. 3:199-205.

91. Siegfried JM, Guentert PJ, Gaither AL (1993) Effects of bombesin and gastrin-releasing peptide on human bronchial epithelial cells from a series of donors: individual variation and modulation by bombesin analogs. Anat Rec. 236:241-247.

92. King KA, Torday JS, Sunday ME (1995) Bombesin and [Leu8]phyllolitorin promote fetal mouse lung branching morphogenesis via a receptor-mediated mechanism. Proc Natl Acad Sci U S A. 92:4357-4361.

93. Singh G, Katyal SL, Torikata C (1981) Carcinoma of type II pneumocytes: immunodiagnosis of a subtype of "bronchioloalveolar carcinomas". Am J Pathol. 102:195-208.

94. Linnoila RI, Jensen SM, Steinberg SM, Mulshine JL, Eggleston JC, Gazdar AF (1992) Peripheral airway cell marker expression in non-small cell lung carcinoma. Association with distinct clinicopathologic features. Am J Clin Pathol. 97:233-243.

95. Mizutani Y, Nakajima T, Morinaga S, Gotoh M, Shimosato Y, Akino T, Suzuki A (1988) Immunohistochemical localization of pulmonary surfactant apoproteins in various lung tumors. Special reference to nonmucus producing lung adenocarcinomas. Cancer. 61:532-537.

96. Dempo K, Satoh M, Tsuji S, Mori M, Kuroki Y, Akino T (1987) Immunohistochemical studies on the expression of pulmonary surfactant apoproteins in human lung carcinomas using monoclonal antibodies. Pathol Res Pract. 182:669-675.

97. Noguchi M, Nakajima T, Hirohashi S, Akiba T, Shimosato Y (1989) Immunohistochemical distinction of malignant mesothelioma from pulmonary adenocarcinoma with anti-surfactant apoprotein, anti-Lewisa, and anti-Tn antibodies. Hum Pathol. 20:53-57.

98. Bejarano PA, Baughman RP, Biddinger PW, Miller MA, Fenoglio-Preiser C, al-Kafaji B, Di Lauro R, Whitsett JA (1996) Surfactant proteins and thyroid transcription factor-1 in pulmonary and breast carcinomas. Mod Pathol. 9:445-452.

99. Di Loreto C, Puglisi F, Di Lauro V, Damante G, Beltrami CA (1998) TTF-1 protein expression in pleural malignant mesotheliomas and adenocarcinomas of the lung. Cancer Lett. 124:73-78.

100. Moran CA, Wick MR, Suster S (2000) The role of immunohistochemistry in the diagnosis of malignant mesothelioma. Semin Diagn Pathol. 17:178-183.

101. Wick MR, Loy T, Mills SE, Legier JF, Manivel JC (1990) Malignant epithelioid pleural mesothelioma versus peripheral pulmonary adenocarcinoma: a histochemical, ultrastructural, and immunohistologic study of 103 cases. Hum Pathol. 21:759-766.

102. Husain AN, Colby TV, Ordonez NG, Krausz T, Borczuk A, Cagle PT, Chirieac LR, Churg A, Galateau-Salle F, Gibbs AR, Gown AM, Hammar SP, Litzky LA,

Roggli VL, Travis WD, Wick MR (2009) Guidelines for pathologic diagnosis of malignant mesothelioma: a consensus statement from the International Mesothelioma Interest Group. Arch Pathol Lab Med. 133:1317-1331.

103. Maeda Y, Dave V, Whitsett JA (2007) Transcriptional control of lung morphogenesis. Physiol Rev. 87:219-244.

104. Weir BA, Woo MS, Getz G, Perner S, Ding L, Beroukhim R, Lin WM, Province MA, Kraja A, Johnson LA, Shah K, Sato M, Thomas RK, Barletta JA, Borecki IB, Broderick S, Chang AC, Chiang DY, Chirieac LR, Cho J, Fujii Y, Gazdar AF, Giordano T, Greulich H, Hanna M, Johnson BE, Kris MG, Lash A, Lin L, Lindeman N, Mardis ER, McPherson JD, Minna JD, Morgan MB, Nadel M, Orringer MB, Osborne JR, Ozenberger B, Ramos AH, Robinson J, Roth JA, Rusch V, Sasaki H, Shepherd F, Sougnez C, Spitz MR, Tsao MS, Twomey D, Verhaak RG, Weinstock GM, Wheeler DA, Winckler W, Yoshizawa A, Yu S, Zakowski MF, Zhang Q, Beer DG, Wistuba, II, Watson MA, Garraway LA, Ladanyi M, Travis WD, Pao W, Rubin MA, Gabriel SB, Gibbs RA, Varmus HE, Wilson RK, Lander ES, Meyerson M (2007) Characterizing the cancer genome in lung adenocarcinoma. Nature. 450:893-898.

105. Kwei KA, Kim YH, Girard L, Kao J, Pacyna-Gengelbach M, Salari K, Lee J, Choi YL, Sato M, Wang P, Hernandez-Boussard T, Gazdar AF, Petersen I, Minna JD, Pollack JR (2008) Genomic profiling identifies TITF1 as a lineage-specific oncogene amplified in lung cancer. Oncogene. 27:3635-3640.

106. Perry A, Parisi JE, Kurtin PJ (1997) Metastatic adenocarcinoma to the brain: an immunohistochemical approach. Hum Pathol. 28:938-943.

107. Srodon M, Westra WH (2002) Immunohistochemical staining for thyroid transcription factor-1: a helpful aid in discerning primary site of tumor origin in patients with brain metastases. Hum Pathol. 33:642-645.

108. Prok AL, Prayson RA (2006) Thyroid transcription factor-1 staining is useful in identifying brain metastases of pulmonary origin. Ann Diagn Pathol. 10:67-71.

109. Comperat E, Zhang F, Perrotin C, Molina T, Magdeleinat P, Marmey B, Regnard JF, Audouin J, Camilleri-Broet S (2005) Variable sensitivity and specificity of TTF-1 antibodies in lung metastatic adenocarcinoma of colorectal origin. Mod Pathol. 18:1371-1376.

110. Matoso A, Singh K, Jacob R, Greaves WO, Tavares R, Noble L, Resnick MB, Delellis RA, Wang LJ (2010) Comparison of thyroid transcription factor-1

expression by 2 monoclonal antibodies in pulmonary and nonpulmonary primary tumors. Appl Immunohistochem Mol Morphol. 18:142-149.

111. Zhang PJ, Gao HG, Pasha TL, Litzky L, Livolsi VA (2009) TTF-1 expression in ovarian and uterine epithelial neoplasia and its potential significance, an immunohistochemical assessment with multiple monoclonal antibodies and different secondary detection systems. Int J Gynecol Pathol. 28:10-18.

112. Levine PH, Joutovsky A, Cangiarella J, Yee H, Simsir A (2006) CDX-2 expression in pulmonary fine-needle aspiration specimens: a useful adjunct for the diagnosis of metastatic colorectal adenocarcinoma. Diagn Cytopathol. 34:191-195.

113. Chu P, Wu E, Weiss LM (2000) Cytokeratin 7 and cytokeratin 20 expression in epithelial neoplasms: a survey of 435 cases. Mod Pathol. 13:962-972.

114. Johnston WW (1985) The malignant pleural effusion. A review of cytopathologic diagnoses of 584 specimens from 472 consecutive patients. Cancer. 56:905-909.

115. Moldvay J, Jackel M, Bogos K, Soltesz I, Agocs L, Kovacs G, Schaff Z (2004) The role of TTF-1 in differentiating primary and metastatic lung adenocarcinomas. Pathol Oncol Res. 10:85-88.

116. Afify AM, al-Khafaji BM (2002) Diagnostic utility of thyroid transcription factor-1 expression in adenocarcinomas presenting in serous fluids. Acta Cytol. 46:675-678.

117. Hecht JL, Pinkus JL, Weinstein LJ, Pinkus GS (2001) The value of thyroid transcription factor-1 in cytologic preparations as a marker for metastatic adenocarcinoma of lung origin. Am J Clin Pathol. 116:483-488.

118. Ng WK, Chow JC, Ng PK (2002) Thyroid transcription factor-1 is highly sensitive and specific in differentiating metastatic pulmonary from extrapulmonary adenocarcinoma in effusion fluid cytology specimens. Cancer. 96:43-48.

119. Chan JK, Suster S, Wenig BM, Tsang WY, Chan JB, Lau AL (1997) Cytokeratin 20 immunoreactivity distinguishes Merkel cell (primary cutaneous neuroendocrine) carcinomas and salivary gland small cell carcinomas from small cell carcinomas of various sites. Am J Surg Pathol. 21:226-234.

120. Di Loreto C, Di Lauro V, Puglisi F, Damante G, Fabbro D, Beltrami CA (1997) Immunocytochemical expression of tissue specific transcription factor-1 in lung carcinoma. J Clin Pathol. 50:30-32.

121. Folpe AL, Gown AM, Lamps LW, Garcia R, Dail DH, Zarbo RJ, Schmidt RA (1999) Thyroid transcription factor-1: immunohistochemical evaluation in pulmonary neuroendocrine tumors. Mod Pathol. 12:5-8.

122. Ullmann R, Petzmann S, Sharma A, Cagle PT, Popper HH (2001) Chromosomal aberrations in a series of large-cell neuroendocrine carcinomas: unexpected divergence from small-cell carcinoma of the lung. Hum Pathol. 32:1059-1063.

123. Wada A, Tateishi R, Terazawa T, Matsuda M, Hattori S (1974) Case report: Lymphangioma of the lung. Arch Pathol. 98:211-213.

124. Al-Hilli F (1987) Lymphangioma (or alveolar adenoma?) of the lung. Histopathology. 11:979-980.

9. Candidates publications related to the PhD thesis

1. Khoor A, Gray ME, Hull WM, Whitsett JA, Stahlman MT (1993) Developmental expression of SP-A and SP-A mRNA in the proximal and distal respiratory epithelium in the human fetus and newborn. J Histochem Cytochem. 41:1311-1319 (IF: 2.789).

2. Khoor A, Stahlman MT, Gray ME, Whitsett JA (1994) Temporal-spatial distribution of SP-B and SP-C proteins and mRNAs in developing respiratory epithelium of human lung. J Histochem Cytochem. 42:1187-1199 (IF: 3.296).

3. Khoor A, Fleming MV, Purcell CA, Seidman JD, Ashton AH, Weaver DL (1995) Mature teratoma of the uterine cervix with pulmonary differentiation. Arch Pathol Lab Med. 119:848-850 (IF: 1.644).

4. Khoor A, Gray ME, Singh G, Stahlman MT (1996) Ontogeny of Clara cell-specific protein and its mRNA: their association with neuroepithelial bodies in human fetal lung and in bronchopulmonary dysplasia. J Histochem Cytochem. 44:1429-1438 (IF: 2.854).

5. Khoor A, Whitsett JA, Stephenson M, Cagle PT (1996) Correlation between immunoreactivity for surfactant protein B precursor and better prognosis in early stage adenocarcinoma of lung. Mod Pathol. 9:158A.

6. Khoor A, Whitsett JA, Stahlman MT, Halter SA (1997) Expression of surfactant protein B precursor and surfactant protein B mRNA in adenocarcinoma of the lung. Mod Pathol. 10:62-67.

7. Khoor A, Whitsett JA, Stahlman MT, Stephenson M, Cagle PT (1997) Immunoreactivity for thyroid transcription factor-1 (TTF-1) correlates with better prognosis in early stage adenocarcinoma of the lung. Am J Respir Crit Care Med. 155:A36.

8. Burke LM, Rush WI, Khoor A, Mackay B, Oliveira P, Whitsett JA, Singh G, Turnicky R, Fleming MV, Koss MN, Travis WD (1999) Alveolar adenoma: a histochemical, immunohistochemical, and ultrastructural analysis of 17 cases. Hum Pathol. 30:158-167 (IF: 2.749).

9. Khoor A, Whitsett JA, Stahlman MT, Olson SJ, Cagle PT (1999) Utility of surfactant protein B precursor and thyroid transcription factor 1 in differentiating adenocarcinoma of the lung from malignant mesothelioma. Hum Pathol. 30:695-700 (IF: 2.749).

10. Byrd-Gloster AL, Khoor A, Glass LF, Messina JL, Whitsett JA, Livingston SK, Cagle PT (2000) Differential expression of thyroid transcription factor 1 in small cell lung carcinoma and Merkel cell tumor. Hum Pathol. 31:58-62 (IF: 2,906).

11. Khoor A, Stahlman MT, Johnson JM, Olson SJ, Whitsett JA (2004) Forkhead box A2 transcription factor is expressed in all types of neuroendocrine lung tumors. Hum Pathol. 35:560-564 (IF: 3.369).

12. Strickland-Marmol LB, Khoor A, Livingston SK, Rojiani A (2007) Utility of tissue-specific transcription factors thyroid transcription factor 1 and Cdx2 in determining the primary site of metastatic adenocarcinomas to the brain. Arch Pathol Lab Med. 131:1686-1690 (IF: 1. 806).

13. Khoor A, Byrd-Gloster AL, Nicosia SV (2010) Expression of Thyroid Transcription Factor-1 in Malignant Pleural Effusions. Pathol Oncol Res.

10. Candidates publications unrelated to the PhD thesis

1. Kendrey G, Kovacs M, Khoor A (1984) [Fatal myocardial complication of mucoviscidosis in infancy]. Morphol Igazsagugyi Orv Sz. 24:147-151.

2. Szalka A, Telegdy L, Khoor A (1984) [Malignant leptospirosis with fatal outcome]. Orv Hetil. 125:3243-3245.

3. Khoor A, Schaff Z, Lapis K (1986) [Hepatoblastoma]. Morphol Igazsagugyi Orv Sz. 26:307-311.

4. Medek S, Nemes A, Khoor A, Szell A, Dobolyi C, Novak EK (1987) [Acremonium strictum meningitis in prolonged steroid therapy]. Orv Hetil. 128:2529-2532.

5. Khoor A, Tulassay T, Bald M, Rascher W (1990) Changes in plasma concentrations of atrial natriuretic peptide during exchange transfusion in premature infants. Acta Paediatr Scand. 79:513-517 (IF: 0.681).

6. Khoor A, Tulassay T, Rascher W, Bald M, Machay T, Kiszel J, Csomor S (1990) Atrial natriuretic peptide, volume and blood pressure regulation during exchange transfusion of the neonates. Acta Paediatr Hung. 30:191-199.

7. Tulassay T, Khoor A, Bald M, Ritvay J, Szabo A, Rascher W (1990) Cerebrospinal fluid concentrations of atrial natriuretic peptide in children. Acta Paediatr Hung. 30:201-207.

8. Shelton KD, Franklin AJ, Khoor A, Beechem J, Magnuson MA (1992) Multiple elements in the upstream glucokinase promoter contribute to transcription in insulinoma cells. Mol Cell Biol. 12:4578-4589 (IF: 8.291).

9. Reddy VM, Meyrick B, Wong J, Khoor A, Liddicoat JR, Hanley FL, Fineman JR (1995) In utero placement of aortopulmonary shunts. A model of postnatal pulmonary hypertension with increased pulmonary blood flow in lambs. Circulation. 92:606-613 (IF: 8.822).

10. Fonseca R, Witzig TE, Olson LJ, Edwards BS, Khoor A, Walker RC (1998) Disseminated Kaposi's sarcoma after heart transplantation: association with Kaposi's sarcoma-associated herpesvirus. J Heart Lung Transplant. 17:732-736 (IF: 2.854).

11. Khoor A, Leslie KO, Tazelaar HD, Helmers RA, Colby TV (2001) Diffuse pulmonary disease caused by nontuberculous mycobacteria in

immunocompetent people (hot tub lung). Am J Clin Pathol. 115:755-762 (IF: 3.136).

12. Khoor A, Myers JL, Tazelaar HD, Swensen SJ (2001) Pulmonary Langerhans cell histiocytosis presenting as a solitary nodule. Mayo Clin Proc. 76:209-211 (IF: 2.644).

13. Strickland-Marmol LB, Khoor A, Robinson LA, Williams CC, Jr. (2002) Malignant localized fibrous tumor of the pleura. Cancer Control. 9:255-258.

14. Cheung OY, Muhm JR, Helmers RA, Aubry MC, Tazelaar HD, Khoor A, Leslie KO, Colby TV (2003) Surgical pathology of granulomatous interstitial pneumonia. Ann Diagn Pathol. 7:127-138.

15. Megyesi M, Berta M, Khoor A (2003) Endobronchial large cell neuroendocrine carcinoma. Pathol Oncol Res. 9:198-200.

16. Ott MC, Khoor A, Leventhal JP, Paterick TE, Burger CD (2003) Pulmonary toxicity in patients receiving low-dose amiodarone. Chest. 123:646-651 (IF: 3.264).

17. Ott MC, Khoor A, Scolapio JS, Leventhal JP (2003) Pulmonary microcrystalline cellulose deposition from intravenous injection of oral medication in a patient receiving parenteral nutrition. JPEN J Parenter Enteral Nutr. 27:91-92 (IF: 1.714).

18. Persellin ST, Cohen MD, Ginsburg WW, Calamia KT, Waldorf JC, Khoor A (2003) Temporal artery bruits in a patient with giant cell arteritis. J Rheumatol. 30:191-192 (IF: 2.674).

19. Khoor A (2004) Alpha-1 antitrypsin deficiency: a study from the registry. Hum Pathol. 35:1433-1434.

20. Khoor A, Myers JL, Tazelaar HD, Kurtin PJ (2004) Amyloid-like pulmonary nodules, including localized light-chain deposition: clinicopathologic analysis of three cases. Am J Clin Pathol. 121:200-204 (IF: 2.716).

21. Regala RP, Weems C, Jamieson L, Khoor A, Edell ES, Lohse CM, Fields AP (2005) Atypical protein kinase C iota is an oncogene in human non-small cell lung cancer. Cancer Res. 65:8905-8911 (IF: 7.616).

22. Tun HW, Wallace KH, Grinton SF, Khoor A, Burger CD (2005) Etanercept therapy for late-onset idiopathic pneumonia syndrome after nonmyeloablative allogeneic hematopoietic stem cell transplantation. Transplant Proc. 37:4492-4496 (IF: 0.799).

23. Waller EA, Roy A, Brumble L, Khoor A, Johnson MM, Garland JL (2006) The expanding spectrum of Mycobacterium avium complex-associated pulmonary disease. Chest. 130:1234-1241 (IF: 3.924).

24. Reed CE, Graham A, Hoda RS, Khoor A, Garrett-Mayer E, Wallace MB, Mitas M (2008) A simple two-gene prognostic model for adenocarcinoma of the lung. J Thorac Cardiovasc Surg. 135:627-634 (IF: 3.037).

25. Regala RP, Davis RK, Kunz A, Khoor A, Leitges M, Fields AP (2009) Atypical protein kinase C{iota} is required for bronchioalveolar stem cell expansion and lung tumorigenesis. Cancer Res. 69:7603-7611 (IF: 7.514).

26. Khoor A (2010) Diagnosis of metastatic neoplasms: an overview. Arch Pathol Lab Med. 134:192-193.

Total impact factor: 83.848

11. Acknowledgements

I wish to thank everyone who, directly or indirectly, contributed to my Ph.D. quest, including:

- My Program Director
    - Prof. Dr. Péter Lakatos
- My Thesis Supervisor
    - Prof. Dr. Károly Cseh
- My Professors and Mentors
    - Prof. Dr. Harry Jellinek
    - Prof. Dr. Anna Kádár
    - Prof. Dr. Gábor Kendrey
    - Prof. Dr. Károly Lapis
    - Prof. Dr. Zsuzsa Schaff
    - Dr. Mildred T. Stahlman
- My Mentees
    - Dr. Angela L. Byrd-Gloster
    - Dr. Leah B. Strickland-Marmol
- My Co-Investigators
    - Dr. Philip. T. Cagle
    - Dr. William D. Travis
    - Dr. Jeffrey A. Whitsett
- My Family